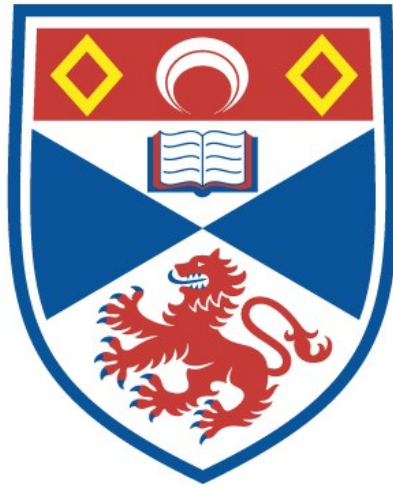


University of St Andrews



Full metadata for this thesis is available in
St Andrews Research Repository
at:

<http://research-repository.st-andrews.ac.uk/>

This thesis is protected by original copyright

(i)

HYDROGEN EXCHANGE ON THE INDOLE NUCLEUS

A Thesis
presented for the degree of
Doctor of Philosophy
in the Faculty of Science of the
University of St. Andrews
by
Eric M. Millar, B.Sc.

October 1968

St. Salvator's College,
St. Andrews.



(ii)

I declare that this thesis is my own composition, that the work of which it is a record has been carried out by myself, and that it has not been submitted in any previous application for a Higher Degree.

The thesis describes results of research carried out at the Chemistry Department, St. Salvator's College, University of St. Andrews (and latterly at the Chemistry Department, Imperial College, University of London) under the supervision of Dr. B.C. Challis since the 1st October 1965, the date of my admission as a research student.

(iii)

I hereby certify that Eric Michael Millar has spent twelve terms at research work under my supervision, has fulfilled the conditions of Ordinance No. 16 (St. Andrews) and is qualified to submit the accompanying thesis in application for the degree of Doctor of Philosophy.

Director of Research

ABSTRACT

Recent theoretical treatments dealing with the magnitude of the primary kinetic hydrogen isotope effect are reviewed, together with the related experimental findings. A short summary of the development of ideas on the mechanism of aromatic hydrogen exchange is also given.

The acid catalysed hydrogen exchange reaction of several substituted indoles is reported. Most of the studies refer to the kinetics of proto-detritiation and proto-dedeuteriation of the appropriately labelled indole in aqueous acetic acid buffer solutions, but some experiments were carried out in dilute hydrochloric acid and in aqueous pyridine buffer solutions.

The values of the kinetic isotope effect and the Brønsted α -exponent for the above reaction are compared with those obtained recently by other workers from studies on closely related systems. In particular it is shown that the variation of the "primary" kinetic isotope effect with ΔpK (the difference in basicities of substrate and catalyst) is much smaller for the aromatic hydrogen exchange reaction than that found for hydrogen abstraction from aliphatic acids. A suggested explanation for this apparent anomaly, in terms of secondary isotope effect considerations, is given.

Studies on the mechanism of the base catalysed hydrogen exchange reaction of indole and several of its derivatives are then reported. The bulk of the experimental evidence indicates

(v)

that the reaction mechanism can be described as a rate determining attack on the indole anion by the conjugate acid of the basic catalyst.

ACKNOWLEDGEMENTS

I should like to thank Dr. B.C. Challis, who suggested this topic of research, for his constant enthusiasm, advice and encouragement throughout the investigation.

I would also like to express my very sincere thanks to Professor J.I.G. Cadogan for his interest in the work.

I am grateful to Professor D.H.R. Barton for permitting me to use the facilities of the Department of Organic Chemistry, Imperial College, London, during my final year of study.

In addition my thanks are due to the many members of the Chemistry Departments, both in St. Andrews and in Imperial College, London, who did so much to assist me throughout the course of this study.

I am indebted to the Science Research Council for the award of a Maintenance Grant.

CONTENTS

Page No.

PART I. INTRODUCTION

CHAPTER I.	The Historical Survey	2
------------	-----------------------------	---

PART II. DISCUSSION OF THE EXPERIMENTAL RESULTS

CHAPTER II.	The Acid-catalysed Hydrogen Exchange Reaction	19
-------------	--	----

CHAPTER III.	Base-catalysed β -Hydrogen Exchange on the Indole Nucleus	77
--------------	--	----

PART III. EXPERIMENTAL

CHAPTER IV.	The Experimental Details	114
-------------	--------------------------------	-----

BIBLIOGRAPHY	143
--------------	-------	-----

(viii)

To Wanda

PART I

Introduction

CHAPTER I

THE HISTORICAL SURVEY

The desire for a better understanding of how chemical reactions occur has been stimulated particularly by the rapid and voluminous development of organic chemistry, both in the number and the complexity of reactions studied. Furthermore, the complete description of all processes involved in a chemical reaction (the "mechanism") must include a knowledge of the sequence and relative speeds of these steps, as well as other non-kinetic information.

Of the many aids to the elucidation of organic reaction mechanisms which have been developed, the hydrogen isotope effect is understandably of major importance, as many reactions involve the process of proton transfer in one way or another. Since the mass ratio of hydrogen (H) and its isotopes, deuterium (D) and tritium (T), is large ($H:D:T = 1:2:3$), changes in both reaction rates and equilibria arising from the replacement of hydrogen by one of its isotopes are normally of an easily measurable magnitude. These changes can be divided into three broad classes and are referred to as primary, secondary, and solvent isotope effects, respectively. The primary isotope effect is associated with the cleavage of the isotopically substituted bond in the rate controlling step of a reaction. The secondary isotope effect is concerned with differences in reaction rates and equilibria which accompany isotopic substitution at sites other than those undergoing bond fission. The solvent isotope effect refers to the differences between ordinary water and deuterium oxide as reaction media.

This introduction is concerned mainly with recent developments,

theoretical and experimental, in the field of primary hydrogen isotope effects, and their bearing on the detailed mechanism of aromatic hydrogen exchange reactions.

The Magnitude of the Primary Kinetic Hydrogen Isotope Effect.

The fundamental requirement for the existence of this phenomenon is that a bond to hydrogen should be broken or formed in the rate-limiting reaction step. Primary kinetic hydrogen isotope effects have been reported for many chemical reactions under a wide variety of experimental conditions. Most of the available data has been discussed in the excellent reviews by Gold and Satchell,⁽¹⁾ Wiberg,⁽²⁾ and Melander,⁽³⁾ and more recently by Gold⁽⁴⁾ and Zollinger.⁽⁵⁾ The wide, and seemingly disordered, variation in the magnitude of the observed effects has led to the development of a number of explanatory theories; in turn, the attention of a few groups of workers has focussed on testing the theoretical arguments.

Theoretical Treatments

In his review of the magnitude of the primary kinetic hydrogen isotope effect, Westheimer⁽⁶⁾ has pointed out that although a few of the experimentally determined values are higher than would be predicted from the simplest theoretical considerations, the vast majority are lower. The simplified treatment is best illustrated by considering the transfer of a hydrogen atom from one molecule to another as illustrated by equation (1.1):



As the hydrogen atom transfers from A to B in forming the transition

state, the molecule A-H loses the degree of freedom associated with the carbon-hydrogen stretching vibration, this vibration becoming the translational motion along the reaction co-ordinate. (Since most data refer to hydrogen transfer from a carbon site within a molecule, carbon-hydrogen vibrations are normally referred to in discussions such as this.) The result is a total loss of the zero-point energy associated with the C-H stretching vibration ($= \frac{1}{2}h\nu_H$) in the ground state, as the proton transfer takes place. The corresponding loss of zero-point energy for the deuterium transfer (equation (1.2))



is $\frac{1}{2}h\nu_D$. The difference in activation energy for the two hydrogen transfer reactions is therefore equal to the difference in zero-point vibrational energies of A-H and A-D. Using reasonable values for the zero-point vibrational frequencies, the difference ($\frac{1}{2} h\nu_H - \frac{1}{2}h\nu_D$) is about 1.15 kcal.per mole. At 25°C this leads to a factor of 6.9 in the reaction rate, i.e.,

$$\frac{k_H}{k_D} = \frac{A e^{\frac{-E_H}{RT}}}{A e^{\frac{-E_D}{RT}}}$$

$$= e^{\frac{-(E_H - E_D)}{RT}}$$

$$= e^{\frac{\Delta Z.P.E.}{RT}}$$

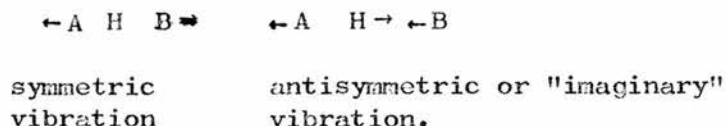
$$= e^{\frac{1.15}{1.98 \times 298}}$$

$$= 6.9$$

where k_H , k_D are the rate coefficients for reactions (1.1) and (1.2) respectively, and the difference in activation energies for the two reactions ($E_D - E_H$) is equal to the difference in zero-point vibrational energies ($\Delta Z.P.E.$) of the C-H and C-D bonds. The pre-exponential factor, A , is assumed to be the same for each reaction.

This treatment, which predicts that all primary carbon-hydrogen isotope effects should have a value of 6.9 at 25°C, must, in view of the experimental findings, be oversimplified. The logical explanation is that other factors associated with the C-H and C-D bonds contribute significant energy differences in the transition state. More elaborate theories have attempted to analyse the origin of these contributions.

Westheimer,⁽⁶⁾ in his treatment of small isotope effects, considered a linear, one-dimensional transition state model in which only two stretching vibrations, one symmetrical and one antisymmetrical, were dependent on the isotopic hydrogen.



The antisymmetric vibration corresponds to the translational motion along the reaction co-ordinate and has no real frequency of vibration. The other vibration has a real frequency which, when the vibration is truly symmetrical, will be independent of the isotopic species. The formation of the transition state should in this case lead to the change in zero-point energy predicted previously from the simplest considerations, and the resulting isotope effect should be at a maximum. However, when the bond-forming capabilities of A and B towards the hydrogen atom are not equal, the vibration will not be

symmetrical. The hydrogen atom will therefore vibrate within the transition state with a higher frequency than the corresponding deuterium atom, and this will lead to a zero-point energy difference for the C-H and C-D bonds. Ultimately, this leads to a lowering of the zero-point energy differences between ground and transition states, and consequently, a lowering of the k_H/k_D ratio. In other words, the magnitude of the primary kinetic isotope effect associated with proton transfer should correlate with the relative base strengths of the sites between which the proton is transferred, and should be at a maximum when these are equal.

The conclusion that isotope effects are dependent on the symmetry of the transition state has been reached subsequently by other authors^(3,7) who have made assumptions and approximations similar to those of Westheimer.⁽⁶⁾ All these theoretical treatments in common have neglected the effects of both bending vibrations and quantum mechanical proton tunnelling (leakage of H or D through the potential energy barrier), on the magnitude of the isotopic effect. Using a coulombic model for the motion of the proton, Bell⁽⁸⁾ has shown that contributions from transition state bending vibrations and proton tunnelling may exactly cancel out if both effects are small. Nevertheless, the omission of these two factors has yet to be justified and it is on this point that subsequent theoretical treatments have differed.

Thus Willi and Wolfsberg⁽⁹⁾ have shown that, depending on the frequency chosen for the antisymmetric ("imaginary") vibration in the transition state, a series of different relationships between the

isotope effect and transition state symmetry (as measured by the relative degree of bond making or bond breaking), can exist. They concluded that, by the choice of an appropriate curvature parameter for the potential energy surface (corresponding to the "imaginary" vibrational frequency) the k_H/k_D ratio, in principle, could be constant for a series of transition states of differing symmetry. The behaviour predicted by Westheimer⁽⁶⁾ can also be obtained with their treatment by selection of another curvature parameter. Since the curvature of the potential energy barrier is closely related to the width of the barrier and hence to the degree of proton tunnelling, the danger of neglecting this effect is apparent. The same authors have noted that transition state bending vibrations may also play a part in determining the magnitude of the primary isotope effect.

This latter view has been expressed also by Bell⁽¹⁰⁾ who criticised the Westheimer treatment since it neglects bending vibrations. Furthermore, Bell considered it doubtful that variations in the "symmetric" vibration for a three-centre transition state model with a realistic potential energy surface could account for the small magnitude of some k_H/k_D ratios. He therefore assumed a more sophisticated five-centre transition state to be a better model (than the three-centre counterpart) for many reactions, and argued that additional stretching vibrations possible in the five-centre model might lead to a more satisfactory explanation of low isotope effects.

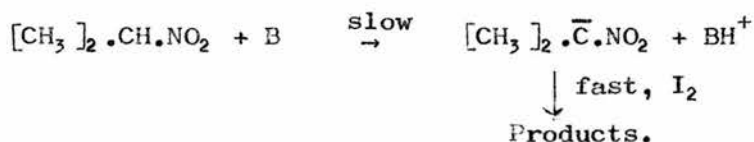
Also, Bader,⁽¹¹⁾ using a perturbed hydrogen bond as his transition state model, has attempted to show the large effects of

bending vibrations on the magnitude of the isotope effect. His simplification, consisting of the neglect of stretching vibrations, reduces the applicability of the treatment, but nevertheless he demonstrated that bending vibrations could produce a considerable lowering of the isotope effect. In addition Bader claimed that a large variation of k_H/k_D should be possible without alteration of transition state symmetry. His calculations also led to the prediction that variation of the base strength of B (cf. equations (1.1) and (1.2)), in a system with an A-H bond which cannot readily delocalise negative charge development, should give rise to a set of k_H/k_D values which pass through a minimum!

On the other hand, Westheimer's approximation that considerations of stretching vibrations alone can account for the observed low isotope effects, has received recent support from two sets of calculations by Albery⁽¹²⁾ and More O'Ferrall and Kouba,⁽¹³⁾ respectively. Albery,⁽¹²⁾ by considering all possible values for transition state force constants in the simple three-centre model, has shown that it is unnecessary to invoke the five-centre model proposed by Bell⁽¹⁰⁾ to explain low observed isotope effects. More O'Ferrall and Kouba,⁽¹³⁾ by means of calculations for four- and five-centred transition state models, have demonstrated that even when bending vibrations and proton tunnelling are taken into account, the same over-all result is obtained as that from considerations only of stretching vibrations, viz., that isotope effects will be at a maximum for a reasonably symmetrical transition state.

Experimental Evidence.

Few systematic investigations have been made so far to test the validity and relative importance of the approximations used in the theoretical calculations. Perhaps the best evidence to date is provided by Bell and his co-workers, who have studied the ionisation of ketonic substances^(10,14) and nitroparaffins.^(10,15) In both series of reactions, abstraction of a hydrogen or deuterium atom from the substrate by an attacking base, is the rate-controlling process, e.g., for nitropropane with base B:

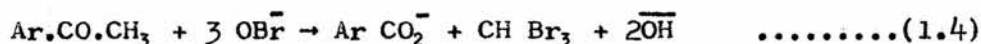


.....(1,3)

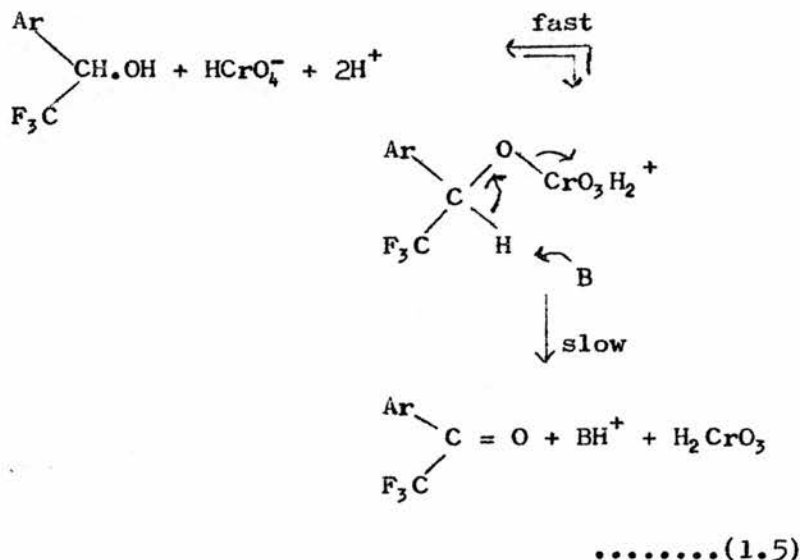
It is evident from the combined data that a plot of $\log_{10} (k_H/k_D)$ against the difference between substrate and catalyst basicities (ΔpK) shows a maximum isotope effect in the neighbourhood of $\Delta \text{pK} = 0$; i.e., when the base strengths of the two species between which the proton is being transferred are equal. As ΔpK becomes positive or negative, the isotope ratios decrease smoothly from either side of the maximum. Although Bell⁽¹⁰⁾ has proposed an alternative explanation based on a five-centre transition state model, these results are in good agreement with Westheimer's suggestion that a maximum value of the isotope effect should correspond to a symmetrical transition state.

Other experimental evidence is less compelling. Thus, as part of a number of investigations on the rates of ionisation of ketonic compounds,⁽¹⁶⁾ Jones and his co-workers^(16c) have shown that for a

series of para- and meta-substituted acetophenones (which react with alkaline solutions of bromine according to the general equation:



where the rate determining process is ionisation of the ketone), a correlation exists between the magnitude of the isotope effect and the pK of the corresponding benzoic acid, an increase in isotope effect being observed as the acid becomes weaker. This correlation is similar to that found by Stewart and Lee⁽¹⁷⁾ for the oxidation of substituted phenyl trifluoromethyl carbinols:

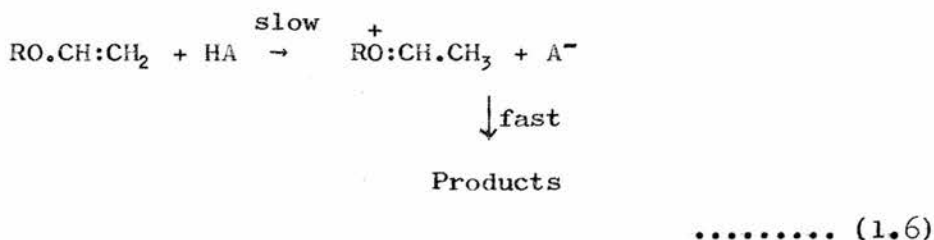


Although the observed isotope effect does not pass through a maximum in either of these instances, there is good evidence that the k_H/k_D ratio increases as the transition state tends towards a symmetrical configuration as measured by differences in basicity.

Ling and Kendall⁽¹⁸⁾ have measured the primary kinetic isotope effect on hydrogen exchange in four substituted dimethylanilines in acid solution. The primary isotope effect increases from 4.1 to 7.2, in parallel with a steady decrease in the specific rate constant

for the exchange process. Again, no maximum value of the isotope effect is realised, but a dependence on substrate basicity (and therefore reactivity) of the magnitude of the k_H/k_D ratio is indicated.

The most recent systematic study on the magnitude of isotope effects is that of Kresge, Sagatys and Chen.⁽¹⁹⁾ They have measured the isotope effects on the hydrolysis of several vinyl ethers for which the initial H^+ transfer is the rate-determining step (equation (1.6)).



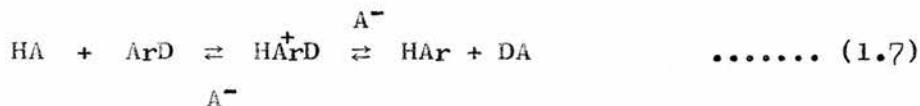
A good correlation between substrate reactivity and isotope effect is observed, increase of reaction rate being accompanied in a regular manner with increased primary isotope effect, and is again taken to indicate the dependence of the isotope effect on transition state structure. The correlation is poor, however, when similar data for other reactions are included on the plot. It therefore seems probable that other effects, specific to the reaction, influence a k_H/k_D ratio, and successful correlations may be restricted to data for a single reaction type only.

Although most of the available data only illustrates in general that isotope effects tend to be smaller than the predicted maximum, very large values have been obtained in a few cases. In particular, Funderburk and Lewis,⁽²⁰⁾ from studies of hydrogen abstraction from 2-nitropropane by a series of increasingly sterically-hindered

pyridine bases (as in equation (1.3)), have found that the isotope effect rises from a value of 9.84 (for pyridine catalysis) to 24.1 and 24.2 (for catalysis by 2,6-lutidine and 2,4,6-collidine, respectively) Bell and Goodall⁽¹⁵⁾ have repeated the measurement for the 2,6-lutidine catalyst and have reported a k_H/k_D of similar magnitude (= 19.5).

The explanation offered for these large isotopic rate ratios is that proton tunnelling is important; this should cause a greater reduction in the pre-exponential factor of the Arrhenius equation for a protium as compared to a deuterium compound,⁽²¹⁾ and thus result in an abnormally high isotope effect. The evidence is in accord with the expectation that tunnelling may be important in those reactions where the transition state is sterically crowded.⁽²⁰⁾

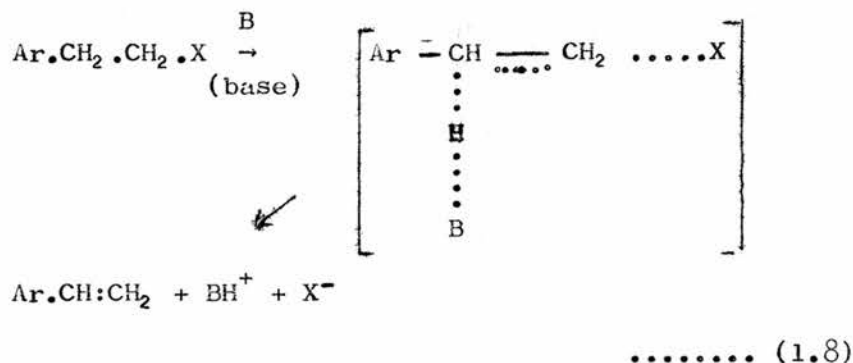
Kresge⁽²²⁾ suggested some time ago that the aromatic hydrogen exchange reaction represented by equation (1.7)



furnishes experimental support for the incidence of substrate dependent primary isotope effects. The data for this reaction has been extended recently by Long and his co-workers^(23,24) from measurements of the primary kinetic isotope effect for isotopic hydrogen exchange with substituted azulenenes. The plot of k_H/k_D against $\Delta pK (= pK_{\text{substrate}} - pK_{\text{HA}})$ is a curve, similar to that found by Bell,⁽¹⁵⁾ exhibiting a maximum isotope effect close to $\Delta pK = 0$. Isotopic rate ratios for other weakly basic aromatic species also correlate with their relative reactivities, and this is taken as evidence that diminishing values of k_H/k_D will be observed outside

the rather limited range covered by the results for azulene.

Other evidence comes from studies of base-catalysed β -elimination reactions in which proton loss is synchronous with anion expulsion as illustrated generally by equation (1.8):



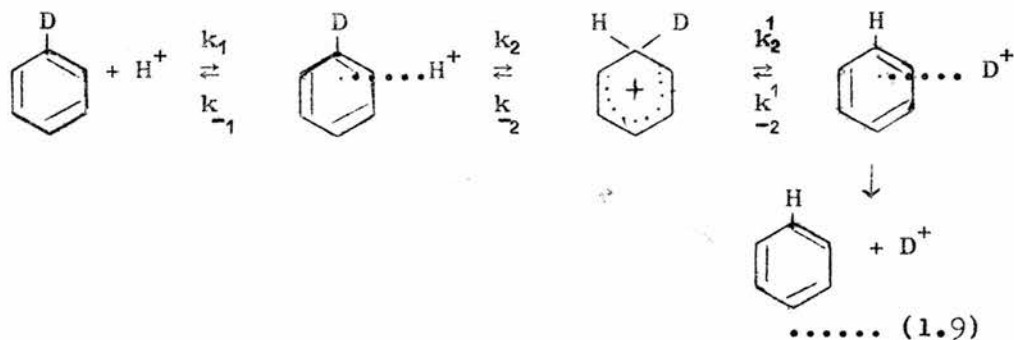
Cockerill⁽²⁵⁾ has found that for the reaction of 2-arylethyldimethylsulphonium bromides ($\text{X} = \text{S}[\text{CH}_3]_2\text{Br}$ in equation (1.8)) with sodium hydroxide in water the $k_{\text{H}}/k_{\text{D}}$ gradually increases with added dimethyl sulphoxide, passes through a maximum, and then decreases. This variation is associated with different degrees of proton transfer in the transition state arising from changes in the structure of the attacking base (i.e. change of hydration) as the medium is changed from pure water to dimethyl sulphoxide - water mixtures. Other interpretations are not excluded and it is interesting to note that the $k_{\text{H}}/k_{\text{D}}$ ratio is independent of dimethyl sulphoxide concentration for the reaction of 2-aryethyl bromides ($\text{X} = \text{Br}$ in equation (1.8)) with potassium t-butoxide in t-butyl alcohol - D.M.S.O. mixtures.⁽²⁶⁾ In this case it has been suggested that the nature of the base (i.e. degree of solvation) remains essentially constant although the base concentration is changing. Furthermore, Cockerill⁽²⁵⁾ has suggested that the tunnel effect may be important in this reaction,

causing a broadening of the region of transition state symmetry over which a maximum isotope effect could occur.⁽⁹⁾ It is apparent that before the variation in primary isotope effect can be ascribed solely to changes in transition state symmetry, further evidence of desolvation specific to the hydroxide ion is necessary.

In conclusion, it appears that the theoretical prediction for variation of the primary isotope effect with the structure of the transition state is borne out, in part at least, by the available experimental studies. The most compelling evidence is that of Bell and Goodall.⁽¹⁵⁾ The limited data of other studies are in general agreement with Bell and Goodall's findings.

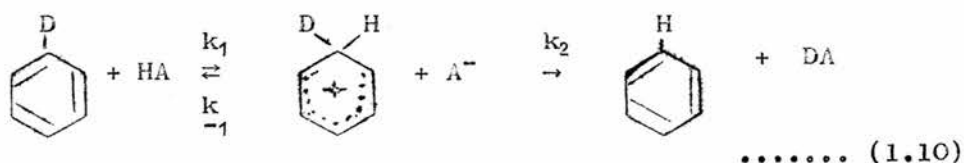
Aromatic Hydrogen Exchange Reactions

Gold⁽⁴⁾ has reviewed studies of acid-catalysed isotopic hydrogen exchange on aromatic substrates carried out prior to 1960. From the collective evidence it can be deduced that the reaction is of an electrophilic nature and is a substitution rather than an addition-elimination process. The reaction mechanism, based mainly on studies of exchange in concentrated mineral acid solutions, was originally thought⁽²⁷⁾ to consist of the sequence of steps illustrated by equation (1.9).



In this, a fast pre-equilibrium addition of H^+ to the substrate to form an "outer" (π - type) complex of hydrogen ion plus aromatic molecule, is followed by a slow (rate-determining) rearrangement of the complex. This mechanism, which predicts specific acid catalysis (i.e., catalysis only by the hydronium ion), and which was consistent with the data available at that time, has since been criticised^(28,29) as a result of studies with more basic aromatic hydrocarbons in dilute aqueous solutions.

Thus Kresge and Chiang⁽²⁸⁾ have shown that hydrogen exchange on trimethoxybenzene is subject to general acid catalysis and have suggested an alternative mechanism which accounts not only for their results, but also those of previous workers. The mechanism, an "orthodox" $A-S_E2$ exchange process (acid-catalysed, bimolecular, electrophilic substitution) is illustrated by equation (1.10):



The reaction involves two slow steps. In the first one (k_1) a proton is transferred from the general acid HA to the substrate; the relatively stable conjugate acid thus formed, then loses either deuterium (k_2) or hydrogen (k_{-1}) to give the product or reactant, respectively. Similarly, hydrogen exchange on a series of azulenes⁽²⁹⁾ was found to be subject to general acid catalysis and the $A-S_E2$ mechanism proposed by Kresge and Chiang again appears to be operative.

Acid-catalysed hydrogen exchange on the indole nucleus was

first studied by Koizumi⁽³⁰⁾ in 1938, but his experiments, which were carried out under heterogeneous conditions, gave only a qualitative estimate of the relative ease of deuterium exchange at the various ring positions. Hinman and his co-workers^(31b) have briefly studied the exchange in homogeneous solutions of methyl-substituted indoles in concentrated deuteriosulphuric acid in deuterium oxide. Although no firm conclusions on the reaction mechanism can be drawn from their studies, they have established the site of equilibrium protonation (3-position) and measured the basicity of several substituted indoles.⁽³¹⁾ The site of protonation is consistent with the fact that, normally, electrophilic substitution reactions of indoles involve the 3-position.⁽³²⁾

Challis and Long⁽³³⁾ have demonstrated that, as for azulene⁽²⁹⁾ and trimethoxybenzene,⁽²⁸⁾ the acid-catalysed hydrogen exchange on 2-methylindole and 1,2-dimethylindole is subject to general acid catalysis and a similar $A-S_E2$ exchange mechanism was therefore suggested. As an extension of this work, further studies on the acid-catalysed hydrogen exchange have been undertaken and are reported in Chapter II.

The same workers⁽³³⁾ found that the isotopic exchange reaction is also catalysed by sodium hydroxide when the indole has no nitrogen substituent; general base catalysis for the protodetritiation of 2-methyl-3- $[^3H]$ indole was then established by further experiments.⁽³⁴⁾ No similar base-catalysed process was evident for hydrogen exchange on the other carbon bases.^(28,29) Further investigations on the base-catalysed exchange reactions of several indoles are reported in Chapter III. In connection with these, it is interesting to note that recently, Yagil,⁽³⁵⁾ using a series of substituted indoles as

indicators, established an acidity function for aqueous sodium hydroxide and measured the acid dissociation constants of several substituted indoles.

PART II

DISCUSSION OF THE EXPERIMENTAL RESULTS

CHAPTER II

THE ACID-CATALYSED HYDROGEN EXCHANGE REACTION

The results discussed in this Chapter are concerned with the acid-catalysed hydrogen exchange reactions of several substituted indoles. The exchange processes were studied for most cases in aqueous acetic acid buffer solutions and in dilute hydrochloric acid, but additional measurements on indole itself were made in aqueous pyridine buffer solutions.

The kinetic leaving-atom isotope effect is calculated for nine different substrate-catalyst pairs; supplementary measurements of the kinetic solvent isotope effect on the detritiation of 2-methyl-3- $^{[3]}\text{H}$ indole are also reported. The magnitude of the various isotope effects in relation to the Brønsted α -exponent for general acid catalysed exchange is also discussed.

All the kinetic runs reported herein were at 25°C in solutions maintained at ionic strength (μ) of 0.1 by the addition of NaCl, and followed good first-order kinetics in accordance with equation (2.1)

$$v = k_{\text{obs}}[\text{Indole}] \dots\dots\dots (2.1)$$

where [Indole] refers to the concentration of the isotopically labelled substrate.

2-methylindole

a) Proto-detrition in aqueous acetic acid - sodium acetate buffer solutions.

The acid-catalysed proto-detrition of 2-methyl-3- $[^3\text{H}]$ indole was studied initially in acetic acid - sodium acetate buffer solutions, both to check the previous data of Challis and Long,⁽³³⁾ and to familiarise with the experimental technique. The variation of the experimental first-order rate coefficient (k_{obs}^T) with $[\text{HOAc}]$ (which refers to the concentration of acetic acid) at constant pH is shown in TABLE (2.1).

TABLE (2.1)

Proto-detrition of 2-methyl-3- $[^3\text{H}]$ indole in acetic acid buffers

Buffer ratio* = 1:5.		$[\text{H}_3\text{O}^+]** = 5.58 \times 10^{-6} \text{M}$		$\mu = 0.1$
Kinetic	$[\text{HOAc}]$	$[\text{OAc}^-]$	$[\text{NaCl}]$	$10^4 k_{\text{obs}}^T$
Run	$\cdot 10^3 \text{M}$	$\cdot 10^3 \text{M}$	$\cdot 10^3 \text{M}$	sec^{-1}
31	20	100	-	15.7
32	15	75	25	12.7
34	10	50	50	9.35
33	5	25	75	5.80
30	1	5	95	2.81

* Buffer ratio (for acetic acid) refers throughout the thesis to ratio of acetic acid concentration to acetate anion concentration, i.e. $[\text{HOAc}]:[\text{OAc}^-]$.

** Throughout the thesis, $[\text{H}_3\text{O}^+]$ is calculated in the usual manner for buffer solutions from a value of 2.79×10^{-5} for the dissociation constant of acetic acid.⁽³⁶⁾

In TABLE (2.2) the values of k_{obs}^T referring to varying pH for a constant $[\text{HOAc}]$ are given.

TABLE (2.2)

Proto-detrition of 2-methyl-3-^[3H]indole in acetic acid buffers.

[HOAc] = 10 ⁻³ M, throughout.		μ = 0.1		
Kinetic	[OAc ⁻]	[NaCl]	[H ₃ O ⁺]	10 ⁴ k _{obs} ^T
Run	.10 ³ M	.10 ³ M	.10 ⁶ M	sec. ⁻¹
27	1	99	27.9	11.4
28	2	98	14.0	6.47
29	3	97	9.29	4.38
30	5	95	5.58	2.81
*	-	-	0	0.69

* value obtained from data of TABLE (2.1)

The second-order coefficients for catalysis of the reaction by both acetic acid and H₃O⁺, corresponding to equation (2.2), were obtained

$$v = k_{H_3O^+}^T [H_3O^+] [Indole] + k_{HOAc}^T [HOAc] [Indole] \quad \text{..... (2.2)}$$

from the experimental results by plotting k_{obs}^T against [HOAc] and [H₃O⁺], respectively. In practice, the best straight line was selected by a least squares analysis of the experimental data, and this is demonstrated for experiments at constant pH (to derive k_{HOAc}^T) in FIGURE (2.1). The following values for the second-order coefficients were obtained.

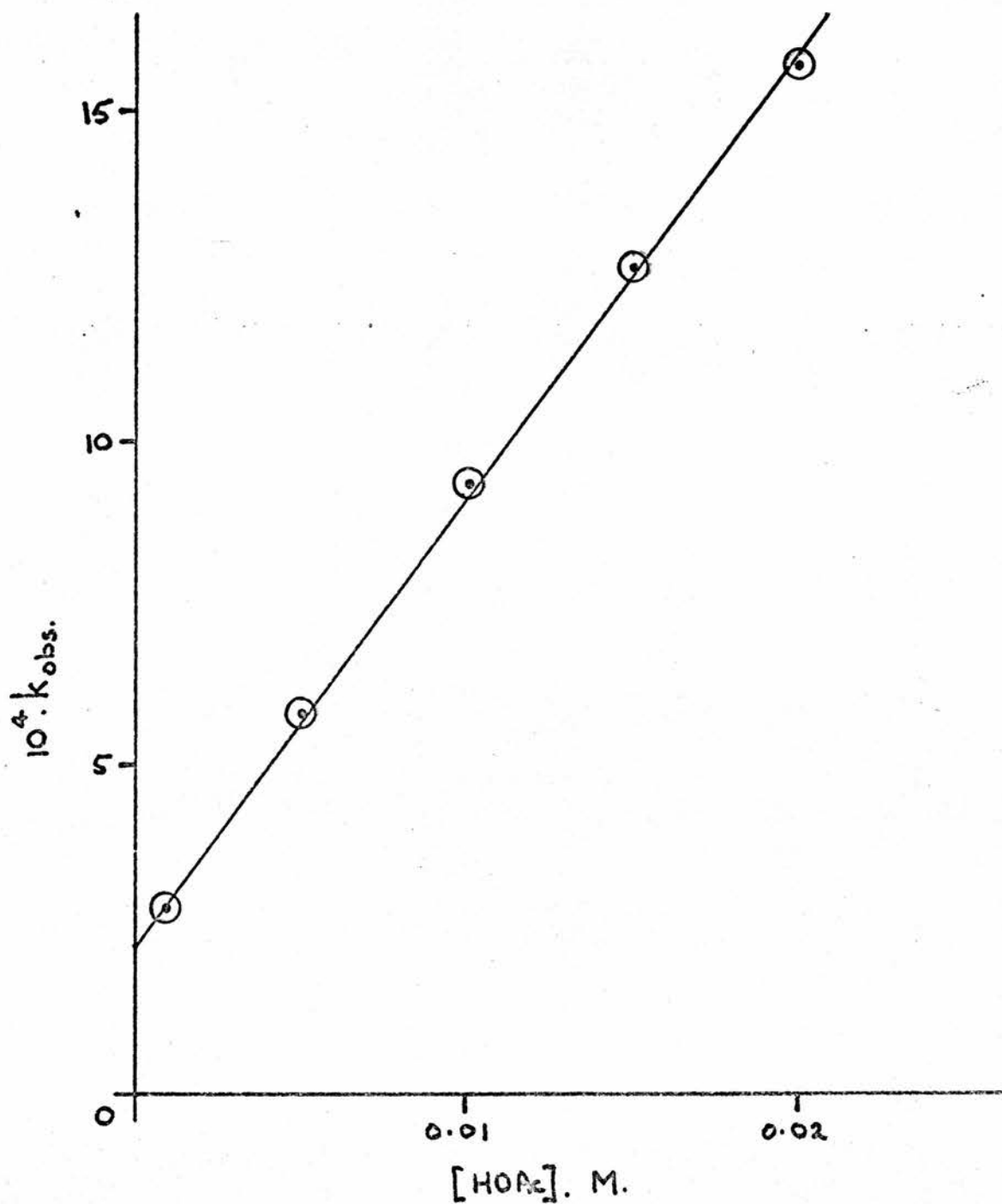
$$k_{HOAc}^T = 0.069 \pm 0.001 \text{ l.mole}^{-1} \text{ sec.}^{-1}$$

$$k_{H_3O^+}^T = 38.6 \pm 1.0 \text{ l.mole}^{-1} \text{ sec.}^{-1}$$

It is of interest to note that the intercept of FIGURE (2.1) (which corresponds to k_{H₃O⁺}^T + [5.58 x 10⁻⁶]) leads to a value of k_{H₃O⁺}^T in excellent agreement with that obtained directly from the data of TABLE (2.2). Similar excellent agreement was found for the

Figure (2.1)

Detritiation of 2-methyl-3- $^{[3]}\text{H}$ indole in acetic acid buffers. Variation of k_{obs} with $[\text{HOAc}]$.



corresponding values of k_{HOAc}^T . Thus the rate equation for isotopic hydrogen exchange in acetic acid buffers (neglecting catalysis by H_2O itself) is given by equation (2.3), and this is in good agreement

$$v = 38.6 [\text{H}_3\text{O}^+][\text{Indole}] + 0.069 [\text{HOAc}][\text{Indole}] \quad \text{..... (2.3)}$$

with the results of Challis and Long.⁽³³⁾

The earlier studies^(33,34) demonstrated the absence of appreciable catalysis by the acetate anion, since the slope of k_{obs}^T vs. $[\text{HOAc}]$ at different buffer ratios was essentially constant; catalysis by water was at the same time shown to be negligible in the acetic acid buffer solutions used above.

b) Proto-dedeuteriation in aqueous acetic acid - sodium acetate buffer solutions.

The rate of proto-dedeuteriation of 2-methyl-3-[^2H]indole was also measured in aqueous acetic acid buffers, and the experimental data is presented in TABLES (2.3) and (2.4)

TABLE (2.3)

Proto-dedeuteriation of 2-methyl-3-[^2H]indole in acetic acid buffers

Buffer ratio = 1:10. $[\text{H}_3\text{O}^+] = 2.79 \times 10^{-6} \text{M}$. $\mu = 0.1$

Kinetic	$[\text{HOAc}]$	$[\text{OAc}^-]$	$[\text{NaCl}]$	$10^4 k_{\text{obs}}^D$
Run	$\cdot 10^3 \text{M}$	$\cdot 10^3 \text{M}$	$\cdot 10^3 \text{M}$	sec. ⁻¹
13	10	100	-	15.9
22	10	100	-	16.6
15	8	80	20	14.0
17	5	50	50	9.10
20	3	30	70	5.40
19	1	10	90	4.10
21	1	10	90	3.30

TABLE (2.4)

Proto-dedeuteriation of 2-methyl-3-[²H]indole in acetic acid buffers

[HOAc] = 10 ⁻³ M, throughout.		μ = 0.1		
Kinetic	[OAc ⁻]	[NaCl]	[H ₃ O ⁺]	10 ⁴ k _{obs} ^D
Run	.10 ³ M	.10 ³ M	.10 ⁶ M	sec. ⁻¹
23	1	99	27.9	24.5
24	2	98	14.0	14.9
25	3	97	9.29	9.40
26	5	95	5.58	6.45
*	-	-	0	1.44

* value obtained from data of TABLE (2.3)

The catalytic coefficients $k_{\text{HOAc}}^{\text{D}}$ and $k_{\text{H}_3\text{O}^+}^{\text{D}}$, for acetic acid and H₃O⁺ catalysis respectively, were obtained by an exactly analogous procedure to that used for the proto-detrutiation reaction, and the results obtained are as follows:

$$k_{\text{HOAc}}^{\text{D}} = 0.144 \pm 0.010 \text{ l.mole}^{-1} \text{ sec.}^{-1}$$

$$k_{\text{H}_3\text{O}^+}^{\text{D}} = 83.1 \pm 4.0 \text{ l.mole}^{-1} \text{ sec.}^{-1}$$

As for proto-detrutiation, satisfactory agreement was obtained between the calculated (from data of TABLE (2.4)) and extrapolated (from data of TABLE (2.3)) values of $k_{\text{H}_3\text{O}^+}^{\text{D}}$.

The rate equation for the reaction has the same kinetic form as that for proto-detrutiation and insertion of the appropriate rate coefficient leads to equation (2.4)

$$v = 83.1 [\text{H}_3\text{O}^+][\text{Indole}] + 0.144 [\text{HOAc}][\text{Indole}] \dots\dots\dots (2.4)$$

c) Deuterio-detrition in aqueous (D_2O) acetic acid buffer solutions.

The replacement of tritium in 2-methyl-3- $[^3H]$ indole by deuterium, was studied in two sets of acetic acid - sodium acetate buffer solutions in D_2O . The atom fraction of deuterium (n_D) in these solutions was at least 99%. These results are given in TABLES (2.5) and (2.6).

TABLE (2.5)

Deuterio-detrition of 2-methyl-3- $[^3H]$ indole in acetic acid buffers in D_2O .

Buffer ratio = 1:10.		$[D_3O^+]^* = 8.53 \times 10^{-7} M.$		$\mu = 0.1$
Kinetic	$[DOAc]$	$[OAc^-]$	$[NaCl]$	$10^4 \bar{k}_{obs}^T$
Run	$.10^3 M$	$.10^3 M$	$.10^3 M$	sec. $^{-1}$
44	10	100	-	4.86
45	7	70	30	3.42
46	4	40	60	2.15
47	1	10	90	0.89

* Values of $[D_3O^+]$ were calculated from the acid dissociation constant of DOAc in D_2O . The difference in pK_A on a molarity scale between HOAc in H_2O , and DOAc in D_2O has recently been set at 0.5145^(37,38)

Since a value of pK_A equal to 4.554 for HOAc in H_2O has been used for the experiments in aqueous solution at ionic strength of 0.1 (see page 20), the corresponding value for DOAc in D_2O can be calculated from:

$$pK_A (DOAc) = pK_A (HOAc) + 0.5145 = 5.069$$

TABLE (2.6)

Deuterio-detrification of 2-methyl-3-[³H]indole in acetic acid buffers in D₂O.

[DOAc] = 0.01M, throughout.		μ = 0.1		
Kinetic	[OAc ⁻]	[NaCl]	[D ₃ O ⁺]	10 ⁴ \bar{k}_{obs}^T
Run	.10 ² M	.10 ² M	.10 ⁷ M	sec. ⁻¹
91	1	9	85.3	10.6
90	2	8	42.6	7.65
89	5	5	17.1	5.70
44	10	-	8.53	4.86
*	-	-	0	4.39

* Value obtained from data of TABLE (2.5)

Analysis of the results in the manner described before, leads to the following values of the second-order rate coefficients for catalysis by DOAc and D₃O⁺, in the medium D₂O:-

(A bar over the coefficient indicates that the value refers to a deuteriated medium.)

$$\bar{k}_{DOAc}^T = 0.044 \pm 0.002 \text{ l.mole}^{-1} \text{ sec.}^{-1}$$

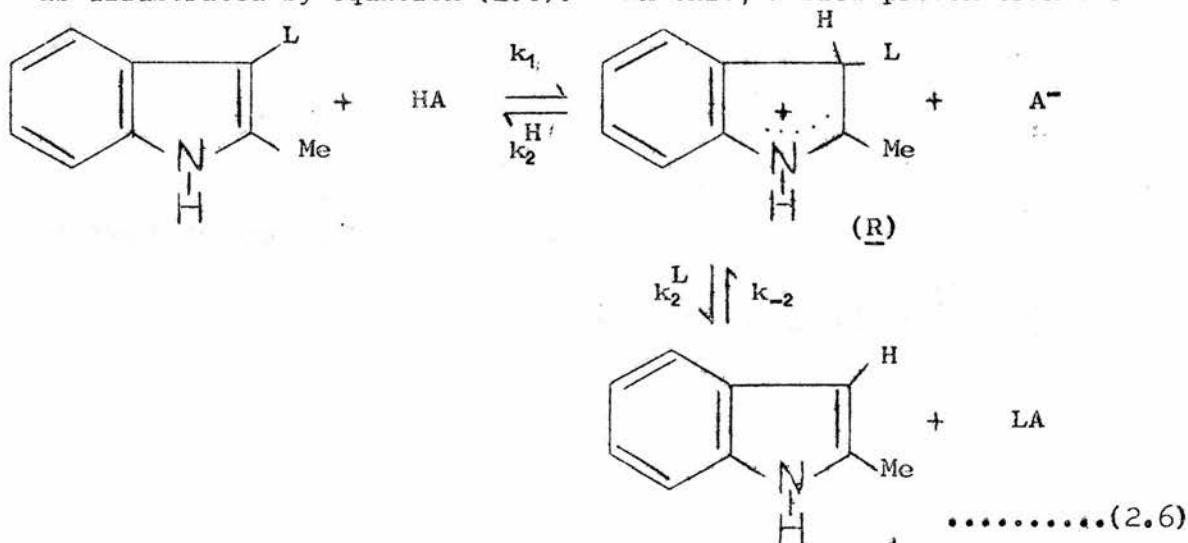
$$\bar{k}_{D_3O^+}^T = 73.7 \pm 5.0 \text{ l.mole}^{-1} \text{ sec.}^{-1}$$

The general acid catalysed reaction in deuterium oxide (neglecting catalysis by both OAc⁻ and D₂O) can thus be represented by equation (2.5).

$$v = 73.7[D_3O^+][\text{Indole}] + 0.044 [\text{DOAc}][\text{Indole}] \dots\dots(2.5).$$

Discussion

The previously reported general acid catalysis for the hydrogen exchange reactions of 2-methylindole, together with Hinman and Whipple's^(31b) conclusion that equilibrium protonation occurs at the 3-position are indicative of an "orthodox" A-S_E2 exchange mechanism, as illustrated by equation (2.6). In this, a slow proton transfer



to the substrate from the general acid HA (k_1) to form the relatively stable conjugate acid (\underline{R}), is followed by slow loss of isotopic hydrogen (where L = D or T) from \underline{R} (k_2^L) to give the product. Since the concentration of LA is always less than 0.1% of that of HA, the reverse of the second step (k_{-2}) may be neglected. The relationship between the observed rate coefficients and those for the individual steps of equation (2.6) can be derived in the usual way⁽³⁹⁾ by assuming that the concentration of the intermediate (\underline{R}) is not a function of time, i.e. steady state conditions prevail. Thus

$$\begin{aligned}
 v &= k_{\text{obs}} [\text{HA}] [2\text{-Me-3-[L]indole}] \\
 &= \frac{k_1 k_2^L}{k_2^H + k_2^L} [\text{HA}] [2\text{-Me-3-[L]indole}]
 \end{aligned}$$

This predicts general acid catalysis, as is observed experimentally.

Although the rate coefficients for the individual steps cannot be determined from k_{obs} directly, the kinetic isotope effects for each step can be obtained in the way described by Kresge and Chiang.⁽⁴⁰⁾

For H_3O^+ (and D_3O^+ , where appropriate) catalysis:

$$(k_{\text{obs}})_I = \frac{k_1 \text{H}_3\text{O}^+}{1 + (k_2^{\text{H}}/k_2^{\text{D}}) 1.442}$$

for proto-detritiation in H_2O .

$$(k_{\text{obs}})_{II} = \frac{k_1 \text{H}_3\text{O}^+}{1 + k_2^{\text{H}}/k_2^{\text{D}}}$$

for proto-dedeuteriation in H_2O

$$(k_{\text{obs}})_{III} = \frac{k_1 \text{D}_3\text{O}^+}{1 + (k_2^{\text{H}}/k_2^{\text{D}}) 0.442}$$

for deuterio-detritiation in D_2O

Thus, $\frac{k_2^{\text{H}}}{k_2^{\text{D}}}$ and $\frac{k_1 \text{H}_3\text{O}^+}{k_1 \text{D}_3\text{O}^+}$ can be obtained by simultaneous solution

of these three equations. In a similar way, counterparts for the kinetic isotope effects associated with the acetic acid catalysed exchange reaction can be deduced. Application of this analysis to the experimental constants obtained for 2-methylindole leads to the following values for the kinetic isotope effects.

For H_3O^+

$$\frac{k_2^{\text{H}}}{k_2^{\text{D}}} = 6.7 \pm 0.9$$

$$\frac{k_1 \text{H}_3\text{O}^+}{k_1 \text{D}_3\text{O}^+} = 2.56 \pm 0.5$$

For HOAc

$$\frac{k_2^H}{k_2^D} = 6.3 \pm 1.0$$

$$\frac{k_1^{HOAc}}{k_1^{DOAc}} = 7.3 \pm 1.4$$

Discussion of these kinetic isotope effect values is deferred until later.

Indole

The rates of hydrogen exchange for both 3-[²H]indole and 3-[³H]indole were determined in aqueous HCl, and in aqueous acetic acid and aqueous pyridine, buffer solutions. As for 2-methylindole, the reaction was subject to general acid catalysis and the same A-S_E2 exchange process appears to be operative.

Aqueous hydrochloric acid solutions.

Indole ($pK_A = -3.5^{(31c)}$) is a much less basic (and therefore less reactive) substrate than 2-methylindole ($pK_A = -0.28^{(31c)}$). It was therefore possible to determine the rate of H_3O^+ -catalysed exchange directly in dilute aqueous HCl, with the ionic strength maintained at a constant 0.1 with the addition of NaCl. The experimental rate coefficients (k_{obs}) for proto-deuteriation are listed in TABLE (2.7).

TABLE (2.7)

Proto-dedeuteration of 3[²H]indole in aqueous HCl

[HCl] = 10 ⁻³ M.		[NaCl] = 0.1M.
Kinetic	10 ⁴ k _{obs}	k _{H₂O⁺} ^D
Run	sec. ⁻¹	ℓ.mole ⁻¹ sec. ⁻¹
192	9.8	0.98
193	9.7	0.97
256	9.7	0.97

$$\therefore k_{\text{H}_2\text{O}^+}^{\text{D}} = 0.97 \text{ l.mole}^{-1} \text{ sec.}^{-1}$$

Also $k_{\text{H}_2\text{O}^+}^T = 0.50 \text{ l.mole}^{-1} \text{ sec.}^{-1}$

was obtained from the rate of proto-detrition of $3[^3\text{H}]\text{indole}$ in $4.81 \times 10^{-3}\text{M}$ HCl ($\mu = 0.1$).

Acetic acid buffer solutions.

Two independent sets of acetic acid buffer solutions were used to determine the rates of the acetic acid catalysed proto-detrutiation and proto-dedeuteriation of 3[³H]indole and 3[²H]indole respectively. These results are listed in TABLES (2.8) → (2.11), and least squares values of the slope (equivalent to k_{HOAc}^T) and the intercept (equivalent to $k_{\text{H}_3\text{O}^+} + [\text{H}_3\text{O}^+]$) for the plot of k_{obs} against [HOAc] are also given at the foot of the corresponding table.

TABLE (2.8)

Proto-detrutiation of 3[³H]indole in acetic acid buffers

Buffer ratio = 1:1		$[\text{H}_3\text{O}^+] = 2.79 \times 10^{-5} \text{ M.}$		$\mu = 0.1.$
Kinetic	[HOAc]	[OAc ⁻]	[NaCl]	$10^5 k_{\text{obs}}$
Run	.10 ² M.	.10 ² M.	.10 ² M.	sec. ⁻¹
163	10	10	-	5.72
184	10	10	-	5.73
164	7.5	7.5	2.5	4.66
166	5	5	5	3.56
185	5	5	5	3.63
167	2.5	2.5	7.5	2.50
168	1	1	9	1.79
186	1	1	9	1.82

$$k_{\text{HOAc}}^T = 4.33 \times 10^{-4} \text{ l.mole}^{-1} \text{ sec.}^{-1}$$

$$[\text{H}_3\text{O}^+] \times k_{\text{H}_3\text{O}^+}^T = 1.40 \times 10^{-5} \text{ sec.}^{-1}$$

TABLE (2.9)

Proto-detrition of 3[³H]indole in acetic acid buffers.

Buffer ratio = 1:3. $[H_3O^+] = 9.3 \times 10^{-6} M.$ $\mu = 0.1.$

Kinetic	[HOAc]	[OAc ⁻]	[NaCl]	$10^6 k_{obs}$
Run	.10 ³ M.	.10 ³ M.	.10 ³ M.	sec. ⁻¹
165	33.33	100	-	19.4
169	25	75	25	15.5
170	16.67	50	50	11.9
171	8.33	25	75	8.4
172	3.33	10	90	6.1

$$k_{HOAc}^T = 4.35 \times 10^{-4} \text{ l.mole}^{-1} \text{ sec.}^{-1}$$

$$k_{H_3O^+}^T [H_3O^+] = 4.70 \times 10^{-6} \text{ sec.}^{-1}$$

TABLE (2.10)

Proto-dedeuteriation of 3[²H]indole in acetic acid buffers.

Buffer ratio = 1:1. $[H_3O^+] = 2.79 \times 10^{-5} M.$ $\mu = 0.1.$

Kinetic	[HOAc]	[OAc ⁻]	[NaCl]	$10^5 k_{obs}$
Run	.10 ² M.	.10 ² M.	.10 ² M.	sec. ⁻¹
194	10	10	-	10.9
199	10	10	-	11.5
176	7.5	7.5	2.5	9.05
177	5	5	5	7.10
195	5	5	5	7.00
174	2.5	2.5	7.5	5.00
175	1	1	9	3.62
*	0	-	-	2.71

* value calculated from $k_{H_3O^+}^D [H_3O^+]$

$$k_{HOAc}^D = 8.39 \times 10^{-4} \text{ l.mole}^{-1} \text{ sec.}^{-1}$$

$$k_{H_3O^+}^D [H_3O^+] = 2.80 \times 10^{-5} \text{ sec.}^{-1}$$

TABLE (2.11)

Proto-dedeuteriation of 3^[2H]indole in acetic acid buffers

Buffer ratio = 1:3 $[H_3O^+] = 9.3 \times 10^{-6} M.$ $\mu = 0.1.$

Kinetic	[HOAc]	[OAc ⁻]	[NaCl]	$10^5 k_{obs}$
Run	$\cdot 10^3 M.$	$\cdot 10^3 M.$	$\cdot 10^3 M.$	sec. ⁻¹
196	33.33	100	-	3.60
197	25	75	25	3.10
178	16.67	50	50	2.40
179	8.33	25	75	1.64
198	3.33	10	90	1.22
*	0	-	-	0.91

* value calculated from $k_{H_3O^+}^D [H_3O^+]$

$$k_{HOAc}^D = 8.22 \times 10^{-4} \text{ l.mole}^{-1} \text{ sec.}^{-1}$$

$$k_{H_3O^+}^D [H_3O^+] = 0.96 \times 10^{-5} \text{ sec.}^{-1}$$

Two features of the results in TABLES (2.8) → (2.11) are of commentable interest. Firstly, the two values of both $k_{\text{HOAc}}^{\text{T}}$ and $k_{\text{HOAc}}^{\text{D}}$ obtained from the two sets of buffers are closely similar; this suggests that any catalysis by acetate ion under these conditions is negligibly small. The average values of the respective rate coefficients are therefore

$$k_{\text{HOAc}}^{\text{T}} = 4.34 (\pm 0.01) \times 10^{-4} \text{ l.mole}^{-1} \text{ sec.}^{-1}$$

$$k_{\text{HOAc}}^{\text{D}} = 8.31 (\pm 0.23) \times 10^{-4} \text{ l.mole}^{-1} \text{ sec.}^{-1}$$

These values are used in subsequent calculations of the kinetic isotope effects. Secondly, the conclusions above are further supported by the general concordancy between the values of $k_{\text{H}_3\text{O}^+}^{\text{T}}$ and $k_{\text{H}_3\text{O}^+}^{\text{D}}$ obtained by extrapolation of the results for acetic acid buffers to zero acetic acid concentration, and those obtained directly by measurements in dilute hydrochloric acid. Furthermore, this agreement suggests that catalysis by water must be negligibly small.

Aqueous pyridine-pyridine hydrochloride buffer solutions.

The exchange reactions of both tritio- and deuterio-indole were also studied in three sets of pyridine-pyridine hydrochloride buffer solutions of differing buffer ratio. The values of k_{obs} together with the buffer concentrations are listed in TABLES (2.12) → (2.17). For each set of data, the slope of the best straight line for k_{obs} versus $[\text{PyH}^+]$ calculated by least squares analysis is given at the foot of the table.

TABLE (2.12)

Proto-detrutiation of 3[³H]indole in pyridine buffers

Buffer ratio* = 6:1		$\mu = 0.1$		
Kinetic	[Py]	[PyH ⁺]	[NaCl]	$10^6 k_{\text{obs}}$
Run	.10 ² M.	.10 ² M.	.10 ² M.	sec. ⁻¹
243	60	10	-	14.6
242	42	7	3	10.4
241	24	4	6	6.42
240	6	1	9	1.82

* Buffer ratio for pyridine solutions, refers (in TABLES (2.12) → (2.17)) to the ratio [Py]:[PyH⁺].

$$\text{Slope} = 14.1 \times 10^{-5} \text{ l.mole}^{-1} \text{ sec.}^{-1}$$

TABLE (2.13)

Proto-detrutiation of 3[³H]indole in pyridine buffers

Buffer ratio = 3:1		$\mu = 0.1.$		
Kinetic	[Py]	[PyH ⁺]	[NaCl]	$10^6 k_{\text{obs}}$
Run	.10 ² M.	.10 ² M.	.10 ² M.	sec. ⁻¹
247	30	10	-	13.5
246	21	7	3	9.71
245	12	4	6	6.45
244	3	1	9	2.21

$$\text{Slope} = 12.2 \times 10^{-5} \text{ l.mole}^{-1} \text{ sec.}^{-1}$$

TABLE (2.14)

Proto-detrition of 3[³H]indole in pyridine buffers

Buffer ratio = 1:2		$\mu = 0.1$		
Kinetic	[Py]	[PyH ⁺]	[NaCl]	10 ⁶ k _{obs}
Run	.10 ² M.	.10 ² M.	.10 ² M.	sec. ⁻¹
255	5	10	-	16.2
254	3.75	7.5	2.5	13.7
253	2.5	5	5	11.1
252	1.5	3	7	9.06
251	0.5	1	9	6.54

$$\text{Slope} = 10.3 \times 10^{-5} \text{ l.mole}^{-1} \text{ sec.}^{-1}$$

TABLE (2.15)

Proto-dedeuteration of 3[²H]indole in pyridine buffers

Buffer ratio = 6:1		$\mu = 0.1.$		
Kinetic	[Py]	[PyH ⁺]	[NaCl]	10 ⁶ k _{obs}
Run	.10 ² M.	.10 ² M.	.10 ² M.	sec. ⁻¹
261	60	10	-	28.2
260	42	7	3	19.7
259	24	4	6	11.0
258	15	2.5	7.5	6.86
257	6	1	9	3.35

$$\text{Slope} = 27.8 \times 10^{-5} \text{ l.mole}^{-1} \text{ sec.}^{-1}$$

TABLE (2.16)

Proto-dedeuteriation of 3[²H]indole in pyridine buffers

Buffer ratio = 3:1		$\mu = 0.1$		
Kinetic	[Py]	[PyH ⁺]	[NaCl]	$10^6 k_{\text{obs}}$
Run	.10 ² M.	.10 ² M.	.10 ² M.	sec. ⁻¹
272	30	10	-	25.3
273	24	8	2	19.8
274	18	6	4	15.3
275	12	4	6	10.7
276	3	1	9	3.90

$$\text{Slope} = 23.5 \times 10^{-5} \text{ l.mole}^{-1} \text{ sec.}^{-1}$$

TABLE (2.17)

Proto-dedeuteriation of 3[²H]indole in pyridine buffers

Buffer ratio = 1:2		$\mu = 0.1$		
Kinetic	[Py]	[PyH ⁺]	[NaCl]	$10^6 k_{\text{obs}}$
Run	.10 ² M.	.10 ² M.	.10 ² M.	sec. ⁻¹
266	5	10	-	29.5
265	3.75	7.5	2.5	25.9
264	2.5	5	5	22.0
263	1.5	3	7	17.5
262	0.5	1	9	13.3

$$\text{Slope} = 18.1 \times 10^{-5} \text{ l.mole}^{-1} \text{ sec.}^{-1}$$

Unlike acetic acid catalysis, the changes in buffer ratio produce different ~~by~~ slopes, as is apparent from FIGURE (2.2), when k_{obs} (equation (2.1)) is plotted against the concentration of protonated pyridine, $[PyH^+]$. This indicates that catalysis by more than one buffer component (probably both PyH^+ and Pyridine, itself) contributes to the overall rate equation. The contribution (and therefore the specific rate coefficient) for each catalyst may be easily evaluated from the experimental results by solution of the appropriate sets of simultaneous equations. For proto-detrutiation, these equations are:-

$$k_{PyH^+}^T + 6k_{Py}^T = 14.1 \times 10^{-5} \text{ l.mole}^{-1} \text{ sec.}^{-1}$$

(line B, FIGURE (2.2))

$$k_{PyH^+}^T + 3k_{Py}^T = 12.2 \times 10^{-5} \text{ l.mole}^{-1} \text{ sec.}^{-1}$$

(line C, FIGURE (2.2))

$$k_{PyH^+}^T + 0.5k_{Py}^T = 10.3 \times 10^{-5} \text{ l.mole}^{-1} \text{ sec.}^{-1}$$

(line A, FIGURE (2.2))

From which one obtains as the best solution

$$k_{PyH^+}^T = 10.1 (\pm 0.2) \times 10^{-5} \text{ l.mole}^{-1} \text{ sec.}^{-1}$$

$$k_{Py}^T = 6.9 (\pm 0.5) \times 10^{-6} \text{ l.mole}^{-1} \text{ sec.}^{-1}$$

The corresponding equations for proto-dedeuteriation are:-

$$k_{PyH^+}^D + 6k_{Py}^D = 27.8 \times 10^{-5} \text{ l.mole}^{-1} \text{ sec.}^{-1}$$

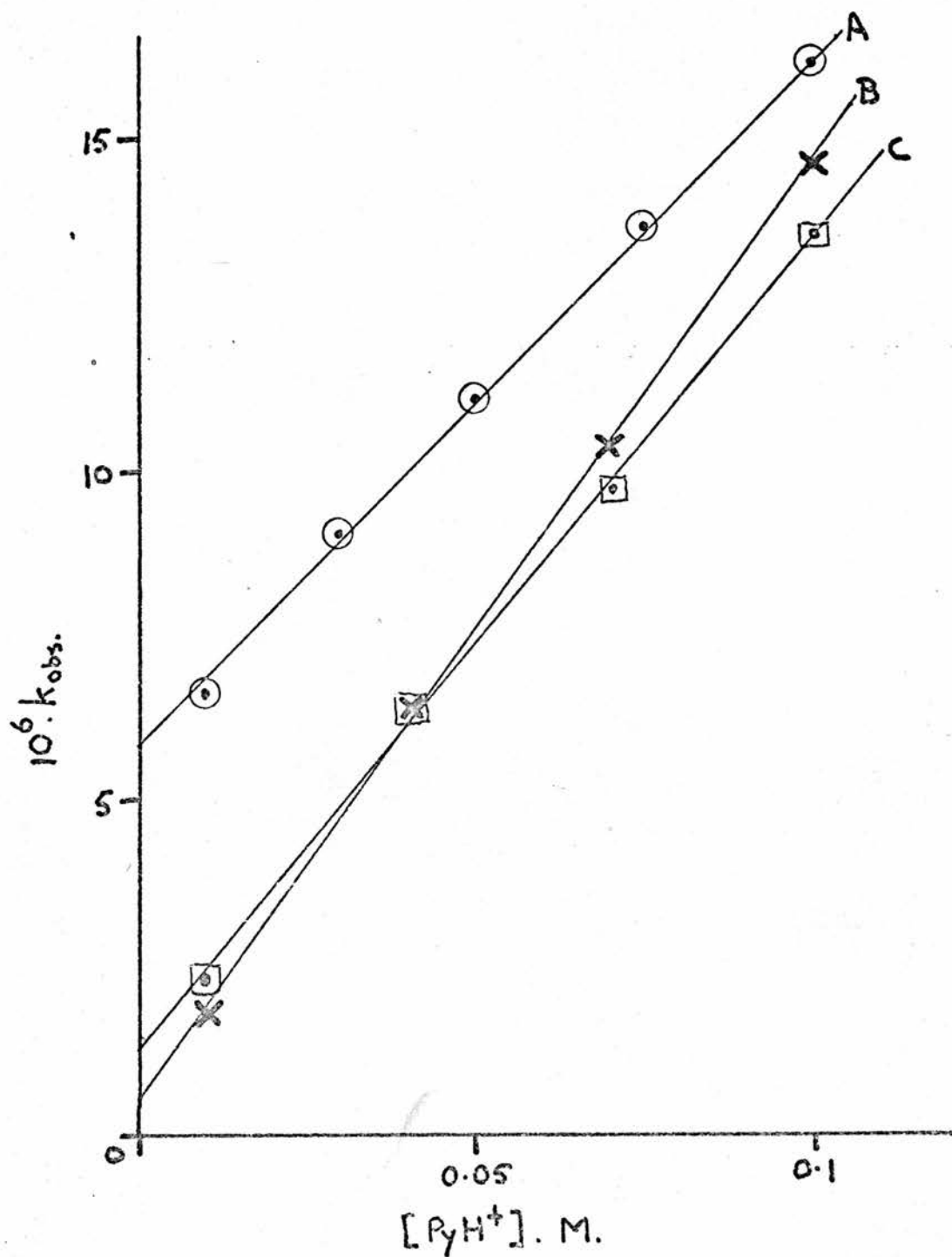
$$k_{PyH^+}^D + 3k_{Py}^D = 23.5 \times 10^{-5} \text{ l.mole}^{-1} \text{ sec.}^{-1}$$

$$k_{PyH^+}^D + 0.5k_{Py}^D = 18.1 \times 10^{-5} \text{ l.mole}^{-1} \text{ sec.}^{-1}$$

Figure (2.2)

Detritiation of 3- ^{3}H indole in pyridine buffers.

Variation of k_{obs} with $[\text{PyH}^+]$.



And the best solution leads to values of:-

$$k_{\text{PyH}^+}^{\text{D}} = 17.8 (\pm 1.0) \times 10^{-5} \text{ l.mole}^{-1} \text{ sec.}^{-1}$$

$$k_{\text{Py}}^{\text{D}} = 17.9 (\pm 2.6) \times 10^{-6} \text{ l.mole}^{-1} \text{ sec.}^{-1}$$

Consideration of additional catalytic terms such as $k[\text{PyH}^+][\text{Py}]$, where k is the catalytic coefficient for simultaneous catalysis by pyridine and its conjugate acid, does not lead to a satisfactory solution of the simultaneous equations. Also, the intercepts of the k_{obs} versus $[\text{PyH}^+]$ plots, are in good agreement with values calculated from the previously determined catalytic coefficients for the hydronium ion, in conjunction with a value of 5.18 for the pK_A of pyridine hydrochloride in 0.1 M salt solution.⁽⁴¹⁾ Calculation of a possible contribution to the overall rate by hydroxide ion catalysis, $k_{\text{OH}}^- [\text{OH}^-]$ (where k_{OH}^- is equal to about $10^{-5} \text{ l.mole}^{-1} \text{ sec.}^{-1}$, page 103), shows this to be negligible at the pH of the pyridine buffer solutions. Catalysis by water can also be ruled out on the basis of the intercept values, both here and for the measurements in acetic acid buffers. It therefore seems that only pyridine, its conjugate acid and H_3O^+ , are effective catalysts under the conditions of these experiments, and each contributes an independent term to the overall reaction rate. Thus the kinetic analysis of the slopes (k_{obs} versus $[\text{PyH}^+]$) in terms of $k_{\text{PyH}^+} [\text{PyH}^+]$ and $k_{\text{Py}} [\text{PyH}^+]$ only, is valid.

Summary and Calculation of Kinetic Isotope Effects.

The various rate coefficients for the proto-detritiation and proto-dedeuteriation of labelled indole by the various catalysts are

summarised below.

$$\begin{aligned} \text{H}_3\text{O}^+ : \quad k^{\text{T}} &= 0.50 \text{ l.mole}^{-1} \text{ sec.}^{-1} \\ k^{\text{D}} &= 0.97 \text{ l.mole}^{-1} \text{ sec.}^{-1} \end{aligned}$$

$$\begin{aligned} \text{HOAc} : \quad k^{\text{T}} &= 4.34 \times 10^{-4} \text{ l.mole}^{-1} \text{ sec.}^{-1} \\ k^{\text{D}} &= 8.31 \times 10^{-4} \text{ l.mole}^{-1} \text{ sec.}^{-1} \end{aligned}$$

$$\begin{aligned} \text{PyH}^+ : \quad k^{\text{T}} &= 10.1 \times 10^{-5} \text{ l.mole}^{-1} \text{ sec.}^{-1} \\ k^{\text{D}} &= 17.8 \times 10^{-5} \text{ l.mole}^{-1} \text{ sec.}^{-1} \end{aligned}$$

$$\begin{aligned} \text{Py} : \quad k^{\text{T}} &= 6.9 \times 10^{-6} \text{ l.mole}^{-1} \text{ sec.}^{-1} \\ k^{\text{D}} &= 17.9 \times 10^{-6} \text{ l.mole}^{-1} \text{ sec.}^{-1} \end{aligned}$$

Following the procedure outlined previously for 2-methylindole (page 28) the kinetic isotope effects for loss of a lyonium ion from the intermediate ($k_2^{\text{H}}/k_2^{\text{D}}$) can be calculated from the experimental results. The following values are obtained.

$$\text{For } \underline{\text{H}_3\text{O}^+} \quad k_2^{\text{H}}/k_2^{\text{D}} = 5.6 \pm 0.3$$

$$\text{For } \underline{\text{HOAc}} \quad k_2^{\text{H}}/k_2^{\text{D}} = 5.3 \pm 0.4$$

$$\text{For } \underline{\text{PyH}^+} \quad k_2^{\text{H}}/k_2^{\text{D}} = 4.5 \pm 0.8$$

The result for catalysis by pyridine itself is discussed in Chapter III. The further discussion of the other (acid-catalysed reaction) results is deferred until later.

5-methoxyindole

This compound is too reactive ($pK_A = -2.9$) for isotopic hydrogen exchange to be studied easily in dilute HCl, thus the catalysis by both H_3O^+ and HOAc was measured in two sets of acetic acid buffer solutions with buffer ratios ($[acid]:[salt]$) of 1:1 and 5:1. The results are contained in TABLES (2.18) - (2.21), and as for the previous compounds the optimum least squares value of the slopes (k_{HOAc}^L) and intercepts ($\equiv k_{H_3O^+}^L + [H_3O^+]$) of plots of k_{obs} (equation (2.1)) versus $[HOAc]$, are listed at the foot of each table.

TABLE (2.18)

Proto-detrition of 5-methoxy-3 3 H indole in acetic acid buffers

Buffer ratio = 1:1		$[H_3O^+] = 2.79 \times 10^{-5} M.$		$\mu = 0.1.$
Kinetic	$[HOAc]$	$[OAc^-]$	$[NaCl]$	$10^5 k_{obs}$
Run	.10 ² M.	.10 ² M.	.10 ² M.	sec. ⁻¹
217	10	10	-	15.4
218	7.5	7.5	2.5	12.5
214	5	5	5	9.25
215	2.5	2.5	7.5	6.35
216	1	1	9	4.25

$$k_{HOAc}^T = 1.21 \times 10^{-3} \text{ l.mole}^{-1} \text{ sec.}^{-1}$$

$$k_{H_3O^+} [H_3O^+] = 3.3 \times 10^{-5} \text{ sec.}^{-1}$$

TABLE (2.19)

Proto-detritiation of 5-methoxy-3[³H]indole in acetic acid buffers

Buffer ratio = 5:1		$[H_3O^+] = 1.40 \times 10^{-4} M.$		$\mu = 0.1.$
Kinetic	$[HOAc]$	$[OAc^-]$	$[NaCl]$	$10^4 k_{obs}$
Run	$.10^2 M.$	$.10^2 M.$	$.10^2 M.$	$sec.^{-1}$
213	50	10	-	7.62
211	40	8	2	6.45
212	30	6	4	5.02
209	15	3	7	3.40
210	5	1	9	2.14

$$k_{HOAc}^T = 1.22 \times 10^{-3} \text{ l.mole}^{-1} \text{ sec.}^{-1}$$

$$k_{H_3O^+} [H_3O^+] = 1.53 \times 10^{-4} \text{ sec.}^{-1}$$

The concordancy between the two values of k_{HOAc}^T shows that catalysis by acetate anion is negligible and confirms that the slope represents only acetic acid catalysis,

i.e. $k_{HOAc}^T = 1.22 (\pm 0.01) \times 10^{-3} \text{ l.mole}^{-1} \text{ sec.}^{-1}$

The agreement of the $k_{H_3O^+}^T$ values calculated from the two intercepts ($k_{H_3O^+}^T = 1.18 \text{ l.mole}^{-1} \text{ sec.}^{-1}$ from TABLE (2.18), $k_{H_3O^+}^T = 1.09 \text{ l.mole}^{-1} \text{ sec.}^{-1}$ from TABLE (2.19)) is evidence that, as in the previous cases, catalysis by water is negligible. Thus the full kinetic equation for tritium exchange in acetic acid - sodium acetate buffers can be represented by equation (2.7) below

$$k_{obs}^T = 1.14[H_3O^+] + 1.22 \times 10^{-3} [HOAc] \quad \dots\dots\dots (2.7)$$

where the average value of $k_{H_3O^+}^T = 1.14 \pm 0.04 \text{ l.mole}^{-1} \text{ sec.}^{-1}$

The corresponding rate equation for the parallel proto-dedeuteriation reaction may be derived in an analogous manner from the data in TABLES (2.20) and (2.21).

TABLE (2.20)

Proto-dedeuteriation of 5-methoxy-3[²H]indole in acetic acid buffers

Buffer ratio = 1:1 [H ₃ O ⁺] = 2.79 x 10 ⁻⁵ M. μ = 0.1				
Kinetic	[HOAc]	[OAc ⁻]	[NaCl]	10 ⁵ k _{obs}
Run	.10 ² M.	.10 ² M.	.10 ² M.	sec. ⁻¹
229	10	10	-	32.8
225	7.5	7.5	2.5	25.4
228	5	5	5	19.1
226	2.5	2.5	7.5	12.4
227	1	1	9	8.20

$$k_{\text{HOAc}}^{\text{D}} = 2.57 \times 10^{-3} \text{ l.mole}^{-1} \text{ sec.}^{-1}$$

$$k_{\text{H}_3\text{O}^+}^{\text{D}} [\text{H}_3\text{O}^+] = 6.0 \times 10^{-5} \text{ sec.}^{-1}$$

$$\therefore k_{\text{H}_3\text{O}^+}^{\text{D}} = 2.15 \text{ l.mole}^{-1} \text{ sec.}^{-1}$$

TABLE (2.21)

Proto-dedeuteriation of 5-methoxy-3-[²H]indole in acetic acid buffers

Buffer ratio = 5:1 $[H_3O^+] = 1.40 \times 10^{-4} M.$ $\mu = 0.1$

Kinetic	[HOAc]	[OAc ⁻]	[NaCl]	$10^4 k_{obs}$
Run	.10 ² M.	.10 ² M.	.10 ² M.	sec. ⁻¹
221	50	10	-	15.7
222	40	8	2	13.1
220	30	6	4	10.5
219	15	3	7	7.55
223	5	1	9	4.78

$$k_{HOAc}^D = 2.45 \times 10^{-3} \text{ l.mole}^{-1} \text{ sec.}^{-1}$$

$$k_{H_3O^+}^D [H_3O^+] = 3.50 \times 10^{-4} \text{ sec.}^{-1}$$

$$\therefore k_{H_3O^+}^D = 2.50 \text{ l.mole}^{-1} \text{ sec.}^{-1}$$

Thus the average values of the rate coefficients for proto-dedeuteriation (including errors in the slope measurements) are:

$$k_{HOAc}^D = 2.51 (\pm 0.12) \times 10^{-3} \text{ l.mole}^{-1} \text{ sec.}^{-1}$$

$$k_{H_3O^+}^D = 2.33 (\pm 0.17) \text{ l.mole}^{-1} \text{ sec.}^{-1}$$

The proto-dedeuteriation in acetic acid - sodium acetate buffer solutions can therefore be expressed by equation (2.8):

$$k_{obs}^D = 2.33[H_3O^+] + 2.51 \times 10^{-3} [HOAc] \quad \dots\dots\dots (2.8)$$

The kinetic isotope effects (k_2^H/k_2^D) for both acetic acid and hydronium ion catalysis are obtained as usual from equations (2.7) and (2.8):

$$\text{For } \underline{\text{H}_3\text{O}^+} \quad k_2^H/k_2^D = 6.0 \pm 1.2$$

$$\text{For } \underline{\text{HOAc}} \quad k_2^H/k_2^D = 6.2 \pm 0.6$$

The discussion of these results, too, is deferred until later.

5-cyanoindole

The rate of isotopic hydrogen exchange on 5-cyanoindole was determined for catalysis by the hydronium ion in dilute hydrochloric acid, and for acetic acid by the reaction in buffer solutions. The results for the former reaction are collected in TABLES (2.22) and (2.23).

TABLE (2.22)

Proto-detritiation of 5-cyano-3[³H]indole in dilute HCl

$\mu = 0.1$

Kinetic	[HCl]	[NaCl]	$10^5 k_{\text{obs}}$	$10^3 \frac{k_{\text{obs}}}{[\text{HCl}]}$
Run	$\cdot 10^2 \text{ M.}$	$\cdot 10^2 \text{ M.}$	sec.^{-1}	$\ell.\text{mole}^{-1} \text{ sec.}^{-1}$
187	10	-	51.5	5.15
190	10	-	53.2	5.32
188	5	5	26.3	5.26
189	5	5	26.4	5.28
191	1	9	5.32	5.32

Average $k_{\text{H}_2\text{O}^+}^{\text{T}} = 5.27 (\pm 0.05) \times 10^{-3} \ell.\text{mole}^{-1} \text{ sec.}^{-1}$

-49-
TABLE (2.23)

Proto-dedeuteration of 5-cyano-3-[²H]indole in dilute HCl.

$\mu = 0.1$

Kinetic	[HCl]	[NaCl]	$10^5 k_{\text{obs}}$	$10^3 \frac{k_{\text{obs}}}{[\text{HCl}]}$
Run	.10 ² M.	.10 ² M.	sec. ⁻¹	l.mole ⁻¹ sec. ⁻¹
203	10	-	93.5	9.35
202	5	5	48.4	9.68
201	1	9	10.8	10.8
200	1	9	9.5	9.50

Average $k_{\text{H}_3\text{O}^+}^{\text{D}} = 9.81 (\pm 0.47) \times 10^{-3} \text{ l.mole}^{-1} \text{ sec.}^{-1}$

Acetic acid catalysis

The proto-detrutiation of 5-cyano-3-[³H]indole was studied mainly in buffer solutions with the ratio [HOAc] : [OAc⁻] set at 5:1. Supplementary measurements were also made in solutions with [HOAc] : [OAc⁻] of 2:1, to check the extent of acetate ion catalysis. These results are listed in TABLES (2.24) and (2.25). As for the other substrates, the slope of k_{obs} versus [HOAc] was estimated by least squares analysis; the value of this is listed at the bottom of the TABLES.

TABLE (2.24)

Proto-detrition of 5-cyano-3[³H]indole in acetic acid buffers

Buffer ratio = 5:1 $[H_3O^+] = 1.40 \times 10^{-4} M.$ $\mu = 0.1$

Kinetic	[HOAc]	[OAc ⁻]	[NaCl]	$10^7 k_{obs}$
Run	$\cdot 10^2 M.$	$\cdot 10^2 M.$	$\cdot 10^2 M.$	sec. ⁻¹
204	50	10	-	27.6
205	40	8	2	23.8
206	30	6	4	19.9
207	15	3	7	13.5
208	5	1	9	9.7

$$\text{Slope} = 4.04 \times 10^{-6} \text{ l.mole}^{-1} \text{ sec.}^{-1}$$

TABLE (2.25)

Proto-detrition of 5-cyano-3[³H]indole in acetic acid buffers

Buffer ratio = 2:1 $[H_3O^+] = 5.60 \times 10^{-5} M.$ $\mu = 0.1$

Kinetic	[HOAc]	[OAc ⁻]	[NaCl]	$10^7 k_{obs}$
Run	$\cdot 10^2 M.$	$\cdot 10^2 M.$	$\cdot 10^2 M.$	sec. ⁻¹
248	20	10	-	11.6
249	16	8	2	9.90
250	12	6	4	7.80
*	0	-	-	2.95

* calculated from $k_{H_3O^+}^T [H_3O^+]$

$$\text{Slope} = 4.30 \times 10^{-6} \text{ l.mole}^{-1} \text{ sec.}^{-1}$$

The difference in slopes (6%) for the two series of measurements (TABLES (2.24) and (2.25)) is somewhat larger than the estimated error ($\pm 2\%$) in the determination of each slope. This may indicate that a small fraction of the reaction, under these conditions, is proceeding by a base-catalysed pathway involving the acetate anion. However, the second-order rate coefficients for reaction catalysed by both acetic acid and acetate anion can be evaluated directly from the two slope measurements, via solution of the relevant simultaneous equations below:

$$k_{\text{HOAc}}^T + 0.2 k_{\text{OAc}^-}^T = 4.04 \times 10^{-6}$$

$$k_{\text{HOAc}}^T + 0.5 k_{\text{OAc}^-}^T = 4.30 \times 10^{-6}$$

Solve:

$$k_{\text{HOAc}}^T = 3.87 (\pm 0.07) \times 10^{-6} \text{ l.mole}^{-1} \text{ sec.}^{-1}$$

$$k_{\text{OAc}^-}^T = 8.7 (\pm 2.5) \times 10^{-7} \text{ l.mole}^{-1} \text{ sec.}^{-1}$$

The proto-deuteriation reaction of 5-cyano-3 $^{[2}\text{H}]$ indole was studied only in buffer solutions with a $[\text{HOAc}]:[\text{OAc}^-]$ ratio of 5:1, and an estimate was made for catalysis by acetate anion in deriving the value of k_{HOAc}^D from the experimental results listed in TABLE (2.26).

TABLE (2.26)

Proto-dedeuteriation of 5-cyano-3[²H]indole in acetic acid buffers

Buffer ratio = 5:1		$[H_3O^+] = 1.40 \times 10^{-4} M.$		$\mu = 0.1$
Kinetic	[HOAc]	[OAc ⁻]	[NaCl]	$10^7 k_{obs}$
Run	$\cdot 10^2 M.$	$\cdot 10^2 M.$	$\cdot 10^2 M.$	sec. ⁻¹
234	50	10	-	52.5
233	40	8	2	50.2
232	30	6	4	40.8
231	15	3	7	26.8
230	5	1	9	19.3
*	0	-	-	13.8

* value calculated from $k_{H_3O^+}^D [H_3O^+]$

The slope (determined by least squares) of the plot of k_{obs} versus [HOAc] has a value of $8.12 \times 10^{-6} \text{ l.mole}^{-1} \text{ sec.}^{-1}$. Assuming the observed reaction rate arises from catalysis by acetate anion as well as acetic acid catalysis, leads to equation (2.9) for deuterium exchange.

$$k_{HOAc}^D + 0.2 k_{OAc^-}^D = 8.12 \times 10^{-6} \text{ l.mole}^{-1} \text{ sec.}^{-1} \quad \dots\dots\dots(2.9)$$

The value of $k_{OAc^-}^D / k_{OAc^-}^T$ can, by analogy with results for other base catalysts (chapter III) be placed in the range 1.25 - 2.5. Since $k_{OAc^-}^T = 8.7 \times 10^{-7} \text{ l.mole}^{-1} \text{ sec.}^{-1}$, then $k_{OAc^-}^D$ will lie in the range 1.09×10^{-6} to 2.18×10^{-6} (both in $\text{l.mole}^{-1} \text{ sec.}^{-1}$). Substitution in equation (2.9) then gives

$$k_{HOAc}^D = 7.79 (\pm 0.11) \times 10^{-6} \text{ l.mole}^{-1} \text{ sec.}^{-1}$$

The error for the plot of k_{obs} versus $[\text{HOAc}]$ was no greater than $\pm 0.50 \times 10^{-6} \text{ l.mole}^{-1} \text{ sec.}^{-1}$. Thus the second order coefficient for acetic acid catalysis has the value of:

$$k_{\text{HOAc}}^{\text{D}} = 7.79 (\pm 0.61) \times 10^{-6} \text{ l.mole}^{-1} \text{ sec.}^{-1}$$

Summary and calculation of kinetic isotope effects.

The various rate coefficients for the proto-detritiation and proto-dedeuteration of labelled 5-cyanoindole are summarised below.

$$\underline{\text{H}_3\text{O}^+} \quad k^{\text{T}} = 5.27 \times 10^{-3} \text{ l.mole}^{-1} \text{ sec.}^{-1}$$

$$k^{\text{D}} = 9.81 \times 10^{-3} \text{ l.mole}^{-1} \text{ sec.}^{-1}$$

$$\underline{\text{HOAc}} \quad k^{\text{T}} = 3.87 \times 10^{-6} \text{ l.mole}^{-1} \text{ sec.}^{-1}$$

$$k^{\text{D}} = 7.79 \times 10^{-6} \text{ l.mole}^{-1} \text{ sec.}^{-1}$$

The kinetic isotope effects ($k_2^{\text{H}}/k_2^{\text{D}}$), calculated in the usual manner are:

$$\underline{\text{For H}_3\text{O}^+} \quad k_2^{\text{H}}/k_2^{\text{D}} = 5.0 \pm 0.7$$

$$\underline{\text{For HOAc}} \quad k_2^{\text{H}}/k_2^{\text{D}} = 5.9 \pm 0.9$$

Discussion of these values is deferred until later.

2-t-butylindole

Attempts to measure kinetic isotope effects for hydrogen exchange on this substrate were foiled by the low solubility of the compound. For this reason, measurement of the rate of proto-dedeuteriation of 2-t-butyl-3-[^2H]indole in acidic solution could not be made, but nevertheless, the proto-detritiation of 2-t-butyl-3-[^3H]indole in two sets of acetic acid buffer solutions of different buffer ratio was studied. The experimental first-order rate coefficients (equation (2.1)) had the normal high precision expected for the detritiation technique and these are collected in TABLES (2.27) and (2.28). As before, both the slope ($\equiv k_{\text{HOAc}}^T$) and the intercept ($\equiv k_{\text{H}_3\text{O}^+}^T [\text{H}_3\text{O}^+]$) values of the plot of k_{obs} versus $[\text{HOAc}]$ are listed at the foot of each TABLE.

TABLE (2.27)

Proto-detritiation of 2-t-butyl-3-[^3H]indole in acetic acid buffers

Buffer ratio = 1:1		$[\text{H}_3\text{O}^+] = 2.79 \times 10^{-5} \text{M.}$ $\mu = 0.1$		
Kinetic	$[\text{HOAc}]$	$[\text{OAc}^-]$	$[\text{NaCl}]$	$10^3 k_{\text{obs}}$
Run	$.10^2 \text{M.}$	$.10^2 \text{M.}$	$.10^2 \text{M.}$	sec. $^{-1}$
161	10	10	-	5.05
160	7.5	7.5	2.5	4.00
159	5	5	5	2.97
158	2.5	2.5	7.5	1.94
152	1	1	9	1.28

$$k_{\text{HOAc}}^T = 0.0416 \text{ l.mole}^{-1} \text{sec.}^{-1}$$

$$k_{\text{H}_3\text{O}^+}^T [\text{H}_3\text{O}^+] = 8.80 \times 10^{-4} \text{ sec.}^{-1}$$

TABLE (2.28)

Proto-detrition of 2-t-butyl-3[³H]indole in acetic acid buffers

Buffer ratio = 1:3. $[H_3O^+] = 9.3 \times 10^{-6} M.$ $\mu = 0.1$

Kinetic	[HOAc]	[OAc ⁻]	[NaCl]	$10^4 k_{obs}$
Run	$\cdot 10^3 M.$	$\cdot 10^3 M.$	$\cdot 10^3 M.$	sec. ⁻¹
157	33.33	100	-	16.8
156	25	75	25	13.4
155	16.67	50	50	9.75
154	8.33	25	75	6.45
153	3.33	10	90	4.30

$$k_{HOAc}^T = 0.0416 \text{ l.mole}^{-1} \text{ sec.}^{-1}$$

$$k_{H_3O^+}^T [H_3O^+] = 3.00 \times 10^{-4} \text{ sec.}^{-1}$$

The combined data lead to the following values for the second order rate coefficients.

$$k_{H_3O^+}^T = 31.9 \text{ l.mole}^{-1} \text{ sec.}^{-1}$$

$$k_{HOAc}^T = 4.16 \times 10^{-2} \text{ l.mole}^{-1} \text{ sec.}^{-1}$$

These results are useful later (p. 65) in calculation of Brønsted α -factors for the general-acid catalysed isotopic hydrogen exchange on the indole nucleus.

6-nitroindole

The low basicity of 6-nitroindole ($pK_A = -6.9^{(31c)}$) makes this an ideal compound for studying the effects of substrate basicity on the kinetic isotope effect. Unfortunately, as for 2-t-butylindole, this compound proved to be too insoluble to obtain reliable data for the rate of dedeuteriation. However, measurement of the second-order coefficient for H_3O^+ -catalysed proto-detrutiation was undertaken to provide an additional datum for the Brønsted plot relating reaction rate with substrate basicity. These results are summarised in TABLE (2.29) and lead to an average value of $k_{H_3O^+}^T = 2.75 \times 10^{-3} \text{ l.mole}^{-1} \text{ sec.}^{-1}$

TABLE (2.29)

Proto-detrutiation of 6-nitro-3-[3H]indole in dilute HCl

$\mu = 0.1$

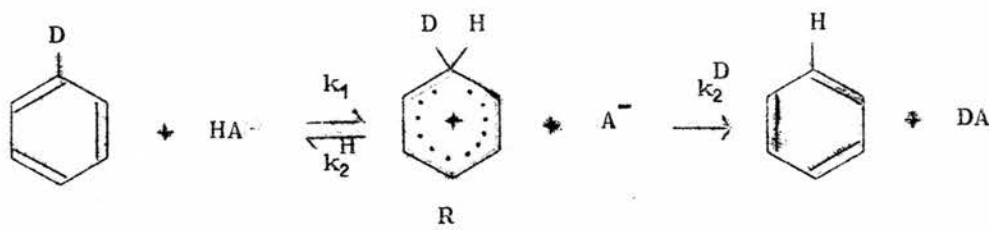
Kinetic	[HCl]	[NaCl]	$10^4 k_{\text{obs}}$	$10^3 \frac{k_{\text{obs}}}{[\text{HCl}]}$
Run	$\cdot 10^2 \text{ M.}$	$\cdot 10^2 \text{ M.}$	sec.^{-1}	$\text{l.mole}^{-1} \text{ sec.}^{-1}$
48	10	-	2.76	2.76
49	10	-	2.70	2.70
52	8	2	2.20	2.75
50	5	5	1.37	2.74
51	4	6	1.10	2.78

$$\text{Average } \frac{k_{\text{obs}}}{[\text{HCl}]} = k_{H_3O^+}^T = 2.75 \times 10^{-3} \text{ l.mole}^{-1} \text{ sec.}^{-1}$$

Discussion

The Magnitude of the Kinetic Isotope Effects.

The kinetic isotope ratios (k_2^H/k_2^D) for the indoles studied, (where k_2^H and k_2^D are the respective rates of loss of hydrogen and deuterium from the conjugate acid intermediate \underline{R} , formed in the aromatic hydrogen exchange reaction depicted generally by equation (2.10)



are summarised

.....(2.10)

in TABLE (2.30) and plotted (FIGURE (2.3)) as a function of ΔpK , the difference between the pK of the substrate and that of the catalyst, following the procedure of Longridge and Long⁽²⁴⁾ and Bell and Goodall.⁽¹⁵⁾

It should be noted that the reported k_2^H/k_2^D ratios are uncorrected for any secondary isotope effects. These may arise both in the initial protonation of the aromatic substrate and in the deprotonation of the conjugate acid intermediate. Although it has been emphasised elsewhere⁽⁴²⁾ that such a correction is desirable, the correction is not made here because of the uncertainty in its magnitude and because it should not affect intercomparison of results obtained for a single reaction in which the only variable is the substrate; thus the results for indoles, azulenes^(23,24) and trimethoxybenzene^(40,43) can be compared.

TABLE (2.30)

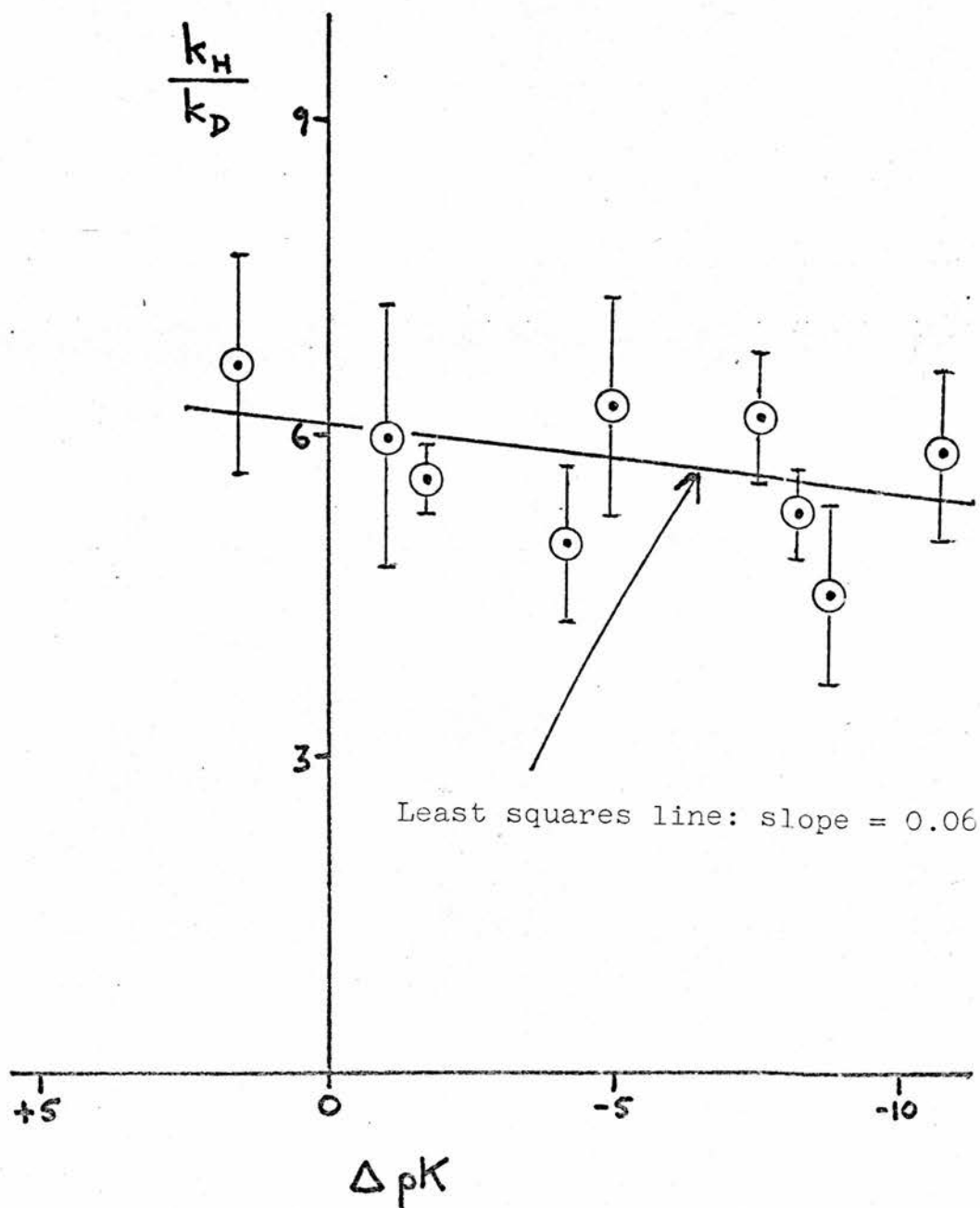
Substrate*	Catalyst*	ΔpK	k_2^H/k_2^D
2-methylindole (-0.28) ^(31c)	H ₃ O ⁺ (-1.75)	+1.47	6.7 ± 0.9
5-methoxyindole (-2.9)	H ₃ O ⁺ (")	-1.15	6.0 ± 1.2
indole (-3.5) ^(31c)	H ₃ O ⁺ (")	-1.75	5.6 ± 0.3
5-cyanoindole (-6.0)	H ₃ O ⁺ (")	-4.25	5.0 ± 0.7
2-methylindole (-0.28) ^(31c)	HOAc (4.76)	-5.04	6.3 ± 1.0
5-methoxyindole (-2.9)	HOAc (")	-7.66	6.2 ± 0.6
indole (-3.5) ^(31c)	HOAc (")	-8.26	5.3 ± 0.4
indole (-3.5) ^(31c)	PyH ⁺ (5.25)	-8.75	4.5 ± 0.8
5-cyanoindole (-6.0)	HOAc (4.76)	-10.76	5.9 ± 0.9

* values in parenthesis are pK_A's. Measurements of pK_A for

5-methoxy- and 5-cyanoindole are reported in the Experimental Section (Chapter IV).

Figure (2.3).

Variation of kinetic isotope effect with pK difference
of the reacting systems. - Indole data only.



The data contained in FIGURE (2.3) show that for the exchange of β -hydrogen on the indole nucleus, there is very little change in the k_2^H/k_2^D ratio over a ΔpK range of 12 logarithmic units; a least squares analysis of the experimental points shows that k_2^H/k_2^D falls by only 0.06 per ΔpK . This decrease is in the direction predicted from Westheimer's arguments,⁽⁶⁾ but is lower than that reported for other recent investigations.^(15,24) Furthermore, there is no clear indication that the isotope effect passes through a maximum value as suggested by recent theoretical arguments.⁽⁶⁾ However, the highest k_2^H/k_2^D value (for H_3O^+ -catalysed exchange with 2-methylindole) is in the region of $\Delta pK = 0$, and the results, apart from this single datum, refer only to negative values of ΔpK . Thus, location of a clear maximum would hardly be expected for these results.

It is of interest to compare the data obtained by Long et al.^(23,24) for substituted azulenes and by Kresge and Chiang⁽⁴⁰⁾ and Batts and Gold⁽⁴³⁾ for trimethoxybenzene (TABLE (2.31)) with the results of the present investigation, and this is done graphically in FIGURE (2.4)

TABLE (2.31)

Substrate	Catalyst	Δ pK	k_2^H/k_2^D
guaiazulene	H_3O^+	+3.3	6.3 ^(a)
guaiaz-2-SO ₃ ⁻	H_3O^+	+1.1	7.4
azulene	H_3O^+	0	9.2
trimethoxybenzene	H_3O^+	-3.5	6.8 ^(b)
azulene	HCO ₂ H	-5.5	6.3
azulene	HOAc	-6.5	6.1
trimethoxybenzene	HOAc	-10.0	5.14

(a) Long et al⁽²⁴⁾ quote a value of 6.0, but this arises from an error in the conversion of the experimental k_2^H/k_2^T value to k_2^H/k_2^D .

(b) Average of values of 6.68⁽⁴⁰⁾ and 6.84⁽⁴³⁾.

The datum from trimethylazulene has been neglected in TABLE (2.31) and FIGURE (2.4), since its value (k_2^H/k_2^D) was reported as unreliable. The dotted line of FIGURE (2.4) is the one drawn by Longridge and Long⁽²⁴⁾ through the experimental data available in 1967; the solid line is that obtained (FIGURE (2.3)) for the indole results. It is evident that the data for the azulenes and trimethoxybenzene are not inconsistent with those for the indole system, with the exception of the experimental point for the H_3O^+ -catalysed exchange for azulene. There is no obvious reason for this apparent discrepancy, although it is of interest to note that the k_2^H/k_2^D for the reaction has been revised repeatedly and published values range from 5.6 to 9.2.

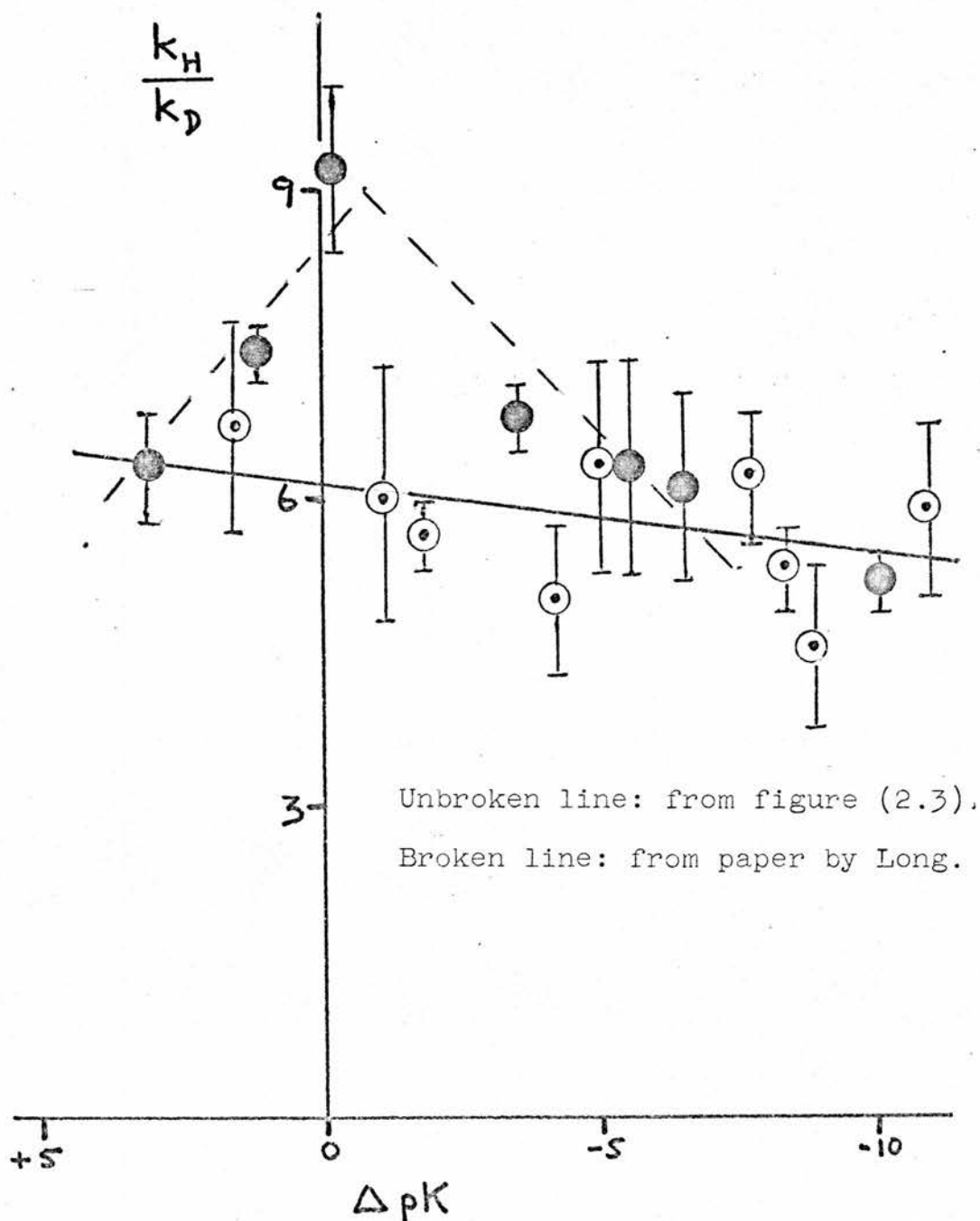
The combined data of FIGURE (2.4) lead to the conclusion that

Figure (2.4).

Variation of kinetic isotope effect with pK difference
of the reacting systems.

(Indole data: open circles.)

Other data: filled circles.)



the kinetic isotope effect (k_2^H/k_2^D) for aromatic hydrogen exchange, contrary to earlier conclusions,^(22,24) is relatively insensitive to the ΔpK value. Hence, if the isotope ratio is a measure of transition state symmetry, then the latter must in turn be almost independent of ΔpK and therefore of substrate reactivity. Similarly, only tenuous support can be given to the theoretical predictions that the ratio might pass through a maximum for catalyst and substrate of equal base strength (i.e. $\Delta pK = 0$).

(Kinetic isotope ratios for H exchange with other aromatic species were summarised by Kresge⁽²²⁾ but cannot be included on FIGURE (2.4) since the pK_A values of most of the substrates are unknown. However, when this data is correlated in terms of relative substrate reactivity (which is related to ΔpK), a decrease in k_2^H/k_2^D accompanies a reduced reactivity (i.e. a more negative value of ΔpK). These results are therefore consistent with those of FIGURE (2.4) where the same trend is detectable.)

Brønsted Acid Catalysis

This conclusion above receives support from the relative magnitudes of the exponent α of the Brønsted relationship⁽⁴⁴⁾ for general acid catalysis (equation (2.11)).

$$k_{HA} = K_{HA}^{\alpha} \quad \dots\dots\dots (2.11)$$

In equation (2.11) k_{HA} refers to the second order rate coefficient for catalysis by the general acid (HA) whose dissociation constant is represented by K_{HA} . The exponent α may be considered as a measure of the degree of proton transfer in the transition state,⁽⁴⁵⁾ and

as such, should correlate with the primary isotope effect. It has been established that the value of α for hydrogen exchange on 2-methylindole^(33,34) and trimethoxybenzene⁽²⁸⁾ is largely insensitive to the nature of the catalyst and is of constant magnitude for catalysts of widely different acidity. For azulene however, the value of α depends on the nature of the catalysing acid as well as on its strength.⁽²⁹⁾ Thus for comparative purposes, it seems reasonable to compare relative values of α for the substrates listed in TABLES (2.30) and (2.31), derived from the catalytic coefficients for isotopic hydrogen exchange by acetic acid and the hydronium ion only. The suitability of this comparison receives some support from the fact that the α values obtained from extensive studies on 2-methylindole (0.58) and trimethoxybenzene (0.52) are reasonably similar to those calculated from acetic acid and hydronium catalysis only (0.42 and 0.48 for 2-methylindole and trimethoxybenzene respectively).

The α values for several 'aromatic' hydrogen exchange reactions derived in this manner are listed in TABLE (2.32), together with the rate coefficients for exchange by H_3O^+ and HOAc catalysts. Two features of these results are of prime interest. Firstly, the magnitude of the α factor is largely insensitive to the reactivity of the aromatic substrate. Thus α only ranges from 0.41 to 0.49, although the reactivity changes by 10^4 as measured from the rate of exchange, and by 10^7 in terms of basicity. Thus the small changes in the α -exponent parallel those for the $k_2^{\text{H}}/k_2^{\text{D}}$ ratio. Secondly, there is an ill-defined trend towards larger α values for the least reactive substrates. Again this parallels the changes in $k_2^{\text{H}}/k_2^{\text{D}}$ ratios reported previously. Thus if both the α -parameters and the

TABLE (2.32)

Approximate Values of the Brønsted Exponent α for Aromatic
Proto-detritiation

Tritiated Substrate (pK_{HA} in parenthesis)		$k_{H_2O^+}^T$ $\ell.mole^{-1} sec.^{-1}$	k_{HOAc}^T $\ell.mole^{-1} sec.^{-1}$	α
2-methylindole	(-0.28)	38.6	6.9×10^{-2}	0.42
2- <u>t</u> -butylindole	(-0.80)	31.9	4.2×10^{-2}	0.44
guaiazulene ⁽²⁴⁾	(1.35)	6.1	1.4×10^{-2}	0.41
5-methoxyindole	(-2.9)	1.14	1.2×10^{-3}	0.46
guaiaz-2-SO ₃ ⁻⁽²⁴⁾	(-0.63)	0.85	5.9×10^{-4}	0.49
indole	(-3.5)	0.50	4.34×10^{-4}	0.47
azulene ⁽²⁴⁾	(-1.76)	0.18	2.5×10^{-4}	0.44
trimethoxybenzene ⁽⁴⁰⁾	(-5.25)	0.008	6.4×10^{-6}	0.48
5-cyanoindole	(-6.0)	0.0053	3.87×10^{-6}	0.48

k_2^H/k_2^D ratios reflect the degree of proton transfer in the transition state, then it is evident that the degree of proton transfer for 'aromatic' hydrogen exchange is not an appreciable function of substrate basicity, and for all the reactions listed in TABLES (2.30) and (2.31) the proton is about 50% transferred in the transition state. This conclusion is in sharp contrast to other results for hydrogen abstraction from aliphatic substrates (see page 70).⁽¹⁵⁾

This conclusion clearly raises two important questions:-

- i) are α -exponents or k_2^H/k_2^D ratios reliable indicators of transition state configuration? ii) if so, is there any special reason why the

extent of proton transfer should be independent of reactivity for aromatic hydrogen exchange? There is some evidence that the magnitude of the α factor may not be a reliable measure of proton transfer in the transition state. This is illustrated by the fact that when the substrate rather than the catalyst is varied, a different value of α is obtained for the same reaction. Thus, for the proto-detritiation of 2-methyl-3-[^3H]indole by several acid catalysts, Challis and Long^(33,34) report an α value of 0.58. However, the calculated value of α for several substituted indoles with a single catalyst (either the hydronium ion or acetic acid), has values of 0.67 and 0.75 respectively. These latter α values are based on the results of TABLE (2.32) together with the datum for the hydronium ion catalysed proto-detritiation of 6-nitro-3-[^3H]indole, and the excellent fit obtained for the experimental points is illustrated by FIGURES (2.5) and (2.6). This is not the first time that such an apparent discrepancy in the values of α , obtained by two different procedures for the same reaction, has been noted. Thus Bell,⁽⁴⁶⁾ in a discussion of results for the reactions of a series of carbonyl compounds with bases, has pointed out that the value of α depends on whether the substrate- or catalyst-basicity is the variable parameter. Similar behaviour of the α -exponent has been pointed out in two recent papers concerned with the acid catalysed hydrolysis of ketal acetals. In these Gold and Waterman⁽⁴⁷⁾ have discussed the further difficulties involved in regarding the α -exponent as a measure of the degree of proton transfer in the transition state. In particular, the results of Gold and Waterman raise considerable

Figure (2.5).

Detritiation of 3-tritio-indoles. - Variation of $k_{H_3O^+}^T$
with pK of indole.

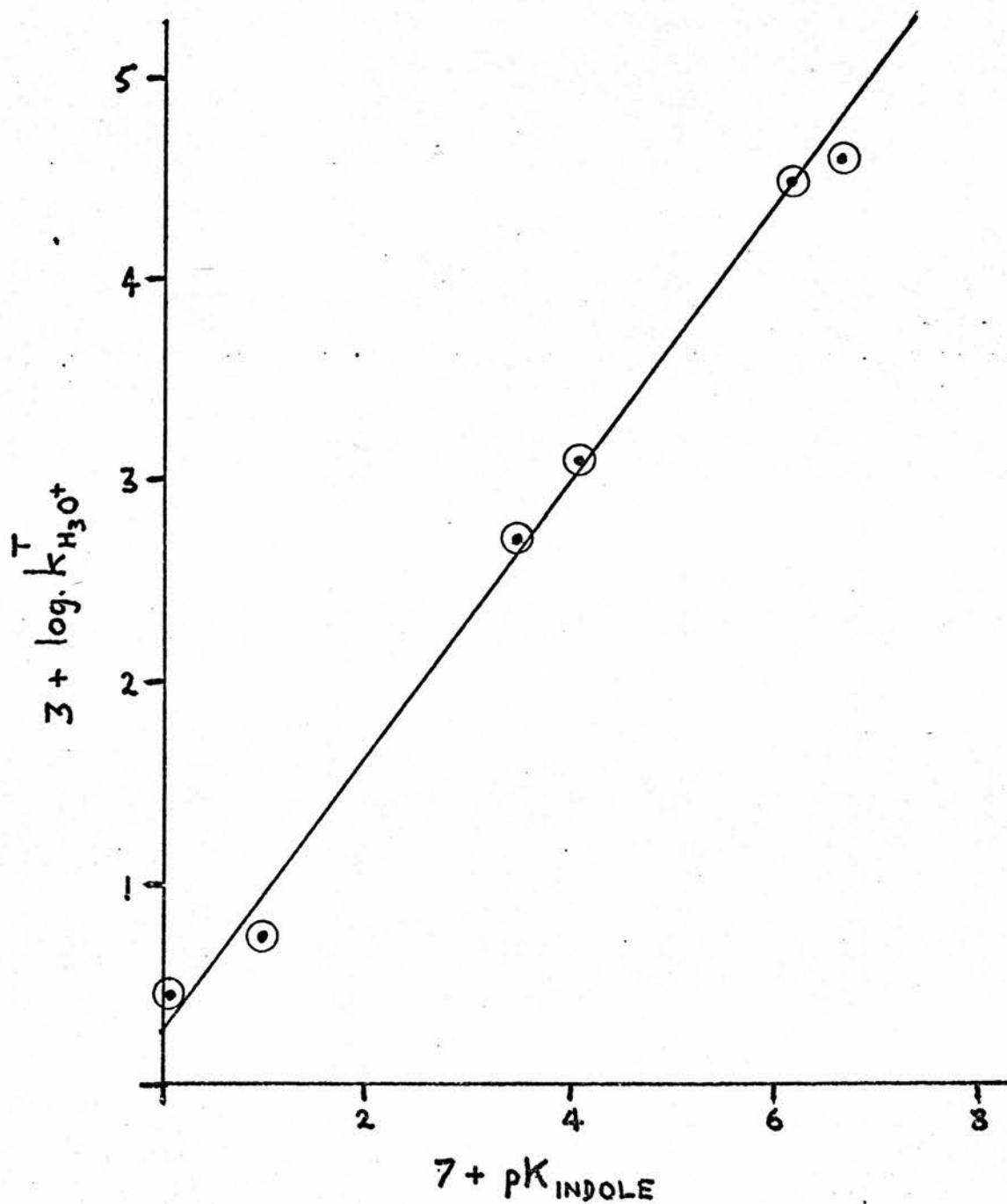
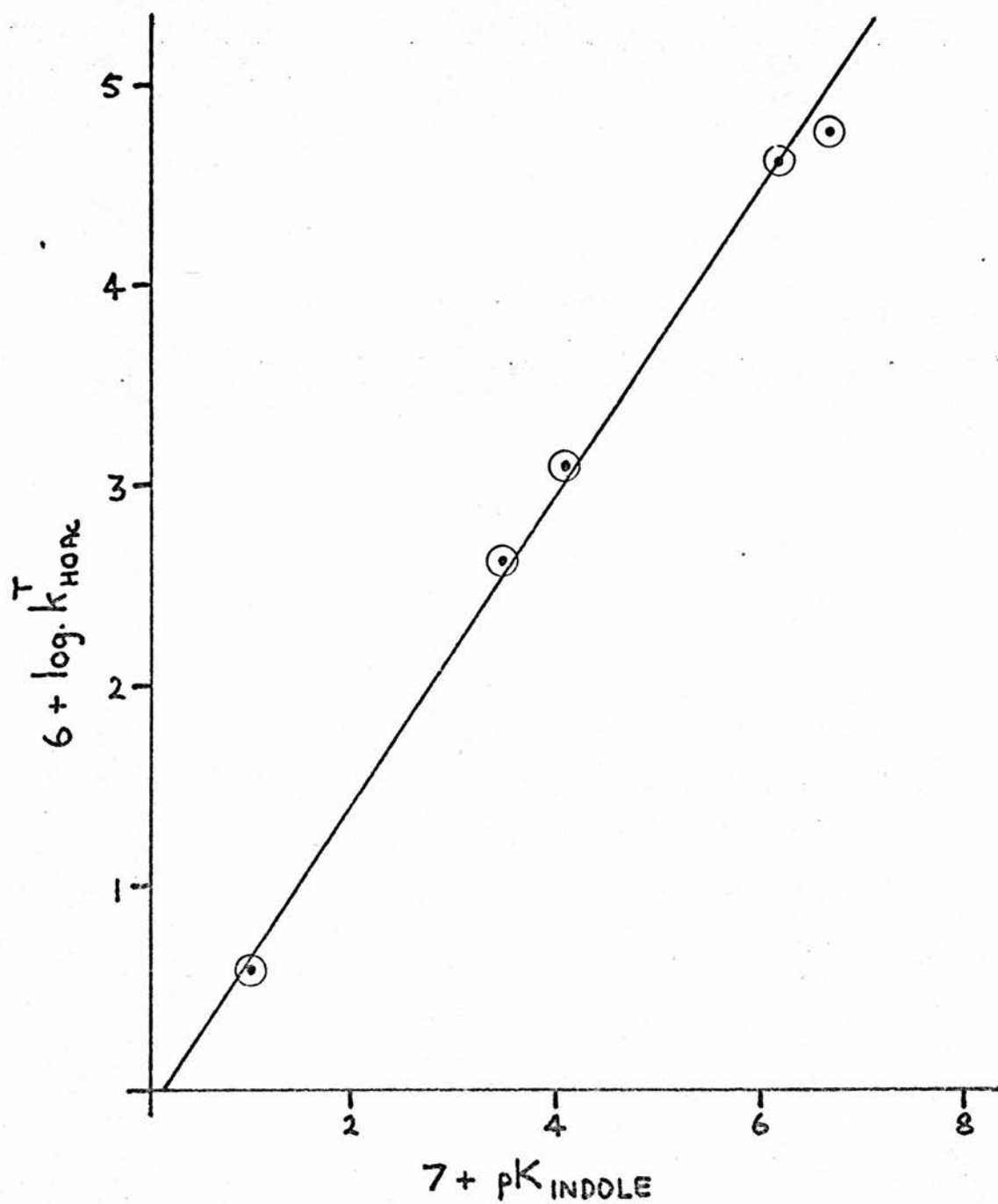


Figure (2.6).

Detritiation of 3-tritio-indoles. - Variation of $k_{\text{HOAc}}^{\text{T}}$
with pK of indole.



doubt on the question of whether either, or both, of the parameters, k^H/k^D and α , reflect transition state symmetry, since when $\alpha = 0.5$ (for the hydrolysis of 2-dichloromethylene-1,3-dioxolon) the corresponding rate isotope effect (k^H/k^D) is smaller than that found for the case $\alpha = 0.6$ (for the hydrolysis of cyanoketen dimethyl acetal). If both parameters (k^H/k^D and α) are measures of transition state proton transfer, then a maximum k^H/k^D (for this reaction type) should have corresponded to the value of α equal to 0.5.

Thus the α values for the indole system show the same features found in some other general acid catalysed reactions. Although their interpretation as quantitative measures of the extent of transition state proton transfer is tenuous, it seems probable that one may still regard the α values for a series of related reactions as an indication of the relative amount of proton transfer in the transition state.⁽⁴⁷⁾ The relative constancy of the α -exponents for aromatic hydrogen exchange as is evident from TABLE (2.32) therefore supports the conclusion drawn from the kinetic isotope effects that transition state symmetry is relatively independent of substrate reactivity.

The origin of this independence is less clear, but useful insight to the problem comes from a comparison with the variable isotope effects reported for other reactions. As discussed in the introduction, Bell and Goodall⁽¹⁵⁾ have summarised the primary kinetic isotope effects for hydrogen abstraction by various bases from groups of compounds containing an activated C-H bond. When the isotopic rate ratios (k^H/k^D) are plotted against ΔpK , a relatively smooth curve with a maximum k^H/k^D near to $\Delta pK = 0$ is obtained. This result is taken as

an indication that the primary isotope effect has a maximum value for a symmetrical transition state. The change in magnitude of the kinetic isotope ratio (k^H/k^D) with ΔpK is much more pronounced in these aliphatic reactions (where $\frac{k^H/k^D}{\Delta pK} \doteq 0.6$) than for aromatic hydrogen exchange ($\frac{k^H/k^D}{\Delta pK} \doteq 0.06$). It therefore appears that the kinetic (primary) isotope effect is approximately 10 times more sensitive to changes in ΔpK for hydrogen abstraction from aliphatic species, than it is for aromatic hydrogen exchange.

The two sets of results are obviously different. However, one similarity between the data for aliphatic and aromatic systems is apparent, in that the magnitude of the isotope effect correlates reasonably well in both cases with the Brønsted exponent. Thus Bell et al^(10,14,15) found that significant changes in β , the Brønsted exponent for general base-catalysed ionisation of the aliphatic substrates in water, were parallel with the change in the primary isotope effect. For aromatic hydrogen exchange, as noted previously, both the Brønsted α -exponent and the kinetic isotope effect are reasonably constant over a wide range of reactivity.

These arguments appear to lead back to the questions on pages 65 and 66 which can be modified slightly in view of the above discussion. Firstly, do the variable k^H/k^D ratios and Brønsted β -exponents for aliphatic proton abstraction reflect the changing symmetry of the transition state? Secondly, is there any special feature of aromatic hydrogen exchange that results in a nearly symmetrical transition state irrespective of the ΔpK value?

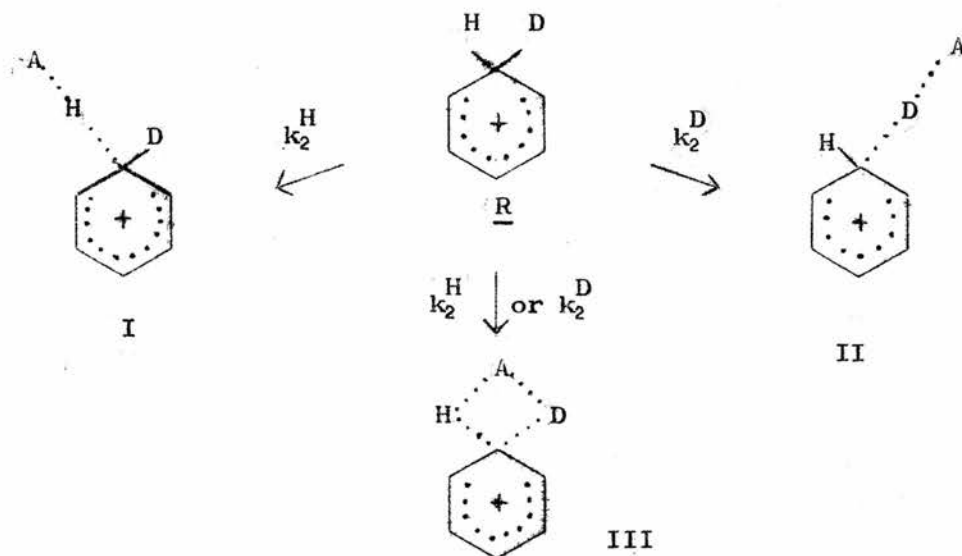
In view of the previous discussion, the answer to the first question must be a qualified yes. This implies that special features are operative in aromatic hydrogen exchange, or, at least, the aromatic

and aliphatic reactions are influenced by different factors.

Bell⁽¹⁰⁾ has considered that the possibilities of additional stretching vibrations (other than those involving C-H bonds) in a five- rather than a three-centre transition state would result in a larger variation of the isotope ratio for aliphatic hydrogen abstraction reactions. Thus if the latter reaction (Bell and Goodall⁽¹⁵⁾) and aromatic hydrogen exchange can be represented by five- and three-centre transition state models respectively, then this could account, in part at least, for the different patterns of results for the two reaction types. However, recent calculations by Albery⁽¹²⁾ and More O'Ferrall and Kouba⁽¹³⁾ both indicate that a three-centre model is adequate to account for the sort of variation of isotope effect (k^H/k^D) found experimentally by Bell et al.^(10,14,15)

It therefore seems dubious that arguments based on differing multi-centre models for the two reactions give a satisfactory answer. Perhaps the solution lies in a consideration of the secondary isotope effects which may be operative in each of the two reaction types (H-abstraction from aliphatic substrates and H-exchange on aromatic substrates). The origin of the secondary isotope effect may be different and more important in aromatic hydrogen exchange than in hydrogen abstraction from aliphatic acids. In the aromatic reaction, the primary isotope effect (k_2^H/k_2^D) refers to the relative rates of loss of hydrogen and deuterium from the intermediate R. The transition states corresponding to H- and D- loss from this intermediate may have structures corresponding to I and II respectively. However, the force constants of the C-D bond in structure (I) and the C-H bond in structure

(II) may be affected by some interaction with the conjugate base A of the catalysing acid, as is illustrated by structure (III).



Since any changes in the force constants of isotopically substituted bonds in the transition state (apart from those bonds which are broken to yield the reaction products) result in a secondary isotope effect, then the $k_2^{\text{H}}/k_2^{\text{D}}$ ratio may contain a significant contribution from a secondary effect.

It should be noted here that Batts and Gold⁽⁴³⁾ have shown that at least for the intermediate (R), structure III is not important. They have reported values of the various isotope ratios ($k_2^{\text{H}}/k_2^{\text{D}}$ and $k_1^{\text{H}_2\text{O}}/k_1^{\text{D}_2\text{O}}$) for H_3O^+ - and acetic acid-catalysed hydrogen exchange on trimethoxybenzene, and these are summarised, together with the corresponding results for 2-methylindole, in TABLE (2.33)

TABLE (2.33)

Comparison of isotope effects for aromatic hydrogen exchange on
2-methylindole and trimethoxybenzene.

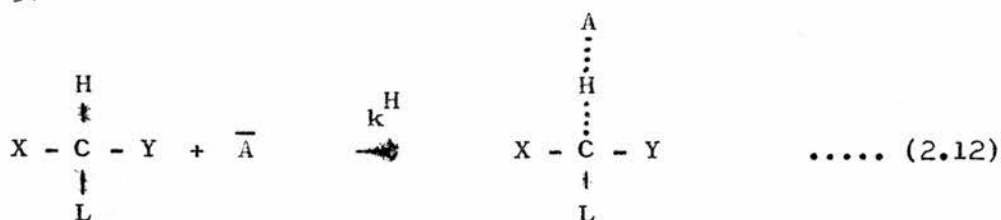
Substrate	Catalyst	k_2^H/k_2^D *	$k_1^{H_2O}/k_1^{D_2O}$
2-methylindole	H_3O^+	6.7 (± 0.9)	2.56 (± 0.5)
1,3,5-trimethoxybenzene	H_3O^+	6.84 (± 0.3)	3.0 (± 0.2)
2-methylindole	HOAc	6.3 (± 1.0)	7.3 (± 1.4)
1,3,5-trimethoxybenzene	HOAc	5.14 (± 0.25)	5.5 (± 0.3)

* uncorrected for secondary isotope effects.

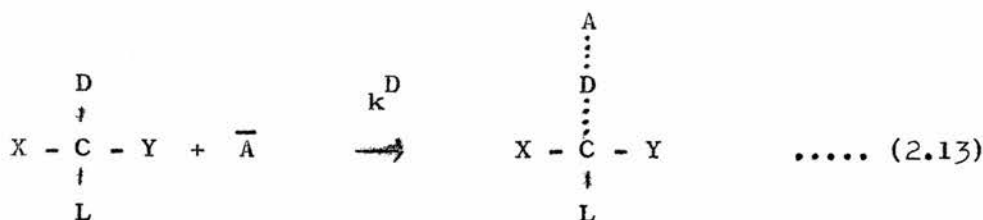
It is evident from TABLE (2.33) that the results for the two substrates agree reasonably well within the limits of the experimental error. Batts and Gold⁽⁴³⁾ have shown that the ratio of dissociation constants of acetic acid in H_2O and D_2O can be calculated from such a set of results. Good agreement between the ratio (K_{HA}/K_{DA}) determined in this manner with the directly determined value $\left(\frac{K_{HA}}{K_{DA}} = 3.3\right)$ can be obtained only by basing the calculation on the hypothesis that the same intermediate (R) is involved for reaction via the two different catalysts H_3O^+ and HOAc. (On this basis a value of K_{HA}/K_{DA} equal to 3.5 was obtained for trimethoxybenzene.) Thus an intermediate of structure corresponding to III, which, on stereochemical grounds would appear to be more feasible for a carboxylic acid than for H_3O^+ can be ruled out, at least for trimethoxybenzene. The value of K_{HA}/K_{DA} obtained from the 2-methylindole results by this method is 4.1, which does not agree quite so well with the directly determined

value of 3.3, as did the value based on the trimethoxybenzene results. This poorer agreement may well result from the larger experimental errors present in the data for 2-methylindole or alternatively it may indicate that there is a tendency towards a structure of the type illustrated by III even for the reaction intermediate, when the conjugate base A of the catalysing acid has a suitable structure. In any case, neither the results for trimethoxybenzene nor those for 2-methylindole, preclude the possibility that the transition state structure may be represented by III, and hence give rise to significant changes in force constant of the non-reacting C-H or C-D bonds, i.e. to the presence of a considerable secondary isotope effect contribution to the measured k_2^H/k_2^D ratios.

For the aliphatic reaction, however, the secondary isotope effect originates from changes in the force constants of the C-L (L refers to H or D) bonds which are not broken in passing from the initial state to the transition state, rather than from an intermediate such as R to the transition state. This is illustrated by equations (2.12) and (2.13) below:



(IV)



(V)

Although stretching of the C-L bond may accompany the loss of H in transition state (IV) or D in transition (V), a structure of the type represented by III (page 72) which describes simultaneous reaction of A (negatively charged) with both H and D (in the positively charged intermediate (R)), cannot be applicable to the aliphatic reaction. Thus, it seems possible that secondary isotope effects may well play a more important role in affecting the experimentally determined "primary" isotope rate ratios (k_2^H/k_2^D) in aromatic exchange than they do in the hydrogen abstraction reactions of aliphatic acids (where the kinetic isotope effect refers to k^H/k^D , equations (2.12) and (2.13)).

Conclusion

The kinetic isotope effects (k_2^H/k_2^D) for the reactions of indole and some of its derivatives, are in good agreement with those obtained from other aromatic hydrogen exchange processes thought to proceed via the same A-S_E2 mechanism, and they correlate well with the Brønsted α -exponents for the reactions.

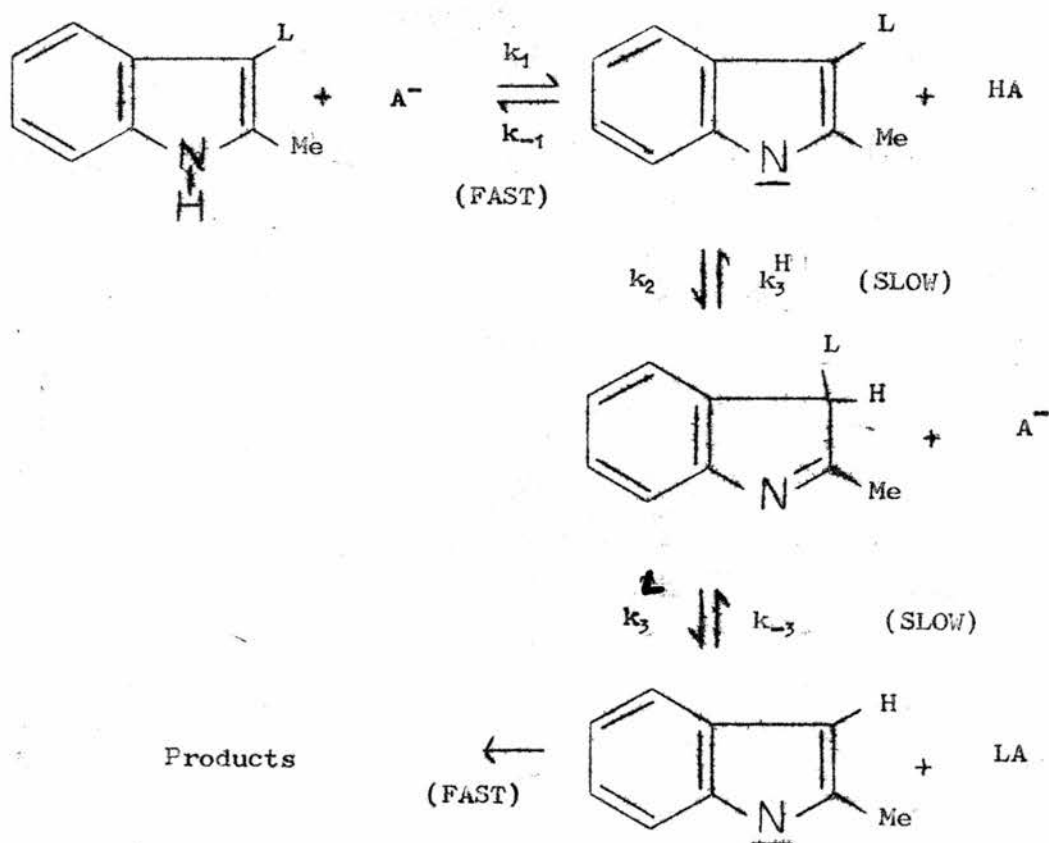
When the values of k_2^H/k_2^D are plotted against the function ΔpK , the resulting correlation is indicative of only a slight decrease in k_2^H/k_2^D from a maximum value in the region $\Delta pK = 0$. This result agrees qualitatively with the predictions of Westheimer⁽⁶⁾ and those of other authors.^(12,13) Compared to the results obtained for a series of aliphatic acids however, the decrease in kinetic isotope effect with ΔpK is a factor of 10 smaller. It is suggested that the probable reason for this reduced variation in aromatic hydrogen exchange arises from an enhanced contribution to the measured isotope

rate ratio from a secondary isotope effect, this effect being a result of considerable interaction in the transition state between the conjugate base of the acid catalyst, and the positively charged reaction intermediate which is indisputably formed in the aromatic hydrogen exchange reaction.

CHAPTER III

BASE-CATALYSED β -HYDROGEN EXCHANGE ON THE INDOLE NUCLEUS.

Base-catalysed hydrogen exchange on the indole nucleus was first studied quantitatively by Challis and Long^(33,34) who showed that proto-detritiation of 2-methyl-3-[³H]indole is subject to general base catalysis (in addition to the general acid catalysed exchange discussed in Chapter II). In contrast to this they also found that, within the limits of experimental error, 1,2-dimethyl-3-[³H]indole does not undergo loss of tritium via any base-catalysed pathway. Although these experiments superficially show that the presence of an amino-hydrogen atom is necessary for base-catalysed hydrogen exchange, no firm conclusions on the reaction mechanism were drawn from the limited data available, although it was suggested that the reaction involved an S_E2 -type process of the conjugate anion (equation (3.1))



Thus a more detailed study of the base-catalysed hydrogen exchange reaction was undertaken and is reported in this Chapter. Studies of kinetic isotope effects, Brønsted catalysis and the kinetic form of the reaction in concentrated solutions of aqueous caustic soda are shown to largely resolve the mechanism of the base-catalysed exchange process.

Proto-detrition Studies in Concentrated Aqueous Solutions of Sodium Hydroxide.

The most definitive evidence for the mechanism of the base-catalysed exchange comes from the kinetic form of the reaction in concentrated NaOH solutions. It may be recalled that Challis and Long⁽³³⁾ found the rate of proto-detrition of 2-methyl-3-[³H]indole showed a first-order dependence in [OH⁻] (equation (3.2)) over the limited range of NaOH concentrations studied (up to about 0.1M NaOH). Early on in the present investigation, however, it was found that the

$$v = k_{OH^-}^T [InT][OH^-] \quad \dots\dots\dots (3.2)$$

rate of exchange of more acidic indoles (containing electron-withdrawing groups) had a more complex dependence on the NaOH concentration. In particular, it was apparent that, although the reaction followed equation (3.2) at low NaOH concentrations, the order in [OH⁻] steadily diminished at higher solvent basicities, and the reaction rate reached a maximum value. This is illustrated by the typical results for 5-cyano- and 6-nitro-3-[³H]indole in FIGURES (3.1) and (3.2) respectively, where k_{obs} ($v = k_{obs}(In-T)$) is plotted against the NaOH concentration.

Figure (3.1).

Detritiation of 5-cyano-3- $^{[3]}\text{H}$ indole in sodium hydroxide.

Variation of k_{obs} with $[\text{NaOH}]$.

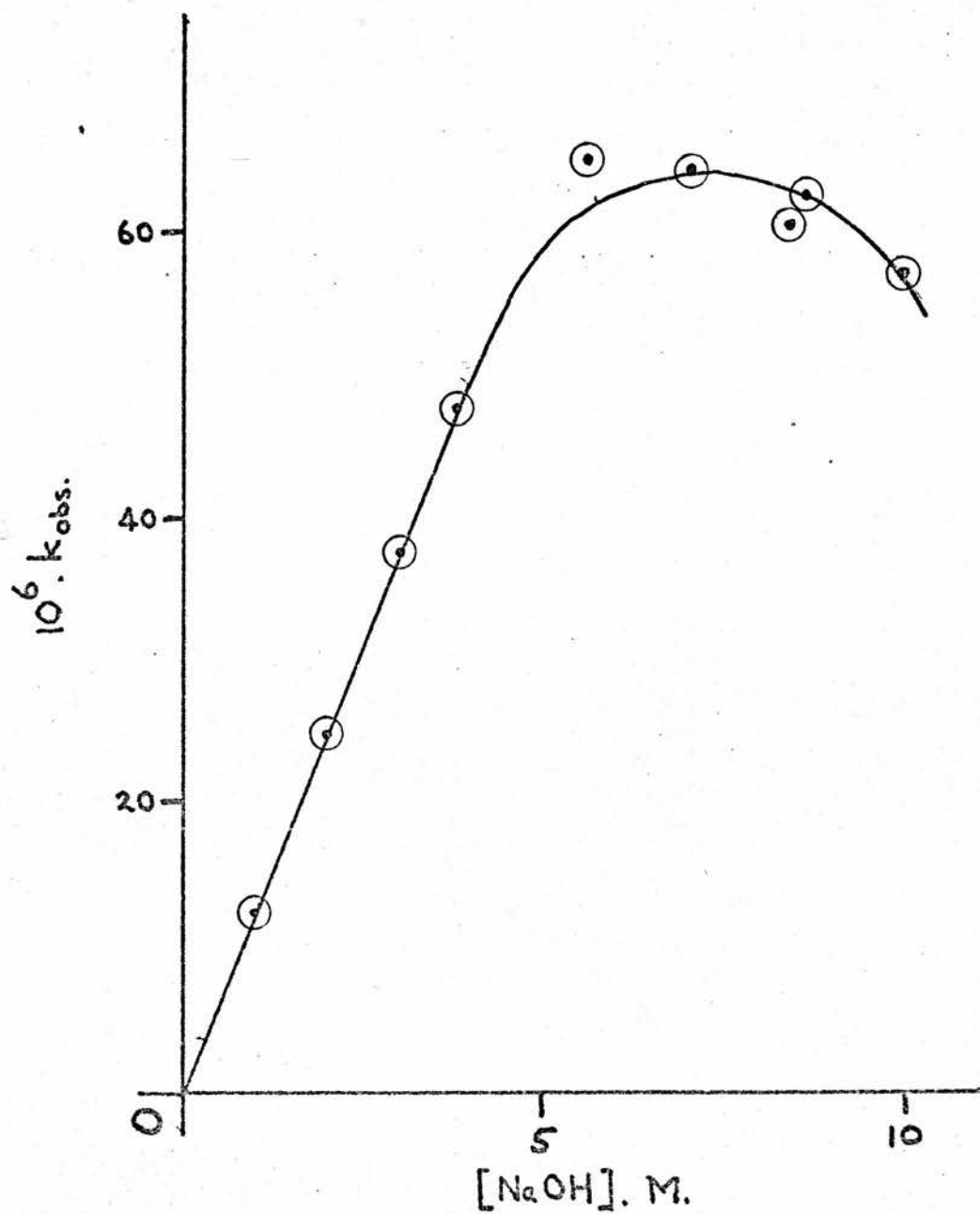
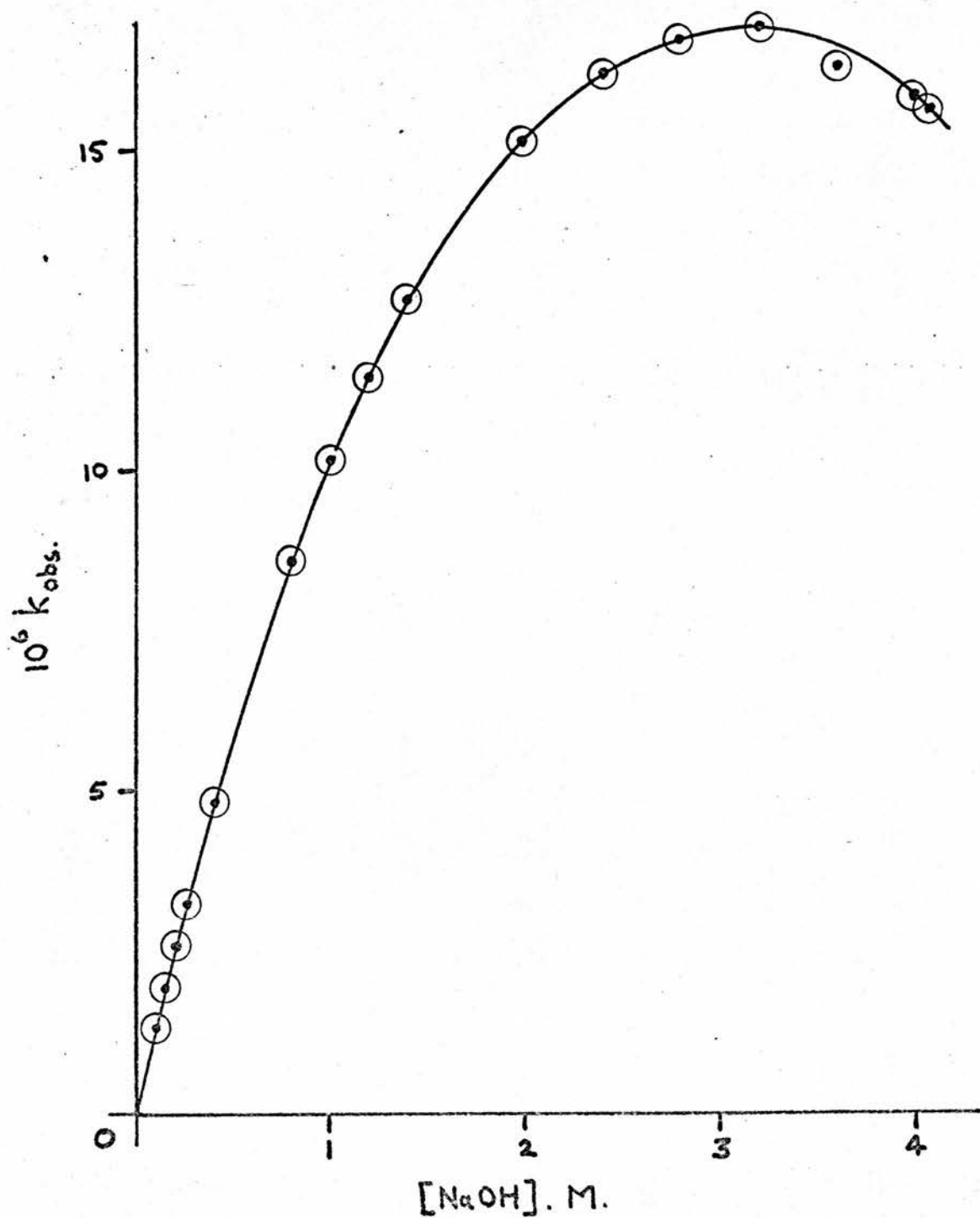


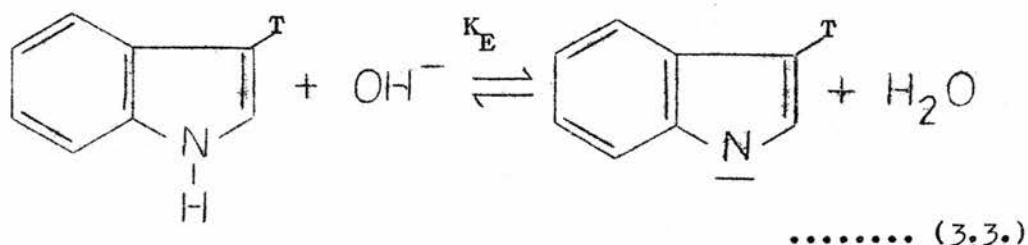
Figure (3.2).

Detritiation of 6-nitro-3- $^{[3]}\text{H}$ indole in sodium hydroxide

Variation of k_{obs} with $[\text{NaOH}]$.

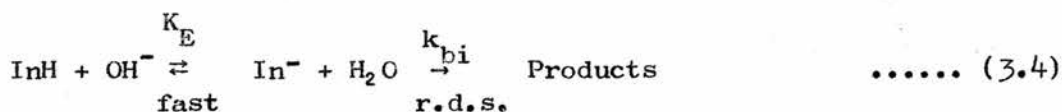


The most obvious explanation of these results, consistent with the mechanism outlined in equation (3.1), is that the bulk component of the substrate at the higher basicities is the indole anion, and the reaction is therefore independent of the solvent basicity. In this situation, it is possible to calculate the equilibrium constant (K_E) for ionisation of the amino-hydrogen (equation (3.3)) and hence the acid dissociation constant of the indole, from the kinetic



results, for comparison with independently determined values from equilibrium studies. (35)

The details of the kinetic analysis to obtain K_E are given below. The exchange reaction (equation (3.1)) is more conveniently written in a shorthand manner as,



where k_{bi} is the composite second-order rate coefficient for the reaction steps involving isotopic exchange at the 3-position

$$\text{i.e. } k_{bi} = \frac{k_2 k_3^T}{k_3^H + k_3^T}$$

k_{bi} is defined by equation (3.5) as:

$$v = k_{bi} [\text{In}^-] [\text{H}_2\text{O}] \quad \text{..... (3.5)}$$

The observed first-order coefficient (k_{obs}) refers to the stoichiometric indole concentration (InH), thus

$$\begin{aligned} v &= k_{\text{obs}} (\text{InH}) \\ &= k_{\text{obs}} ([\text{In}^-] + [\text{InH}]) \end{aligned} \quad \dots\dots (3.6)$$

From equations (3.5) and (3.6)

$$k_{\text{obs}} ([\text{In}^-] + [\text{InH}]) = k_{\text{bi}} [\text{In}^-] [\text{H}_2\text{O}] \quad \dots\dots (3.7)$$

$$\therefore \frac{[\text{H}_2\text{O}]}{k_{\text{obs}}} = \frac{1}{k_{\text{bi}}} \left(1 + \frac{[\text{InH}]}{[\text{In}^-]} \right) \quad \dots\dots (3.8)$$

The relationship between the substrate ratio $\frac{[\text{InH}]}{[\text{In}^-]}$ and the solvent basicity in concentrated solutions of sodium hydroxide may be evaluated by reference to the b_- acidity function derived by Yagil and his co-workers for the ionisation of indole and related compounds. (35,48) They showed that

$$\frac{[\text{InH}]}{[\text{In}^-]} = \frac{K_W}{K_{\text{HIn}} b_-} \quad \text{where,}$$

K_{HIn} = acid dissociation constant of HIn

$$= \frac{[\text{H}^+][\text{In}^-]}{[\text{InH}]}$$

and K_W = ionic product for water

$$= 10^{-14} \text{ at } 25^\circ \text{ (49)}$$

Thus substituting for $\frac{[\text{InH}]}{[\text{In}^-]}$ in equation (3.8)

leads to

$$\frac{[\text{H}_2\text{O}]}{k_{\text{obs}}} = \frac{1}{k_{\text{bi}}} \left(1 + \frac{K_W}{K_{\text{HIn}} \cdot b_-} \right)$$

$$\therefore \frac{[\text{H}_2\text{O}]}{k_{\text{obs}}} = \frac{K_W}{K_{\text{HIn}} \cdot k_{\text{bi}}} \cdot \frac{1}{b_-} + \frac{1}{k_{\text{bi}}}$$

Thus a plot of $[H_2O]/k_{obs}$ vs. $1/b_-$ should lead to a straight line of slope = $\frac{K_W}{K_{HIn} \cdot k_{bi}}$ and intercept = $1/k_{bi}$, from which both k_{bi} and K_{HIn} may be evaluated.

The experimental data for the proto-detritiation of five substituted indoles in aqueous NaOH have been analysed in the manner outlined above, and the results are presented in TABLES (3.1) - (3.5). For each compound, the plot of $\frac{[H_2O]}{k_{obs}}$ vs $1/b_-$ was closely linear, although small deviations close to $1/b_- = 0$, were observed for the nitro-derivatives; these were ignored in the slope determination which was based on the excellent linear behaviour of the other points. Typical plots, for 5-cyano- and 6-nitro-3-[3H]indole, are shown in FIGURES (3.3) and (3.4) respectively. At the foot of each table (pages 85-89) the value of k_{bi} , calculated from measurements in dilute NaOH according to equation (3.9)*

$$k_{bi} = k_{OH^-}^T \cdot \frac{K_{H_2O}}{K_{HIn}} \quad \dots\dots (3.9)$$

is detailed. (In equation (3.9), $k_{OH^-}^T$ is the experimental second-order rate coefficient for the hydroxide-ion catalysed detritiation reaction and may be calculated in dilute NaOH by dividing the observed first-order rate coefficient k_{obs} , by the appropriate hydroxide-ion concentration; K_{H_2O} and K_{HIn} are the acid dissociation constants of water and the indole respectively. The K_{HIn} value used in the calculation of k_{bi} from equation (3.9) was that obtained from the kinetic analysis.) The value of k_{bi} obtained, as described earlier,

* The derivation of equation (3.9) is deferred until later (page 100).

from the intercept of the plot of $\frac{[H_2O]}{k_{obs}}$ vs $1/b_-$, is also noted at the foot of each table. In addition, the pK_{HI_n} values from these kinetic studies are compared with those from the equilibrium measurements.⁽³⁵⁾

The values of $[H_2O]$ for concentrated sodium hydroxide used in the calculations were computed by multiplying the normalised values listed by Yagil and Anbar⁽⁵⁰⁾ by 55.5. b_- was calculated from the value of $H_-^{(35)}$ at the appropriate molarity of NaOH ($b_- = \frac{K_W}{h_-}$; $H_- = -\log h_-$).

TABLE (3.1)

Proto-detrition of 5-cyano-3[³H]indole in aqueous NaOH.

T = 25°C.

Kinetic Run	[OH ⁻] M.	b ₋	1/b ₋	10 ⁶ k _{obs} sec. ⁻¹	10 ⁻⁵ [H ₂ O] $\frac{k_{obs}}{\ell.^{-1} \text{mole sec.}}$
115	0.5			6.31	
116	1			12.3	
117	2			24.7	
119	3			37.7	
121	3.77			47.7	
<hr/>					
120	4.70	13.19	0.0758	57.6	7.05
122	5.60	20.41	0.0490	65.3	5.77
123	6.98	38.94	0.0257	64.6	5.08
143	7.00	41.67	0.0240	64.6	5.07
124	8.40	75.76	0.0132	60.5	4.57
144	8.60	83.20	0.0120	62.7	4.30
145	10.03	162.3	0.0062	57.6	3.73

From [OH⁻] ≤ 3.77M, $k_{OH^-}^T = 12.5 \times 10^{-6} \ell.\text{mole}^{-1} \text{sec.}^{-1}$

∴ $k_{bi} = 2.55 \times 10^{-6} \ell.\text{mole}^{-1} \text{sec.}^{-1}$

from equation (3.9)

From [OH⁻] ≥ 4.70M, plot of $\frac{[H_2O]}{k_{obs}}$ vs $\frac{1}{b^-}$

(least squares method)

gives $k_{bi} = 2.62 \times 10^{-6} \ell.\text{mole}^{-1} \text{sec.}^{-1}$

and $pK_{HIn} = 15.05$, (5-cyanoindole)

cf. $pK_{HIn} = 15.21$

from equilibrium measurement. (35)

TABLE (3.2)

Proto-detrition of 5-bromo-3-[³H]indole in aqueous NaOH.

T = 25°C.

Kinetic	[OH ⁻]	b ₋	1/b ₋	10 ⁵ k _{obs}	10 ⁻⁵ $\frac{[H_2O]}{k_{obs}}$
Run	M.			sec. ⁻¹	ℓ. ⁻¹ mole sec.
125	0.5			1.17	
126	1			2.30	
127	2			4.76	
<hr/>					
128	3	4.464	0.2240	7.68	6.01
129	4.50	11.50	0.0870	12.8	3.26
130	6.13	26.32	0.0380	19.0	1.89
131	7.70	54.95	0.0182	18.9	1.63
132	9.65	135.0	0.0074	20.9	1.13

From [OH⁻] ≤ 2M, $k_{OH^-}^T = 2.34 \times 10^{-5} \text{ ℓ.mole}^{-1} \text{ sec.}^{-1}$

∴ $k_{bi} = 8.50 \times 10^{-6} \text{ ℓ.mole}^{-1} \text{ sec.}^{-1}$

from equation (3.9)

From [OH⁻] ≥ 3M, plot of $\frac{[H_2O]}{k_{obs}}$ vs $\frac{1}{b_-}$

(least squares), gives:

$$k_{bi} = 8.93 \times 10^{-6} \text{ ℓ.mole}^{-1} \text{ sec.}^{-1}$$

and $pK_{HIn} = 15.30$ (5-bromoindole)

cf. $pK_{HIn} = 16.32$

from equilibrium measurement. (35)

TABLE (3.3)

Proto-detrition of 6-nitro-3^[3H]indole in aqueous NaOH

T = 25°C

Kinetic	[OH ⁻]	b ₋	1/b ₋	10 ⁶ k _{obs}	10 ⁻⁶ $\frac{[H_2O]}{k_{obs}}$
Run	M.			sec. ⁻¹	ℓ. ⁻¹ mole sec.
61	0.1			1.36	
62	0.12			1.59	
63	0.15			1.96	
64	0.2			2.62	
65	0.25			3.27	
<hr/>					
54	0.4	0.400	2.500	4.88	11.1
56	0.8	0.833	1.200	8.65	6.16
55	1.0	1.047	0.955	10.2	5.14
66	1.2	1.231	0.812	11.5	4.50
68	1.4	1.446	0.692	12.7	4.02
53	2.0	2.345	0.426	15.2	3.25
58	2.4	3.021	0.331	16.3	2.95
59	2.8	3.984	0.251	16.8	2.79
60	3.2	5.249	0.191	17.0	2.68
67	3.6	6.757	0.148	16.4	2.71
69	4.0	8.929	0.112	15.9	2.71
88	4.08	9.346	0.107	15.7	2.72

From [OH⁻] ≤ 0.25M, $k_{OH^-}^T = 1.32 \times 10^{-5} \text{ ℓ.mole}^{-1} \text{ sec.}^{-1}$

∴ $k_{bi} = 7.25 \times 10^{-7} \text{ ℓ.mole}^{-1} \text{ sec.}^{-1}$ (from equation (3.9))

From [OH⁻] ≥ 0.4M, plot of 1/b₋ vs $\frac{[H_2O]}{k_{obs}}$ (line through experimental

points drawn by inspection) gives:

$$k_{bi} = 7.69 \times 10^{-7} \text{ ℓ.mole}^{-1} \text{ sec.}^{-1}$$

and $pK_{HIn} = 14.48$, (6,nitroindole)

cf $pK_{HIn} = 14.59$

from equilibrium measurement, (51)

TABLE (3.4)

Proto-detrition of 5-nitro-3-[³H]indole in aqueous NaOH.

T = 25°C.

Kinetic	[OH ⁻]	b ₋	1/b ₋	10 ⁶ k _{obs}	10 ⁻⁶ $\frac{[H_2O]}{k_{obs}}$
Run	M.			sec. ⁻¹	ℓ. ⁻¹ mole sec.
99	0.2	0.200		1.57	
100	0.3	0.302	3.31	2.24	24.3
96	0.5	0.513	1.95	3.62	14.9
93	1.0	1.047	0.955	6.72	7.80
92	2	2.345	0.426	11.1	4.45
94	2.6	3.472	0.288	13.1	3.62
95	3.2	5.128	0.195	14.1	3.23
97	4.155	9.346	0.107	14.5	2.94
98	5.17	16.99	0.059	13.1	3.00

From [OH⁻] = 0.2M, $k_{OH^-}^T = 7.85 \times 10^{-6} \text{ ℓ.mole}^{-1} \text{ sec.}^{-1}$

∴ $k_{bi} = 7.67 \times 10^{-7} \text{ ℓ.mole}^{-1} \text{ sec.}^{-1}$ (from equation 3.9)

From [OH⁻] ≥ 0.3M, plot of 1/b₋ vs $\frac{[H_2O]}{k_{obs}}$ (inspection method) gives:

$$k_{bi} = 7.69 \times 10^{-7} \text{ ℓ.mole}^{-1} \text{ sec.}^{-1}$$

and $pK_{HIn} = 14.73$, (5-nitroindole)

cf. $pK_{HIn} = 14.69$

from equilibrium measurement. (35)

TABLE (3.5)

Proto-detrition of 2-methyl-5-nitro-3-[^3H]indole in aqueous NaOH.

T = 25°C.

Kinetic	$[\text{OH}^-]$	b_-	$1/b_-$	$10^5 k_{\text{obs}}$	$10^{-4} \frac{[\text{H}_2\text{O}]}{k_{\text{obs}}}$
Run	M.			sec. $^{-1}$	$\ell.$ $^{-1}$ mole sec.
80	0.2			5.50	
81	0.3			7.95	
82	0.4			10.3	
<hr/>					
72	0.6	0.617	1.62	15.0	35.7
86	0.92	0.935	1.07	22.0	24.0
74	1	1.047	0.955	23.4	22.4
83	1.4	1.445	0.692	30.8	16.6
71	2	2.345	0.426	39.2	12.6
75	2.8	3.922	0.255	46.2	10.2
78	3.6	6.757	0.148	51.5	8.6
102	4.145	9.551	0.105	51.3	8.3
103	5.11	16.60	0.060	47.5	8.3

From $[\text{OH}^-] \leq 0.3\text{M}$, $k_{\text{OH}^-}^T = 2.70 \times 10^{-4} \ell.\text{mole}^{-1}\text{sec.}^{-1}$

$\therefore k_{\text{bi}} = 1.49 \times 10^{-5} \ell.\text{mole}^{-1}\text{sec.}^{-1}$ (from equation (3.9))

From $[\text{OH}^-] \geq 0.6\text{M}$, plot of $1/b_-$ vs $\frac{[\text{H}_2\text{O}]}{k_{\text{obs}}}$

(inspection method), gives:

$$k_{\text{bi}} = 1.75 \times 10^{-5} \ell.\text{mole}^{-1}\text{sec.}^{-1}$$

and $\text{pK}_{\text{HIn}} = 14.48$, (2-methyl-5-nitroindole)

(No available value of pK_{HIn} for comparison)

Figure (3.3).

Detritiation of 5-cyano-3- $^{[3]}\text{H}$ indole in sodium hydroxide. - Variation of $\frac{[\text{H}_2\text{O}]}{k_{\text{obs}}}$ with $\frac{1}{b_-}$.

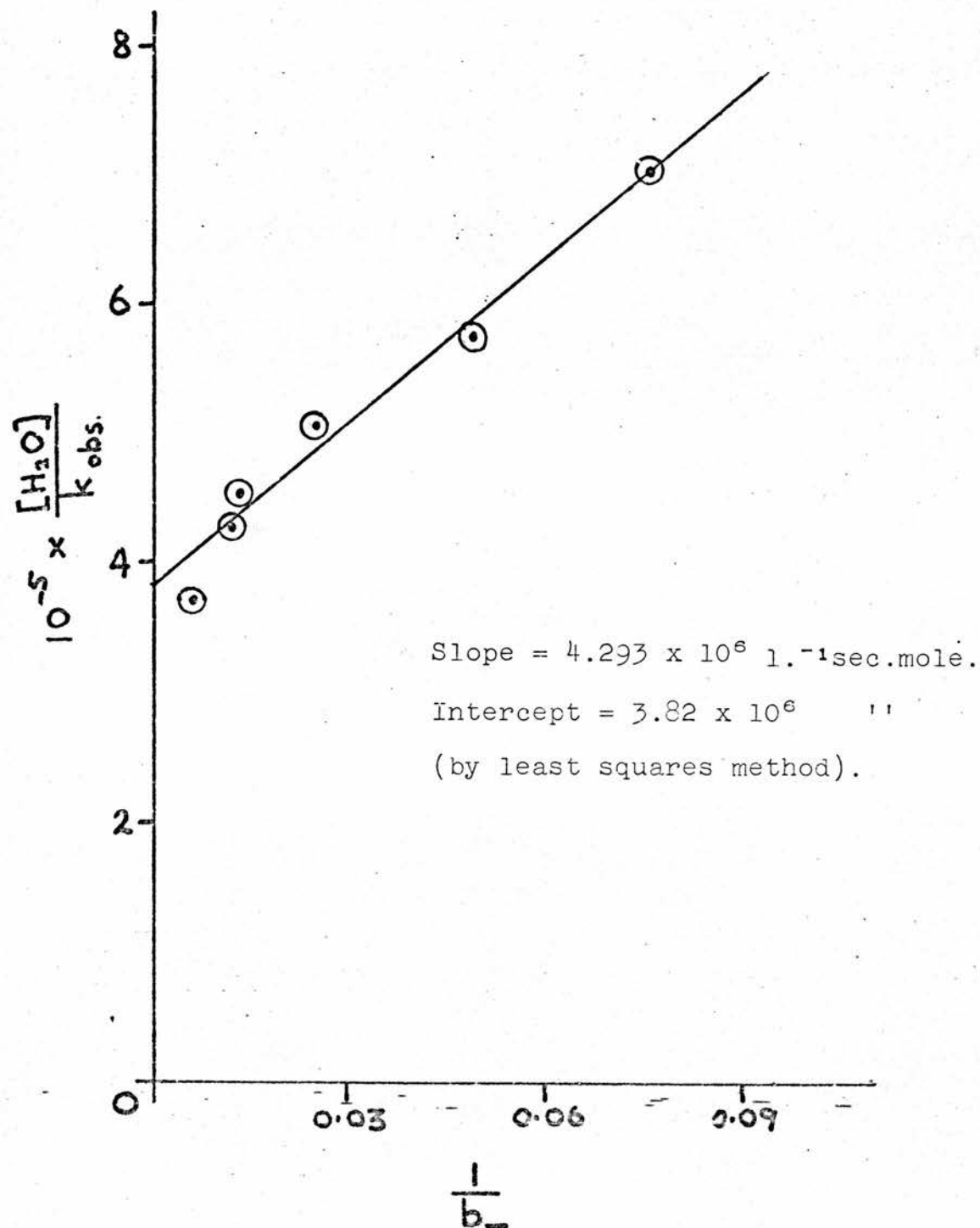
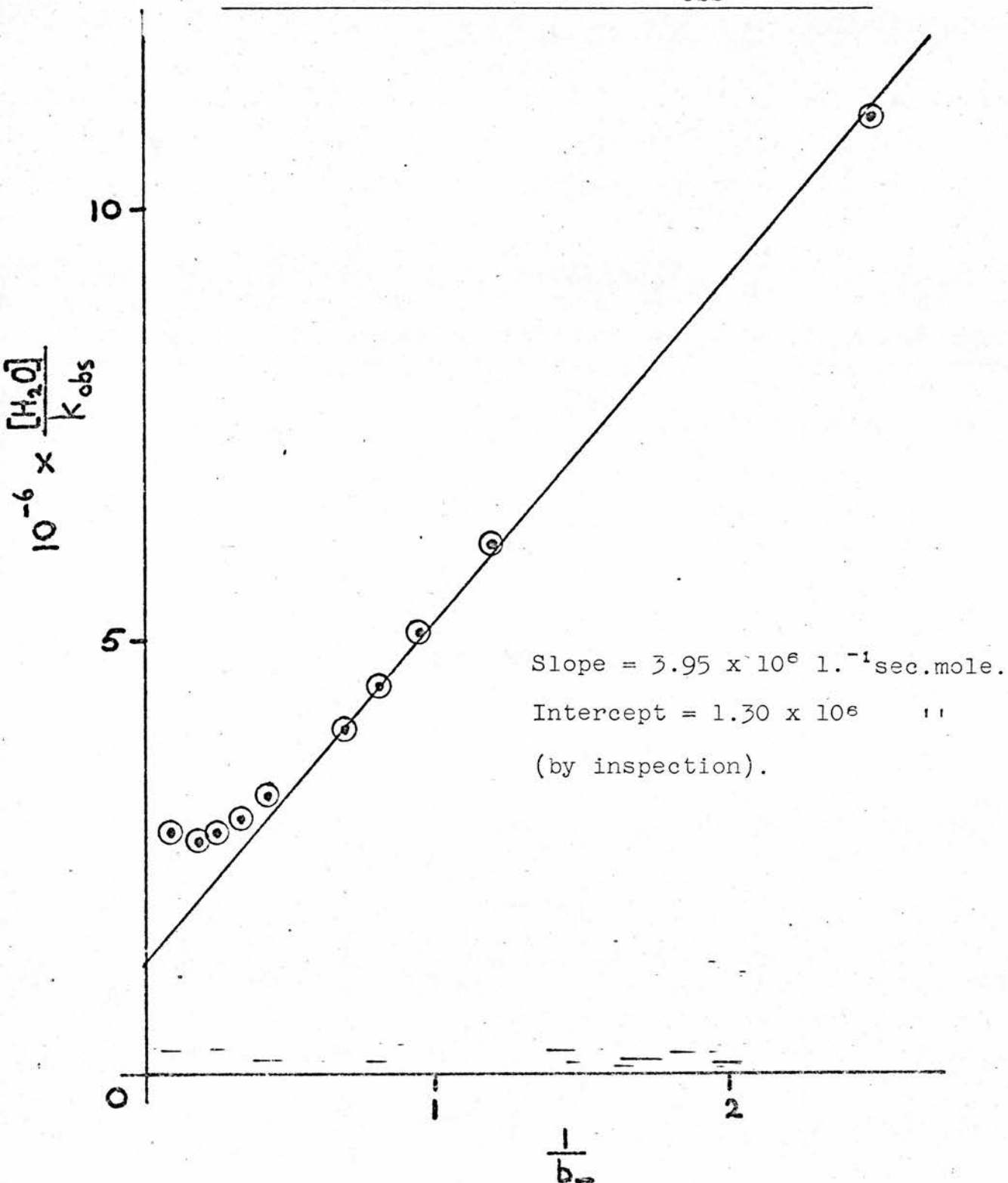


Figure (3.4).

Detritiation of 6-nitro-3- $[^3\text{H}]$ indole in sodium hydroxide. - Variation of $\frac{[\text{H}_2\text{O}]}{k_{\text{obs}}}$ with $\frac{1}{b_-}$



The general consistency of the preceding results and the satisfactory agreement between the values of pK_{HIn} from kinetic and equilibrium measurements seem to vindicate the analysis of the kinetic data. This, in turn, strongly suggests that the mechanistic scheme for the base-catalysed isotopic-hydrogen exchange of the 5-substituted indoles, represented by equation (3.1), is the correct one. Further discussion of these results in regard to Brønsted catalysis is deferred until page 106.

Proto-detritiation of 3[^3H]indole in basic solutions.

Indole, itself, is much less acidic ($pK = 16.97^{(35)}$) yet "more reactive" than the 5-substituted compounds discussed in the previous section. Consequently, the rate maximum is not observed until the NaOH concentration exceeds 12M, where uncertainties in the values of H^- and $[\text{H}_2\text{O}]$ make analysis of the data in the manner of the previous section, unreliable. However, the results are in accord with the mechanism of equation (3.1) and lead to an interesting test of acidity function correlations in basic solutions.

The experimentally determined values of k_{obs} (equation (3.10)) for the proto-detritiation of 3[^3H]indole are listed in TABLE (3.6) for

$$v = k_{\text{obs}}(\text{InH}) \quad \dots\dots\dots (3.10)$$

[NaOH] varying from 0.5 to 13.4M.

TABLE (3.6)

Proto-detrition of 3[³H]indole in aqueous NaOH.

T = 25°C

Kinetic Run	[OH ⁻] M.	H ₋	10 ⁶ k _{obs} sec. ⁻¹	6+log k' _{obs} *	[H ₂ O] (normal- ised)	H ₋ + log [H ₂ O]
106	0.5	13.71	8.85	0.947	0.971	13.70
104	1	14.02	17.8	1.25	0.945	14.00
105	2	14.37	37.5	1.57	0.890	14.32
107	3	14.65	63.0	1.80	0.832	14.57
108	3.82	14.90	81.5	1.91	0.787	14.80
109	5.98	15.39	171	2.22	0.655	15.21
111	7.74	15.75	268	2.40	0.543	15.49
112	9.88	16.18	387	2.52	0.400	15.78
113	11.75	16.55	420	-	-	-
114	13.40	16.83	362	-	-	-

* In column 5, k'_{obs} represents the value of k_{obs} after correction for the concentration of indole anion present at each molarity of NaOH. The values of k'_{obs} were computed using pK = 16.97 for indole. (35)

If the reaction involves a rate-determining attack of H_2O on the indole anion, then it may be expected that the rate coefficient k_{obs} will be related to the solvent basicity by equations (3.11) and (3.12). It should be noted that these equations apply⁽⁴⁸⁾ only when $[In^-] \ll [InH]$,

$$k_{obs} = \text{const. } b_- \cdot [H_2O] \quad \dots\dots\dots (3.11)$$

$$\therefore \log k_{obs} = H_- + \log [H_2O] \quad \dots\dots\dots (3.12)$$

or when k_{obs}

is corrected (as in column 5 of TABLE (3.6)) to allow for the presence of an appreciable contribution of anion to the stoichiometric concentration of indole. As illustrated by FIGURE (3.5) a plot of $\log k'_{obs}$ versus $H_- + \log [H_2O]$ gives a line of slope 0.76 ± 0.22 , which is rather less than the value of unity predicted by equation (3.12). This lack of agreement may arise from errors in the H_- scale at high basicities,⁽³⁵⁾ which in addition would affect the value of pK_{HIn} . (The results have been analysed in an identical manner using unpublished H_- values based on the ionisation of 6-nitroindole only;⁽⁵¹⁾ in this case a straight line of slope equal to 1.00 was obtained.) Furthermore, when $\log k'_{obs}$ is plotted against H_- itself, a curved plot of average slope 0.64 is obtained. This indicates that

$$\log k'_{obs} = H_- + \log [H_2O]$$

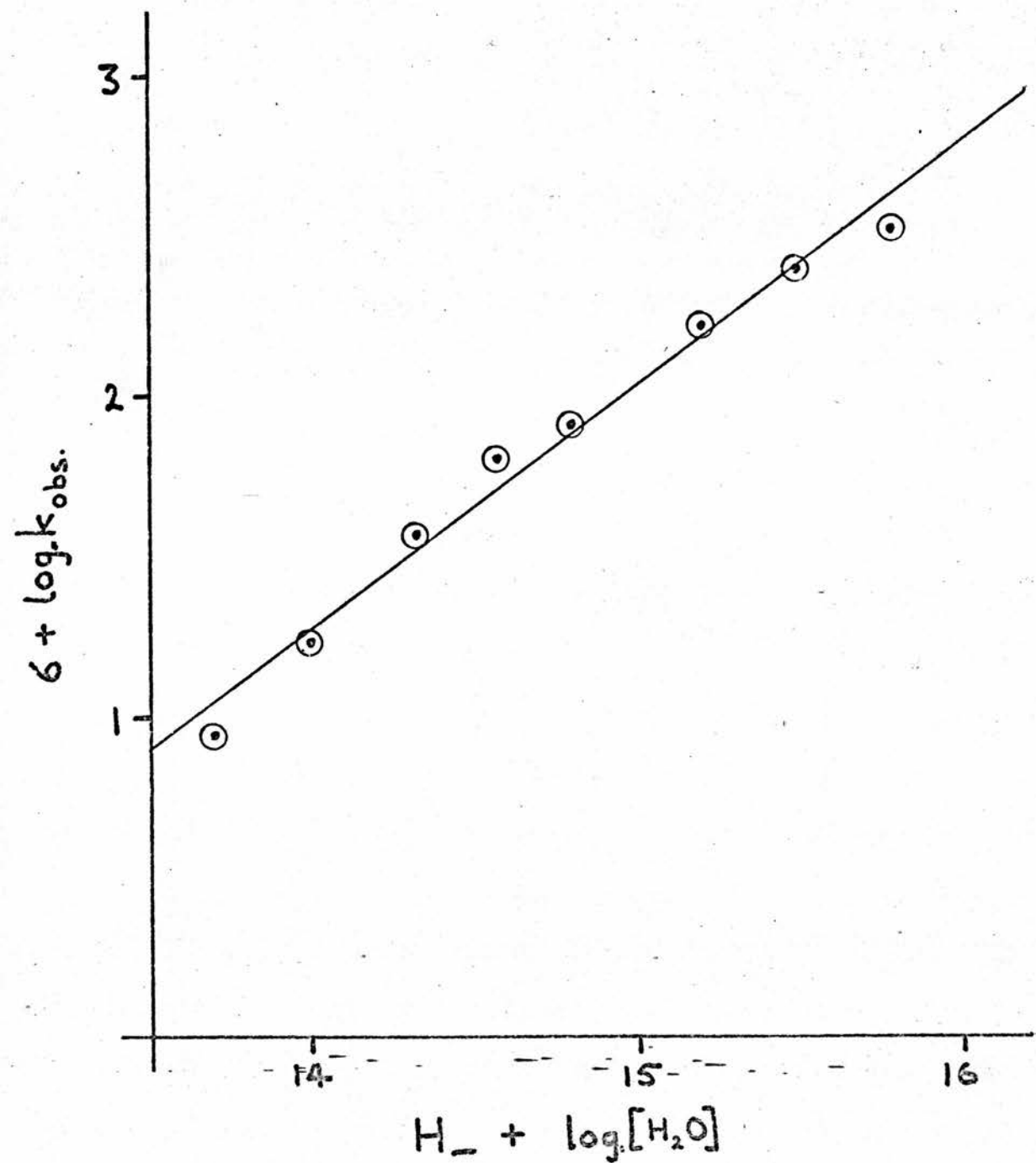
is a better description of the experimental results than alternative formulations such as those suggested by Yagil and his co-workers.⁽⁴⁸⁾

The kinetic form of the results for indole are therefore not inconsistent with the reaction scheme for the base-catalysed hydrogen exchange outlined in the previous section, (equation (3.4)).

Figure (3.5).

Detritiation of 3- ^{3}H indole in sodium hydroxide.

Variation of $\log. k_{\text{obs}}$ with $(H_- + \log. [\text{H}_2\text{O}])$.



Measurement of Kinetic Isotope Effects.2-methylindole.

The rate of proto-detritiation of 2-methyl-3[³H]indole in aqueous sodium hydroxide at an ionic strength of 0.1 (maintained by addition of NaCl) was measured. The bimolecular rate coefficient for the hydroxide ion, defined by equation (3.13)

$$v = k_{\text{OH}^-}^{\text{T}} [\text{Indole-T}][\text{NaOH}] \quad \dots\dots\dots (3.13)$$

was found to be

$$k_{\text{OH}^-}^{\text{T}} = 4.54 \times 10^{-4} \text{ l.mole}^{-1} \text{ sec.}^{-1}$$

in excellent agreement with the previous study.⁽³³⁾

The analogous results for the proto-dedeuteriation of 2-methyl-3[²H]indole are presented in TABLE (3.6)a.

The detritiation of 2-methyl-3[³H]indole was also studied in solutions of aqueous (D₂O) sodium deuterioxide, in which the atom fraction of deuterium was greater than 0.99. These results are summarised in TABLE (3.7).

TABLE (3.6)_aProto-dedeuteriation of 2-methyl-3-[²H]indole in dilute NaOH at 25°C. $\mu = 0.1.$

Kinetic	[NaOH]	[NaCl]	$10^5 k_{\text{obs}}$	$10^4 k_{\text{OH}^-}^{\text{D}} *$
Run	.10 ² M.	.10 ² M.	sec. ⁻¹	l.mole ⁻¹ sec. ⁻¹
4	10	-	9.05	9.05
5	10	-	9.05	9.05
10	8	2	7.30	9.13
9	6	4	6.00	8.57
11	5	5	4.33	8.66
12	3	7	2.90	9.67
7	1	9	0.88	8.80

$$\therefore 10^4 \times \text{Mean value } k_{\text{OH}^-}^{\text{D}} = 9.0 \pm 0.3$$

* The values of $k_{\text{OH}^-}^{\text{D}}$ in column 5 are calculated by dividing the k_{obs} values in column 4 (defined by equation (3.14)), by the

$$v = k_{\text{obs}} [\text{Indole-D}] \quad \dots\dots\dots (3.14)$$

appropriate [NaOH].

TABLE (3.7)

Deuterio-detrutiation of 2-methyl-3-[³H]indole in D₂O/NaOD. $\mu = 0.1044.$

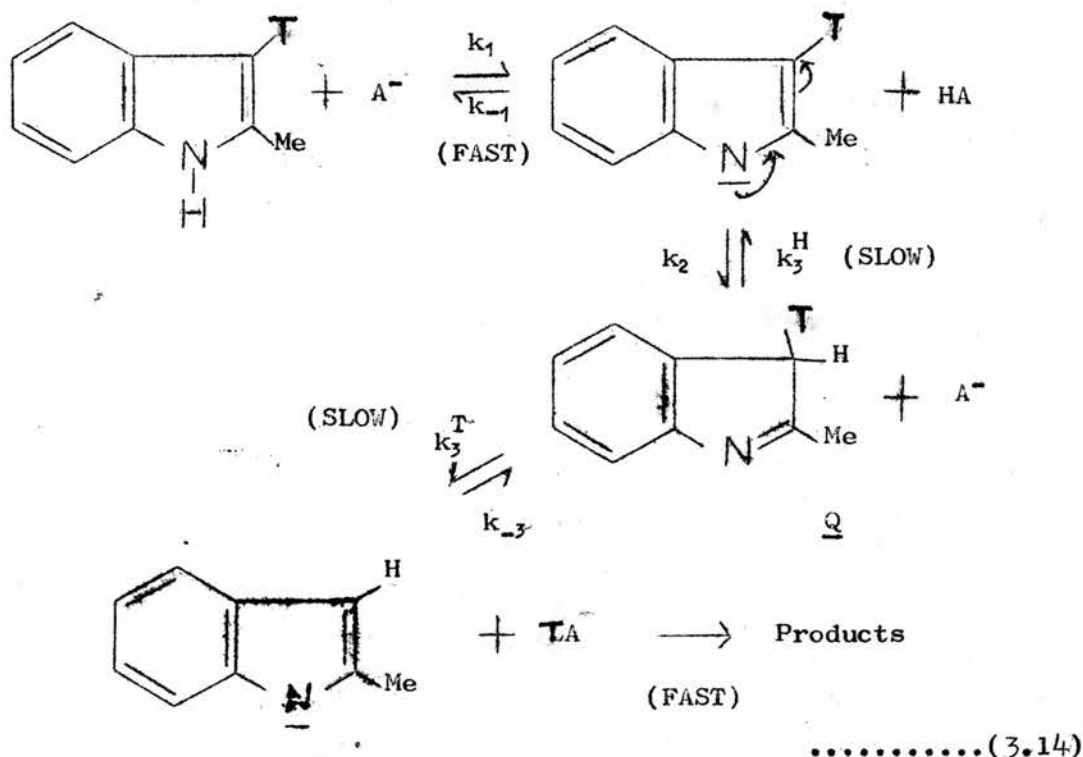
Kinetic	[NaOD]	[NaCl]	$10^5 k_{\text{obs}}$	$10^4 \bar{k}_{\text{OD}^-}^{\text{T}}$
Run	.10 ² M.	.10 ² M.	sec. ⁻¹	l.mole ⁻¹ sec. ⁻¹
40	10.44	-	3.78	3.62
41	6.06	4.38	2.15	3.55
42	3.90	6.54	1.32	3.38
43	0.94	9.50	0.34	3.61

$$\text{Mean value } \bar{k}_{\text{OD}^-}^{\text{T}} = 3.54 (\pm 0.08) \times 10^{-4} \text{ l.mole}^{-1} \text{ sec.}^{-1}$$

where, as before, a bar over the symbol, k, refers to solvent D₂O.

The observation that the rate of loss of deuterium from 2-methyl-3-[^2H]indole is approximately twice that for loss of tritium from 2-methyl-3-[^3H]indole (i.e. there is an appreciable isotope effect) suggests that the rate-controlling process in the base-catalysed exchange reaction is the step, or series of steps, involving isotopic substitution. This conclusion is therefore in good agreement with the suggested reaction scheme (page 81 equation (3.4)) based on the kinetic form of the reaction in concentrated solutions of sodium hydroxide. However, the significance of the observed isotope effect in relation to the detailed reaction mechanism requires further argument.

Since, as noted previously (p. 77), the proto-detrutiation of 1,2-dimethyl-3-[^3H]indole is not catalysed by hydroxide ion, the base-catalysed reaction must involve **initial ionisation of the N-proton**. In addition, direct attack of the base (e.g. OH^-) on the isotopic hydrogen can probably be excluded as the 3-position is a basic rather than an acidic site. A push-pull mechanism involving both the catalysing base (reacting with the N-proton) and its conjugate acid (attacking the 3-position) seems unlikely on the general grounds of the improbability of termolecular reactions, but is not excluded by the above results. These observations, together with the observed isotope effect and the results from kinetic studies of the reaction of other indoles in concentrated sodium hydroxide, suggest that the "most likely" mechanism for hydrogen exchange is that illustrated by equation (3.14) which is identical to equation (3.1). In this, a rapid reversible ionisation of the N-proton (k_1 , k_{-1}) is followed



by two relatively slow steps (k_2 and k_3^T). If k_3^T is slow, then k_3^H is of comparable magnitude, differing from k_3^T by the usual tritium/hydrogen isotope effect (maximum ca. 16). This, in turn, implies that k_2 is not appreciably faster than k_3^T , otherwise spectral changes corresponding to the formation of the indolenine tautomer (Q) would have been observed. Application of steady state kinetics⁽³⁹⁾ then produces the following rate laws (equations (3.15) - (3.17)) for detritiation by this mechanism.

$$v = k_A^T [\text{In-T}][\text{A}^-] \quad \dots\dots\dots (3.15)$$

$$= \frac{k_2 k_3^T}{k_3^H + k_3^T} [\text{In-T}][\text{HA}] \quad \dots\dots\dots (3.16)$$

$$= \frac{k_2 k_3^T}{k_3^H + k_3^T} [\text{In-T}][\text{A}^-] \frac{K_{\text{HIn}}}{K_{\text{HA}}} \quad \dots\dots (3.17)$$

(Since $k_{bi} = \frac{k_2 k_3^T}{k_3^H + k_3^T}$ (see page 81), then for OH^- catalysis,

it follows from equations (3.15) - (3.17) that

$$k_{bi} = k_{\text{OH}^-}^T \cdot \frac{K_{\text{H}_2\text{O}}}{K_{\text{HIn}}} \quad \dots\dots\dots (3.9)$$

In the above equations, K_{HIn} and K_{HA} are the ionisation constants for substrate and catalysing acid respectively, and the symbol In-T represents 2-methyl-3-[^3H]indole. These equations are consistent with the observed general base catalysis and the mechanism differs from that for the acid catalysed reaction discussed in Chapter II, only in that the substrate is now the indole anion rather than the neutral molecule. The base catalysed reaction may therefore be considered as another process of the $\text{S}_{\text{E}}-2$ type.

The observed rates of proto-detritiation and proto-dedeuteriation may be analysed to yield a value of the primary isotope effect (k_3^H/k_3^D) for loss of isotopic hydrogen from the indolenine intermediate, in the manner discussed in p. 28 for the acid catalysed exchange reaction.

$$k_{OH^-}^D = \frac{k_2}{k_3} \frac{k_3^D}{k_3^H} \cdot \frac{K_{HIn}}{K_{H_2O}} \quad \dots\dots\dots (3.18)$$

$$k_{OH^-}^T = \frac{k_2}{k_3} \frac{k_3^T}{k_3^H + k_3^T} \cdot \frac{K_{HIn}}{K_{H_2O}} \quad \dots\dots\dots (3.19)$$

Combination of equations (3.18) and (3.19) with the aid of Schaad's formula⁽⁵²⁾ leads to:

$$\frac{k_3^H}{k_3^D} = 5.7 \pm 0.6$$

for the H₂O-catalysed exchange reaction on the anion of 2-methylindole.

Further support for the proposed mechanism comes from a calculation of the ratio $k_2^{H_2O} / k_2^{D_2O}$ which compares the rates of proton addition to the 3-position (of the indole anion) by the solvents H₂O and D₂O respectively. The rate coefficient relationships for these reactions are given below.

$$k_{OH^-}^T = \frac{k_2^{H_2O} \cdot k_3^T}{k_3^H + k_3^T} \cdot \frac{K_{HIn}}{K_{H_2O}} = 4.54 \quad \dots\dots\dots (3.20)$$

$$k_{OD^-}^T = \frac{k_2^{D_2O} \cdot k_3^T}{k_3^D + k_3^T} \cdot \frac{K_{HIn}}{K_{D_2O}} = 3.54 \quad \dots\dots\dots (3.21)$$

Equations (3.20) and (3.21) can be solved in the manner described on p. 28 for the acid catalysed reaction to yield:

$$\frac{k_2^{H_2O}}{k_2^{D_2O}} \cdot \frac{K_{HIn} \cdot \bar{K}_{D_2O}}{\bar{K}_{HIn} \cdot K_{H_2O}} = 5.6 \quad \dots\dots\dots (3.22)$$

Since the acid dissociation constants at 25° of H₂O (15.74) and 2-methylindole (ca. 17⁽⁵³⁾) are closely similar, the ratio

$\frac{K_{\text{HIn}} \cdot \bar{K}_{\text{D}_2\text{O}}}{\bar{K}_{\text{HIn}} \cdot K_{\text{H}_2\text{O}}}$ is expected to be approximately unity. (54,55)

Thus,
$$\frac{k_2^{\text{H}_2\text{O}}}{k_2^{\text{D}_2\text{O}}} = 5.6 \pm 1$$

Although both the $k_3^{\text{H}}/k_3^{\text{D}}$ and $k_2^{\text{H}_2\text{O}}/k_2^{\text{D}_2\text{O}}$ ratios reported here are uncorrected for secondary isotope effects, their magnitudes are consistent with the exchange mechanism illustrated by equation (3.14).

Indole

Primary isotope effects ($k_3^{\text{H}}/k_3^{\text{D}}$) were measured also for the base-catalysed β -hydrogen exchange with indole, itself. The data for the hydroxide ion catalysed exchange are summarised in TABLE (3.8).

TABLE (3.8)

Proto-detrutiation of 3[³H]indole in aqueous NaOH.

Kinetic Run	[OH ⁻] M.	10 ⁶ k _{obs} sec. ⁻¹	10 ⁶ k _{OH⁻} l.mole ⁻¹ sec. ⁻¹
104	1	17.8	17.8
106	0.5	8.85	17.7

Proto-dedeuteriation of 3[²H]indole in aqueous NaOH.

269	1	33.2	33.2
270	1	32.1	32.1
268	0.8	24.7	30.1
267	0.4	11.5	28.8

The mean values of the respective coefficients in column 4 are:

$$k_{OH^-}^T = 17.8 (\pm 0.1) \times 10^{-6} \text{ l.mole}^{-1} \text{ sec.}^{-1}$$

$$k_{OH^-}^D = 31.1 (\pm 1.6) \times 10^{-6} \text{ l.mole}^{-1} \text{ sec.}^{-1}$$

from which one obtains in the usual way (p. 28)

$$\underline{k_3^H/k_3^D = 4.4 \pm 0.5}$$

for the H_2O -catalysed exchange reaction on the indole anion.

Similarly, the corresponding isotopic rate ratio when the basic catalyst is pyridine can be evaluated from the data presented previously on page 42

$$\underline{k_3^H/k_3^D = 10 \pm 4}$$

for the PyH^+ -catalysed exchange reaction on the indole anion.

Conclusions from Kinetic Isotope Effect Values.

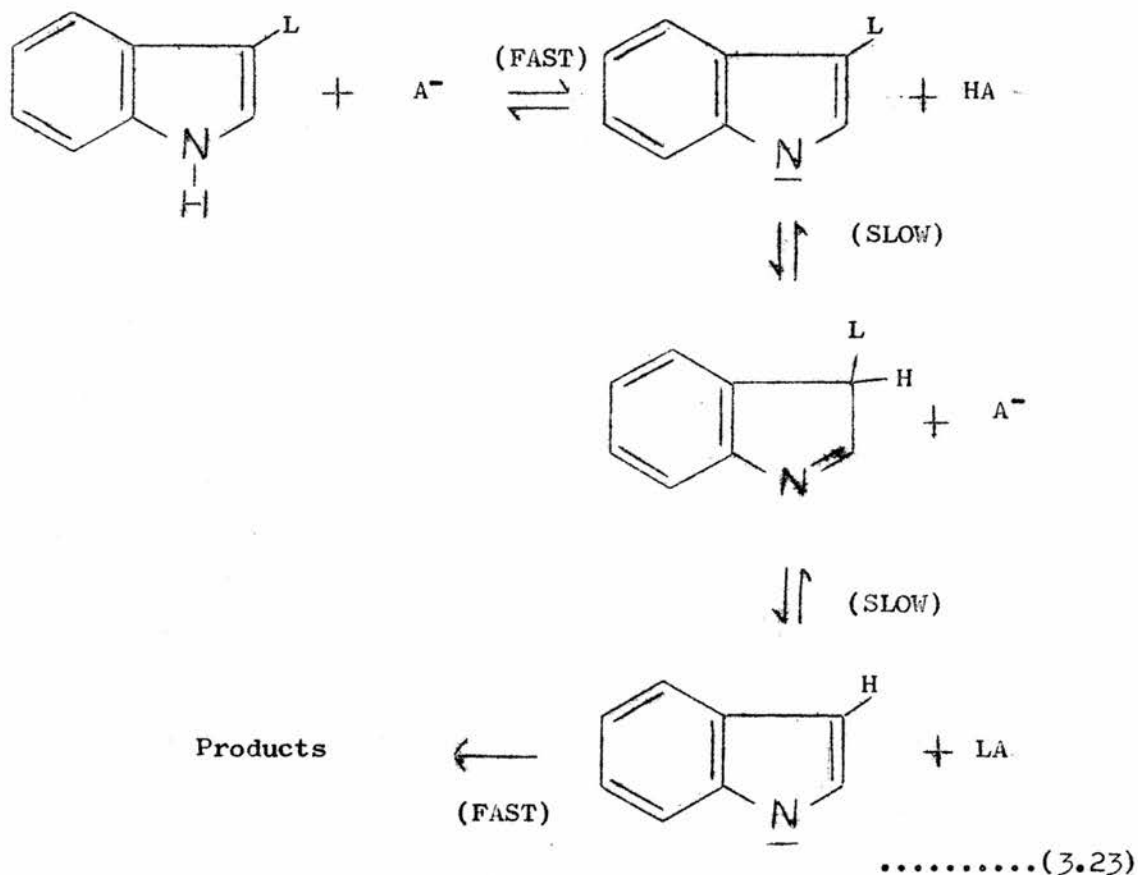
- a) The existence of relatively large difference in the rates of proto-detritiation and proto-dedeuteriation of the labelled substrates 2-methylindole and indole, together with the arguments presented on pages 98-100 , support the proposed reaction mechanism (equation (3.14)) for base catalysed hydrogen exchange on the indole nucleus.
- b) By assuming that this mechanism is correct (i.e., an S_E-2 type exchange on the indole anion), evaluation of the kinetic isotope effect (k_3^H/k_3^D) is possible. Less emphasis can be placed on the value obtained for the pyridine catalysed exchange on indole, due to the large errors involved. Nevertheless, this value (for pyridine catalysis), as well as those obtained for the hydroxide ion catalysed exchange on both indole and 2-methylindole, is consistent with a slow conjugate-acid

catalysed exchange process on the indole anion.

(c) Although the limited amount of experimental data restricts any arguments based on the absolute magnitude of the observed isotopic rate ratios, it is encouraging to note that the values of k_3^H/k_3^D for the base-catalysed exchange reaction are not inconsistent with those previously reported in Chapter II for the $A-S_E2$ reaction.

Discussion

The bulk of the experimental evidence suggests that the general-base catalysed isotopic hydrogen exchange on the indole nucleus is, in fact, a rate-determining reaction of the indole anion with the conjugate acid of the general base, i.e.



This conclusion, however, is in apparent conflict with the magnitude of the Brønsted β -parameter determined by Challis and Long.⁽³⁴⁾ They found $\beta = 0.14$ for the proto-deutritiation of 2-methyl-3-[³H]indole, which leads to a value of $\alpha = 0.86$ ($\equiv 1 - \beta$) for the rate-determining step. This value of α , if considered as a measure of the degree of proton transfer in the transition state is unusual on two counts.

(1) It is considerably lower than the corresponding value for general-acid catalysed exchange of the neutral 2-methyl-3-[³H]indole ($\alpha = 0.58$). Since the anion is obviously the more basic species, the difference in the two α -values is opposite to that expected.

(2) The observed kinetic isotope effect for 2-methyl-3-[³H]indole anion ($k_3^H/k_3^D = 5.7$) is indicative of a nearly symmetrical transition state, whereas the $\alpha = 0.86$ suggests a very unsymmetrical transition state with almost complete proton transfer. Although it has been noted previously on page 66 that the magnitude of the α -parameter may not be a reliable criterion of transition state symmetry, the discrepancies in the present case are sufficiently large to promote further discussion of the mechanism of the base catalysed reaction.

One possible explanation of this unusual α -factor is that it might not refer to a rate-controlling isotopic hydrogen exchange on the indole anion. That is, for the studies with weakly basic catalysts (which lead to evaluation of the α ($\equiv \beta - 1$) factor) the exchange process may be preceded by a slow (rate-determining), rather than a fast pre-equilibrium anion formation. If this is the case, then the β -exponent of the Brønsted equation for general base catalysis would refer to the pre-equilibrium process and hence

would not be convertible to an α -factor for acid catalysed reaction of the indole anion. This explanation is not very satisfactory, since the large isotope effect ($k_3^H/k_3^D = 10$) observed for the pyridine catalysed exchange on indole itself, seems to indicate that even for a weakly basic catalyst, the initial N-H ionisation is not the rate-controlling reaction step.

Another possible explanation for the unusually high value of the α -factor for the general-base catalysed exchange reaction of 2-methylindole is concerned with the stability of the indolenine intermediate. If this species is very unstable, then the proton will, as a consequence, be very close to the remainder of the molecule in the transition state. In this case, the magnitude of the k_3^H/k_3^D ratio, which is indicative of a nearly symmetrical transition state, becomes difficult to interpret. The implication of these considerations may be that the isotopic rate ratio (k_3^H/k_3^D) is reasonably constant, even for unsymmetrical transition states, as in the acid catalysed exchange reaction discussed in Chapter II. Again, this conclusion is difficult to justify entirely, since it suggests that the α -parameter is in fact a reliable measure of the degree of proton transfer in the transition state, whereas the isotope effect is not: this is contrary to the good correlation found, for the acid catalysed reaction, between α and k^H/k^D .

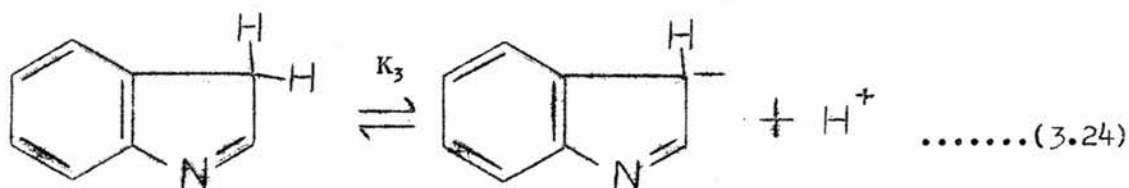
An alternative Brønsted relationship may be evaluated, which refers to the variation in reaction rate of the various substituted indoles studied with a single catalyst - in this case H_2O , from the OH^- -catalysed reactions. Thus the data for these OH^- -catalysed

reactions is summarised in TABLE (3.9) for convenience: $k_{OH^-}^T$ refers to the experimental second-order coefficient obtained from equation (3.2), and k_{bi} is the second-order coefficient calculated on the assumption that the reaction involves rapid formation of the indole anion followed by two relatively slow steps (Equation (3.23)).

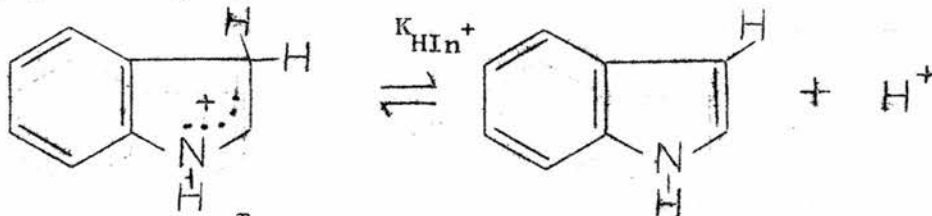
TABLE (3.9)

Substrate	$10^6 k_{OH^-}^T$ $\text{l.mole}^{-1} \text{sec.}^{-1}$	$10^7 k_{bi}$ $\text{l.mole}^{-1} \text{sec.}^{-1}$	pK_{HIn}	pK_{HIn}^+
2-methyl-5-nitroindole	270	149	14.48	-3.6
5-bromoindole	23.4	85.0	15.30	-4.3 ⁽⁵³⁾
5-cyanoindole	12.5	25.5	15.05	-6.0
5-nitroindole	7.85	7.67	14.73	-7.4
6-nitroindole	13.2	7.25	14.48	-6.9
2-methylindole	454	77,000	16.97 ⁽⁵³⁾	-0.3
indole	17.8	3,020	16.97	-3.5

Thus if N-H ionisation were the rate determining step, then a Brønsted correlation should exist between $k_{OH^-}^T$ and the K_{HIn} value (where K_{HIn} is the acid dissociation constant for N-H ionisation). On the other hand, a slow reaction of the indole anion with H_2O should lead to a Brønsted correlation between k_{bi} and some other constant expressing the basicity of the 3-position of the indole anion, i.e. K_3 for equation (3.24). It seems unlikely that K_3 will be directly related



to K_{HIn} , but it should be proportional to (although numerically different from) K_{HIn}^+ , the acid dissociation constant for the conjugate acid, e.g.



The plots of $\log k_{\text{OH}^-}^{\text{T}}$ vs. $\text{p}K_{\text{HIn}}$, and $\log k_{\text{bi}}$ vs. $\text{p}K_{\text{HIn}}^+$ are illustrated by FIGURES (3.6) and (3.7) respectively. The slope of approximately -0.1 obtained for FIGURE (3.6) shows unambiguously that the data are inconsistent with a mechanism involving a slow N-H ionisation.

Furthermore, it can be seen that methyl group substitution in the indole 2-position leads to considerable rate enhancement (relative to the corresponding indoles with no 2-substituent) without significant alteration of the $\text{p}K_{\text{HIn}}$; this is only consistent with a slow attack of H_2O on the indole anion. This latter conclusion receives positive support from the plot of $\log k_{\text{bi}}$ vs. $\text{p}K_{\text{HIn}}^+$ (FIGURE (3.7)), where the slope obtained ($\alpha = 0.37$) is, likewise, consistent with a rate-determining reaction between the indole anion and H_2O . The magnitude of the α -factor is, however, surprisingly different from that obtained for studies of the reaction between 2-methyl-3-[^3H]indole and varying catalysts ($\alpha = 0.86$). This probably arises from the fact that K_{HIn}^+ is only proportional to K_3 (i.e. $\Delta\text{p}K_{\text{HIn}}^+ \approx \Delta\text{p}K_3$) and therefore the slope of the plot of $\log k_{\text{bi}}$ vs. $\text{p}K_{\text{HIn}}^+$ reflects this proportionality too. Also, it is interesting to note that indoles unsubstituted in the aromatic ring give rise to a different, but parallel Brønsted plot. This

FIGURE (3.6) Proto-detrition of indoles in NaOH.

Plot of $\log k_{OH^-}^T$ vs pK_{HIn}

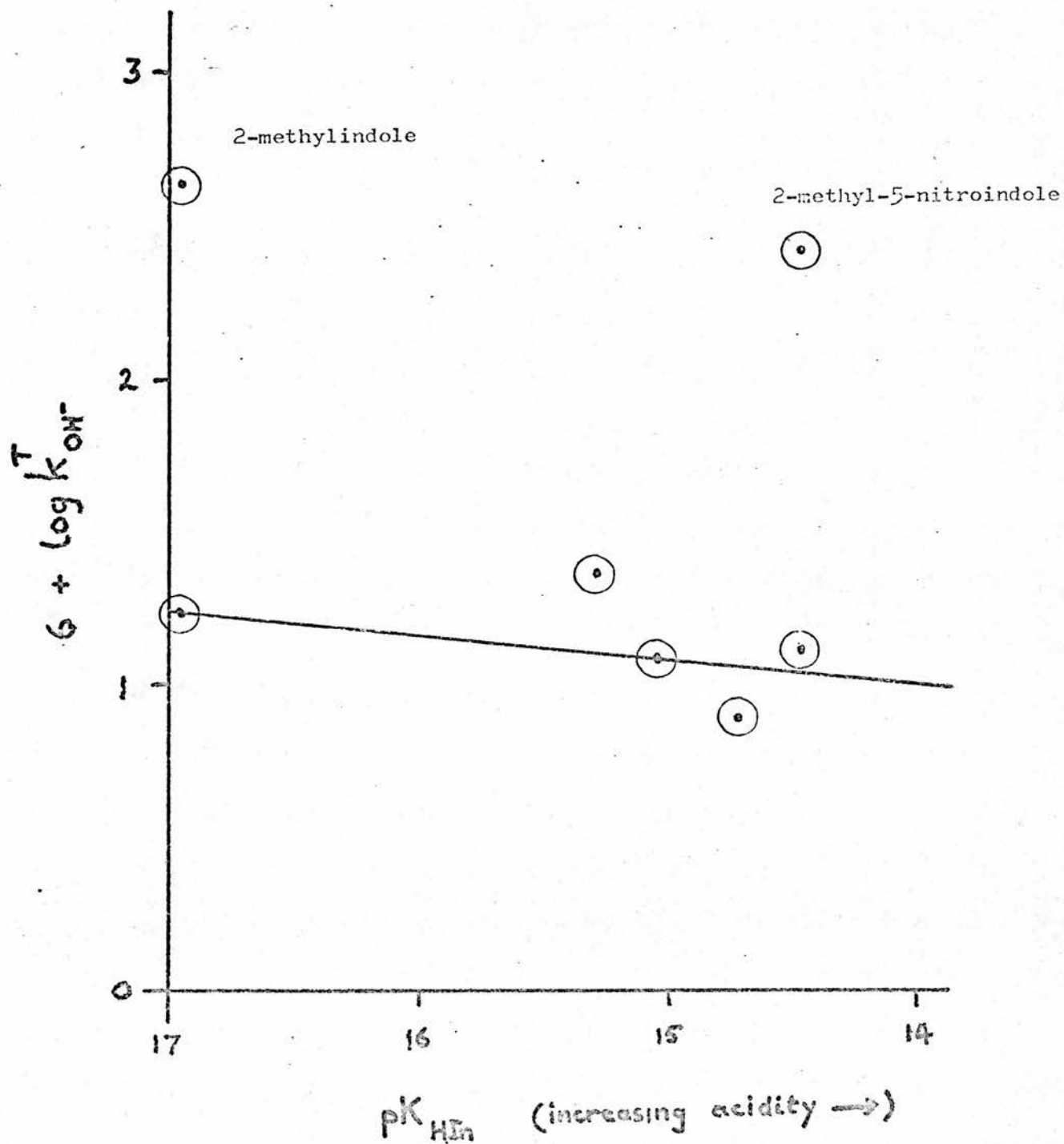
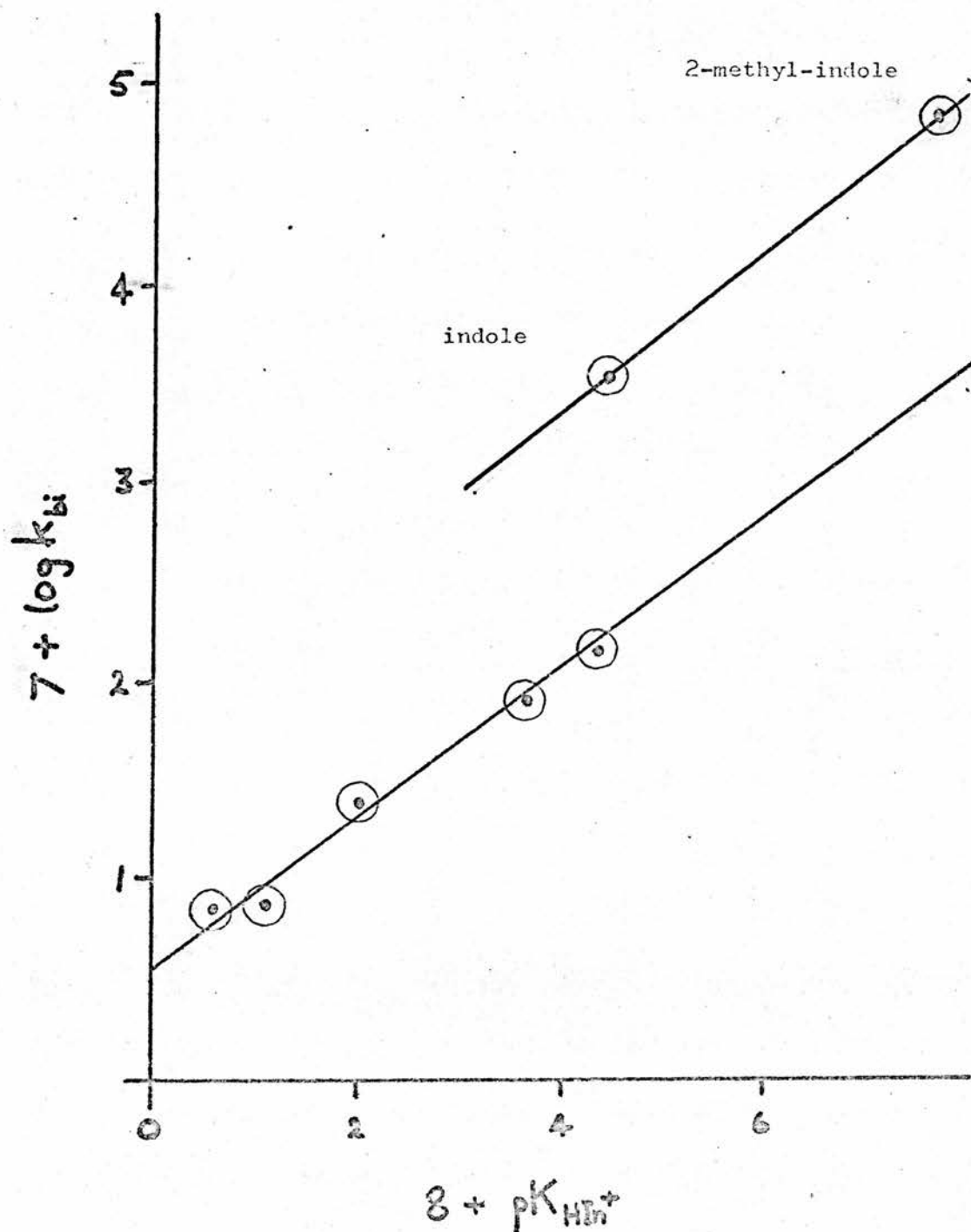
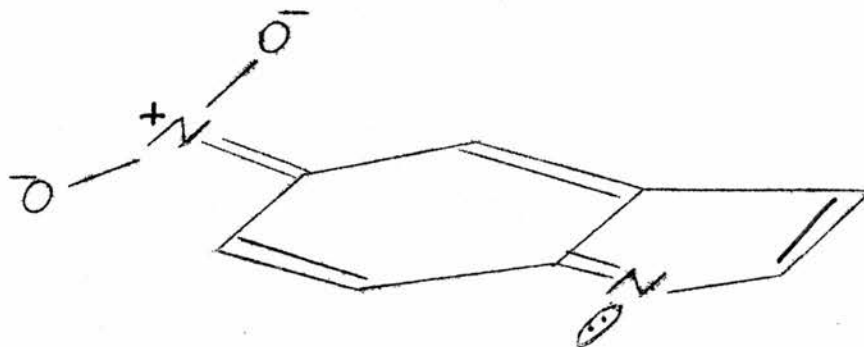
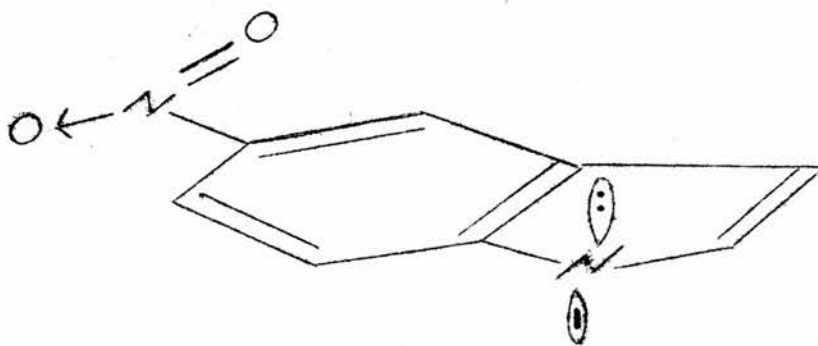


FIGURE (3.7) Proto-detrition of indoles in NaOH

Plot of $\log k_{bi}$ vs pK_{HIn}^+



may arise from conjugation between the 5-substituent and the negative charge on the heterocyclic nitrogen reducing the conjugation of the heterocyclic nitrogen lone pairs with the 3-position. The effect of extensive conjugation with the 5-substituent produces sp^2 hybridisation of the N atom. In this situation, the lone pair orbital will be **planar** with the heterocyclic ring with considerable reduction of the electron overlap (e.g. as shown below for 5-nitroindole).



Conclusion

The proposed mechanism for base catalysed hydrogen exchange on the indole nucleus (equation (3.23), page 104), i.e. a rate-determining attack on the indole anion by the conjugate acid of the basic catalyst, is consistent with most of the experimental evidence, namely

- (1) the existence of appreciable kinetic (primary) isotope effects
- (2) the kinetic form of the reaction in concentrated solutions of sodium hydroxide
- (3) the Brønsted factor ($\alpha = 0.37$) referring to the variation in reaction rate of several substituted indoles with a single catalyst.

The problem of correlating the value of the Brønsted factor ($\alpha = 0.86$) for the reaction of 2-methyl-3-[^3H]indole with varying catalysts, with the other data, remains largely unsolved. It seems doubtful that considerations such as (1) a change in the rate-determining reaction step or (2) the stability of the indolenine intermediate, can successfully account for this unusual Brønsted parameter.

PART III

EXPERIMENTAL

CHAPTER IV

THE EXPERIMENTAL DETAILS

The Kinetic Methods

All kinetic experiments were carried out in stoppered volumetric flasks well immersed in a thermostat at $25 \pm 0.1^{\circ}\text{C}$, and where feasible the ionic strength of the reaction mixture was maintained at 0.1 by the addition of sodium chloride.

Stock buffer solutions were generally prepared so that a tenfold dilution gave the required concentration for the kinetic experiments. Only in the case of pyridine, were the buffer solutions prepared directly for each reaction, by adding a weighed amount of 'Analar' pyridine and a measured volume of standard hydrochloric acid to the reaction flask. To minimise errors, where possible, the same catalyst solution was used for the parallel detritiation and dedeuteriation studies. Good agreement between the calculated and measured values of the pH of the buffer solutions was found.

Proto-detritiation.

Tritium is a soft β -particle emitter with a $t_{\frac{1}{2}} = 12$ years, and the reaction is conveniently followed by measuring the rate of loss of the isotopic species from the labelled substrate. Since tritium has such a long half-life, no significant errors in the rate measurements can occur as a result of spontaneous radio-active decay.

Nearly saturated solutions of the tritiated indole were prepared by stirring the compound in distilled water for about two hours. The necessary amount of the catalyst solution was added to a volumetric

flask. The contents of the flask were then made up to the calibration mark with the filtered aqueous solution of the labelled indole. Normally, catalyst and indole solutions were temperature adjusted to 25°C before mixing. (For the reaction in high [NaOH] however, both solutions were pre-cooled to ca. 5°C, in order to prevent overheating of the mixture upon dilution of the concentrated sodium hydroxide. The temperature was then rapidly adjusted to 25°C.) At suitable timed intervals, 10 ml. aliquots of the reaction solution were removed with a pipette and run into a 60 ml. reagent bottle containing 15 ml. xylene plus, for the acid-catalysed kinetic runs, sufficient aqueous sodium hydroxide solution to neutralise the reaction sample to pH 8-10, which effectively stopped the reaction. The bottle was then shaken manually for 1 minute, after which the contents were allowed to stand for about 1 hour, to effect complete separation of the aqueous and xylene phases. (The distribution coefficient of the indole between water and xylene is such that virtually 100% extraction of the compound from the aqueous to the xylene phase, takes place.) 10 ml. of the xylene layer was then transferred to a low-potassium glass vial containing 5 ml. scintillator solution.* The radioactive assay was made with a Beckmann Liquid Scintillation Counter (Model LS 100). Except in those cases where the indole had an extremely low solubility in water, the initial sample had an activity of ca. 10,000 - 40,000 counts per minute. Readings at infinity, 10 times the measured half-life of reaction, were also taken, but usually were of such a magnitude, as to be

* The scintillator solution consisted of xylene (1 l.)

2,5-diphenyloxazole (10 g.) and

1,4-bis[2-(4-methyl-5-phenyloxazolyl)]benzene (0.25 g.),

negligible in the rate coefficient calculations.

Typical Kinetic Runs.

Three examples are given here to illustrate the various conditions in which the reaction has been studied. The results all refer to an observed first-order rate coefficient (k_{obs}) defined by:

$$\text{Rate} = k_{\text{obs}} [3[^3\text{H}]\text{indole}]$$

k_{obs} is determined from the integrated first-order rate equation:

$$k_{\text{obs}} = \frac{2.303 [\log_{10} (\text{c.p.m.}_{t_1} - \text{c.p.m.}_{t_{\infty}}) - \log_{10} (\text{c.p.m.}_{t_2} - \text{c.p.m.}_{t_{\infty}})]}{t_1 - t_2}$$

In this, $\text{c.p.m.}_t \propto [3[^3\text{H}]\text{indole}]_t$ and t refers to the time at which the sample was taken. Time zero was taken as the time at which the first sample was extracted in each kinetic experiment; this was always after attainment of temperature equilibrium at $25 \pm 0.1^\circ$.

(I) Proto-detrition of 5-nitro-3[³H]indole.

Run 98

[NaOH] = 5.17M.

Time t (hours)	Counts per Minute (c.p.m. _t)	c.p.m. _t - c.p.m. _{t_∞}	% Reaction	10 ⁵ k _{obs} sec. ⁻¹
0	8,238	8,209	-	-
4.1	6,857	6,828	16.5	1.25
10	5,176	5,147	37.2	1.29
22.5	2,854	2,825	65.5	1.32
28	2,209	2,180	73.5	1.32
34	1,682	1,653	79.9	1.31
47	923	894	89.1	1.31
∞	29	-	100	-

mean value k_{obs} = 1.30 x 10⁻⁵ sec.⁻¹

(II) Proto-detrition of 3[³H]indole.

Run 166

[HOAc] = 0.05M.,

[OAc⁻] = 0.05M.,

[NaCl] = 0.05M.

Time t (hours)	Counts per Minute (c.p.m. _{t})	c.p.m. _{t} - c.p.m. _{t_{∞}}	% Reaction	$10^5 k_{\text{obs}}$ sec. ⁻¹
0	33,285	33,242	-	-
1.4	27,628	27,585	17.0	3.70
2.4	24,512	24,469	26.3	3.55
3.5	21,225	21,182	36.2	3.58
5.0	17,638	17,595	47.0	3.53
6.5	14,555	14,512	56.4	3.54
8.5	12,029	11,986	63.9	3.53
∞	43	-	100	-

mean value $k_{\text{obs}} = 3.57 \times 10^{-5} \text{ sec.}^{-1}$

(III) Proto-detrition of 5-cyano-3- ^3H indole.

Run 187

$[\text{HCl}] = 0.099\text{M.}$

Time t (mins.)	Counts per Minute (c.p.m. _{t})	c.p.m. _{t} - c.p.m. _{t_{∞}}	% Reaction	$10^3 k_{\text{obs}}$ sec. ⁻¹
0	25,816	25,729	-	-
7	20,581	20,494	20.3	5.37
14	16,395	16,308	36.7	5.32
21	13,522	13,435	47.8	5.14
28	10,754	10,667	58.5	5.22
35	8,720	8,633	66.5	5.20
42	7,093	7,006	72.8	5.16
∞	87	-	100	-

mean value $k_{\text{obs}} = 5.24 \times 10^{-3} \text{sec.}^{-1}$

Precision of the Measured Rate Coefficients.

The high precision of the kinetic method is shown by the typical kinetic runs. Possible errors arising from temperature differences and mixing of substrate and catalyst solutions were minimised by the choice of the first kinetic point as t_0 . Quenching of samples by pyridine was considerable, causing a reduction of up to 80% of the c.p.m. for some samples. However, the effect was shown to be constant for any single kinetic run, by counting a series of radioactive samples, first without, then with, a constant volume of added pyridine. The detritiation studies in deuterium oxide were done on a reduced scale (25 ml.). It was shown by repeating a proto-detritiation on this smaller scale, that no significant additional errors were introduced by the reduced scale. That the sources of error had been effectively dealt with, is evident from the fact that the error in the rate coefficient measurements never exceeded $\pm 2\%$.

Proto-dedeuteriation

The rate of proto-dedeuteriation was estimated by quantitative measurement of infra-red absorptions corresponding to either C-H or C-D out-of-plane bending vibrations in the $500\text{--}800\text{ cm.}^{-1}$ region of the spectrum.

The kinetic method, itself, was essentially the same as for the proto-detritiations. Thus the reaction was initiated by adding a temperature adjusted aqueous solution of the deuteriated indole to a concentrated solution of the appropriate catalyst contained at

the same temperature in a volumetric flask. At noted time intervals aliquots were withdrawn with a pipette and run into separating funnels containing a few mls. of a suitable organic solvent and, in the case of the acid-catalysed reactions, sufficient dilute sodium hydroxide solution to neutralise the reaction mixture. After manual shaking for about 2 minutes the organic phase was allowed to separate; this usually required about 15 minutes. The organic layer containing the substrate was then removed in readiness for infra-red analysis.

Infra-red analysis

TABLE (4.1) summarises the experimental conditions used for the various substrates. The organic solvent for extraction of the indole was selected by trial and error and was usually a compromise of a solvent a) in which the indole is readily soluble, b) which has a window region at the frequency of interest and c) which is immiscible with water. Either matched Ag Cl-windowed cells (3mm. path-length) or NaCl-windowed cells (0 - 2.5 mm. path-length) were used. Since matched cells were used, solvent absorptions in the region of interest were effectively cancelled out; where these absorptions were relatively high the cell path-length was reduced to a suitable value. With the exception of the indole absorption at 544 cm^{-1} (C-D), all absorptions correspond to C-H vibrational modes.

A constant extraction was obtained for every compound under the given conditions. This was checked via the infra-red absorption at an appropriate frequency for indole, 5-cyanoindole and 5-methoxyindole, prior to kinetics. For 2-methylindole, the constancy of extraction

TABLE (4.1)

<u>Compound</u>	<u>2-methyl-indole</u>	<u>indole</u>	<u>5-cyano-indole</u>	<u>5-methoxy-indole</u>
<u>Reaction scale.</u>	100 ml.	100 ml.	500 ml.	100 ml.
<u>Approx.wt. of substrate used per run.</u>	50 mg.	100 mg.	250 mg.	100 mg.
<u>Aliquot size</u>	10 ml.	10 ml.	50 ml.	10 ml.
<u>Extraction solvent.</u>	2:2:4-tri-methyl-pentane	2:2:4-tri-methyl-pentane	benzene	carbon disulphide.
<u>Vol. of organic solvent used per aqueous aliquot</u>	5 ml.	5 ml.	2.5 ml.	3 ml.
<u>Cell path-length and window</u>	3 mm., AgCl.	3 mm., AgCl or 2.5 mm., NaCl	0.65 mm., NaCl.	1 mm., NaCl.
<u>Instrument used</u>	Perkin Elmer Model 621	P.E.621 or Grubb-Parsons G.S.2.	Grubb-Parsons G.S.2.	Grubb-Parsons G.S.2.
<u>Wavenumber of absorption maximum used in kinetics</u>	778 cm. ⁻¹	720 cm. ⁻¹ or 544 cm. ⁻¹	775 cm. ⁻¹	756 cm. ⁻¹ or 720 cm. ⁻¹

was measured from the ultra-violet absorption of the kinetic samples (diluted 10 times and spectra run in 1 mm. silica cells) in 2:2:4-trimethylpentane at $37,800\text{ cm.}^{-1}$.

The I.R. bands chosen for analyses had intensities which were unaffected by neighbouring peaks, including those of the other isotopic species. This was checked by analysis of mixtures of ordinary and deuteriated indoles. The optical density of the C-H band was unaffected in every case by the presence of the C-D compound.

Calibration.

Calibration of the I.R. spectrometer was made by measuring the absorption of samples of known concentration of the appropriate indole. Reproducible curved plots of [indole] vs. optical density

$$\left(= \log_{10} \frac{100}{\text{measured \% transmittance}} \right)$$

were obtained in all the cases where a C-H absorption was used.

Calibration of the C-D peak at 544 cm.^{-1} in deuteriated indole, gave excellent Beer-Lambert Law behaviour. Since the extent of isotopic substitution was not accurately known, the calibration was made using a series of solutions of $3[{}^2\text{H}]$ indole which had been prepared by dilution from a stock solution of the deuteriated substrate. Thus, only relative concentrations of the labelled **indole were known**, but since direct proportionality between $[3[{}^2\text{H}]$ indole] and optical density, was found, absolute concentrations were unnecessary.

Calibration control settings and the method of setting a standard base-line were reproduced exactly during the estimation of kinetic samples. Frequent checks on the calibrations were made, and whenever

possible, calibration and kinetic spectra were run on the same day.

Additional Checks on Proto-dedeuteriation Data

Since quantitative infra-red analysis is less reliable (mainly due to instrumental factors) than many other analytical techniques, the data were subjected, where possible, to additional checks, as follows:

1. 3[²H]indole

Early work on the dedeuteriation of 3[²H]indole in acetic acid buffers was done using the C-D absorption at 544 cm.⁻¹. The N-D absorption at 540 cm.⁻¹ which was present during calibrations, but not kinetic runs, was not noticed. (The C-D and N-D bands were unresolved under the conditions used.) The reliability of the data was checked by repeating several kinetic runs, using the C-H peak at 720 cm.⁻¹ for the I.R. analysis. The validity of the initial measurements was confirmed.

2. 5-cyano-3[²H]indole

The C \equiv N absorption maximum at 226 cm.⁻¹ was calibrated and used as a check on the constancy of extraction during kinetic runs. It was also possible to estimate the reaction infinity from this calibration as well as from the C-H peak at 775 cm.⁻¹. Good agreement between the two determinations was always obtained.

3. 5-methoxy-3[²H]indole

Two absorption maxima (720 cm.⁻¹ and 756 cm.⁻¹) were suitable for the I.R. analysis of this compound, and this provided a valuable internal check on the measured reaction rates. Separate calculations for each peak were made, and good agreement of the calculated rate

coefficient~~ts~~ was obtained.

Typical Kinetic Runs

The experimental details of four kinetic runs, one for each indole studied, are given overleaf. As for the proto-detritions, the results refer to an observed first-order rate coefficient k_{obs} defined by:

$$\text{Rate} = k_{\text{obs}} [3[{}^2\text{H}]\text{indole}]$$

k_{obs} is calculated from the integrated first-order rate equation:

$$k_{\text{obs}} = \frac{2.303[\log_{10} [\text{In-D}]_{t_1} - \log_{10} [\text{In-D}]_{t_2}]}{t_1 - t_2}$$

where $[\text{In-D}] \equiv$ concentration of the appropriate deuteriated indole and t_1, t_2 are the sampling times.

$[[\text{In-H}] \equiv$ conc. of the delabelled substrate, is also used as an abbreviation in the following pages.]

(1) Proto-dedeuteration of 2-methyl-3-[²H]indole.

Run 9

[NaOH] = 0.07M.,

[NaCl] = 0.03M.

[In-H]_∞ = 4.08 x 10⁻³M. (from U.V. calibration at 37,800 cm.⁻¹)

[In-H]_t estimated from I.R. calibration at 778 cm.⁻¹

[In-D]_t = [In-H]_∞ - [In-H]_t

Time (hours)	[In-H] _t x 10 ³ M.	[In-D] _t x 10 ³ M	% reaction	10 ⁵ k _{obs} sec. ⁻¹
0	0.97	3.11	-	-
0.5	1.28	2.80	10.0	5.75
1.25	1.71	2.37	24.0	6.03
2.75	2.43	1.65	47.0	6.40
4.25	2.90	1.18	62.1	6.35
5.75	3.17	0.91	70.8	5.95
7.65	3.51	0.57	81.7	6.17
10.75	3.75	0.33	89.4	5.80

Mean value k_{obs} = 6.06 x 10⁻⁵ sec.⁻¹.

(2) Proto-dedeuteration of 3[²H]indole.

Run 258

[Pyridine] = 0.15M., [Pyridine-H⁺] = 0.025M.,

[NaCl] = 0.075M.

[In-D]_t estimated from I.R. calibration at 544 cm.⁻¹ of the C-D absorption band.

Values of [In-D]_t are relative; thus no concentration units have been used.

Time	O.D. (544 cm. ⁻¹)	[In-D] _t	%	10 ⁶ k _{obs}
(hours)	α [In-D] _t	-[In-D] _∞	reaction	sec. ⁻¹
0	0.3695	0.3665	-	-
13	0.2675	0.2645	28.0	6.98
25	0.2065	0.2035	44.5	6.54
38.05	0.1475	0.1445	60.5	6.79
49	0.1130	0.1100	70.0	6.82
61.4	0.0830	0.0800	78.2	6.89
69.2	0.0680	0.0650	82.3	6.93
∞	0.0030	-	-	-

mean value k_{obs} = 6.83 x 10⁻⁶ sec.⁻¹

(3) Proto-dedeuteriation of 5-cyano-3-[²H]indole.

Run 202

$$[\text{HCl}] = 0.05\text{M.}, \quad [\text{NaCl}] = 0.05\text{M.}$$

$$[\text{In-H}]_{\infty} = 4.94 \times 10^{-3}\text{M.} \quad (\text{determined from I.R. calibration of} \\ \text{C} \equiv \text{N absorption at } 226 \text{ cm.}^{-1})$$

$$[\text{In-H}]_t \text{ estimated from } 775 \text{ cm.}^{-1} \text{ calibration.}$$

$$[\text{In-D}]_t = [\text{In-H}]_{\infty} - [\text{In-H}]_t$$

Time	$[\text{In-H}]_t$	$[\text{In-D}]_t$	%	$10^4 k_{\text{obs}}$
(mins.)	$\times 10^3 \text{M.}$	$\times 10^3 \text{M.}$	reaction	sec.^{-1}
0	1.32	3.62	-	-
5	1.82	3.12	13.8	4.97
10	2.24	2.70	25.3	4.86
20	2.92	2.02	44.2	4.85
30	3.42	1.52	58.0	4.83
45	3.95	0.99	72.6	4.80
60	4.28	0.66	81.8	4.72

$$\text{mean value } k_{\text{obs}} = 4.84 \times 10^{-4} \text{ sec.}^{-1}$$

(4) Proto-dedeuteriation of 5-methoxy-3[²H]indole.

Run 228

[HOAc] = 0.05M., [OAc⁻] = 0.05M.,

[NaCl] = 0.05M.

All values of [In-H], including infinity reading, were estimated from I.R. calibration at 720 cm.⁻¹

As before, $[In-D]_t \equiv [In-H]_{\infty} - [In-H]_t$

Time	[In-H] _t	[In-D] _t	%	10 ⁴ k _{obs}
(mins.)	x10 ³ M.	x10 ³ M.	reaction	sec. ⁻¹
0	3.45	15.15	-	-
10	5.0	13.6	10.3	1.80
20	6.5	12.1	20.2	1.88
35	8.7	9.9	34.7	2.03
50	10.5	8.1	46.5	2.10
75	11.9	6.7	55.8	1.82
120	14.36	4.25	71.9	1.76
∞	18.6	-	100	-

mean value k_{obs} = 1.90 x 10⁻⁴ sec.⁻¹

(value using 756 cm.⁻¹ peak, k_{obs} = 1.92 x 10⁻⁴ sec.⁻¹)

Precision of the Measured Rate Coefficients.

The errors here are larger than those for the proto-detritions, but with very few exceptions, the estimated error in the rate coefficient was never in excess of $\pm 5\%$. The main, general source of error was in the infra-red estimation of the concentration of the reaction samples. In particular, for those kinetic runs where the appearance of a peak was studied, the infinity value was critical, thus, whenever possible, an independent measure of this was made, by the various methods reported previously. As before, time zero was taken as the time of the first sampling, to minimise mixing and temperature errors.

Decomposition of 2-methylindole in 2:2:4-trimethylpentane.

It was found that solutions of 2-methylindole in 2:2:4-T.M.P. undergo a light-sensitive decomposition, leading eventually to precipitation of a yellow polymeric solid. The extent of decomposition was reduced to a negligible amount by wrapping the sample containers in tin-foil until such time as the spectra could be recorded. No such decomposition was detected for the other substrates in their appropriate extraction solvents.

Equilibrium Protonation Measurements.

The acid dissociation constants (pK_A) for 2-t-butylindole, 5-cyanoindole and 5-methoxyindole respectively, were determined by the U.V. spectral method of Hinman and Lang.^(31c) The wavelength chosen for the pK_A estimation was selected to obtain large differences between the extinction coefficients of the neutral and protonated indole molecules, and changes in optical density with acidity were therefore at a maximum. The selected wavelengths were close to the maxima of the protonated species, in each case:

2- <u>t</u> -butylindole	45,450 cm^{-1}
5-cyanoindole	42,000 cm^{-1}
5-methoxyindole	45,000 cm^{-1}

The equilibrium measurements were made in sulphuric acid on a Beckmann S.P.700 instrument, using either 1 cm. silica cells (for 2-t-butylindole and 5-cyanoindole) or 10 cm. cells (for 5-methoxyindole). 2-t-butylindole and 5-cyanoindole were stable in the acid solutions, but 5-methoxyindole underwent a decomposition which was minimised by working in very dilute solution (ca. 10^{-6} M final indole concentration). Solutions of final concentration 2×10^{-5} M and 1.2×10^{-5} M were used for 2-t-butylindole and 5-cyanoindole respectively. All solutions were temperature adjusted to $25 \pm 0.1^\circ\text{C}$ before the spectra were quickly recorded. Under the conditions finally chosen, there was no change in the spectrum with time; this indicated that no undesirable side reactions were taking place.

Values: 2-t-butylindole, $pK_A = -0.80$
 5-methoxyindole, $pK_A = -2.9$
 5-cyanoindole, $pK_A = -6.0$

Preparation and Purification of Materials.

Substrates.

Indole and 2-methylindole were B.D.H. reagent grade chemicals; 5-bromo-, 5-cyano-, 5-methoxy-, 5-nitro- and 6-nitroindole were purchased from the Aldrich Chemical Co.; 2-methyl-5-nitroindole was obtained from the Regis Chemical Co. 2-t-butylindole was synthesised by the method of Jönsson.⁽⁵⁶⁾

(m.p. 72-73°, lit. m.p. 73-74°. Anal. Found:

C, 83.05; H, 8.75. Calc. for $C_{12}H_9N$:

C, 83.25; H, 8.7%).

For the spectral measurements, all the substrates were purified by vacuum sublimation to a constant melting point. Good agreement with literature values was obtained in every case.

Preparation of labelled indoles.

The indoles were specifically labelled with deuterium or tritium at the 3 position via either a base- (for indole and 5-methoxyindole) or an acid-catalysed (for all other substrates) process. Since the position of tracer level tritium substitution in an organic molecule cannot be determined by conventional analytical techniques, deuteration of several representative indoles was undertaken, using experimental conditions which differed only from the parallel tritiation in the use of deuterium oxide rather than tritiated water. The position of isotopic substitution was then determined by analysis of the N.M.R. and I.R. spectra of the ordinary and deuteriated indoles.

Acid-catalysed exchange was effected by dissolving the indole (0.2 - 0.5 g.) in a homogeneous solution consisting of 1 - 5M deuterio-sulphuric acid in D_2O (4 ml.) absolute alcohol (5 ml.) and anhydrous

ether (3 ml.). (For the tritiation, a solution of 'Analar' sulphuric acid in tritiated water (final activity = 4 mc. per ml.) was used in place of the deuteriosulphuric acid). The reaction mixture was stirred in the dark at room temperature for about 30 mins. and then neutralised to pH 9 by the addition of anhydrous sodium carbonate. The labelled indole was extracted with anhydrous ether (3 x 5 ml. portions) and the ethereal solution then dried over anhydrous calcium sulphate. The solvent was removed at room temperature under vacuum and the residual solid purified by vacuum sublimation to a constant melting point. TABLE (4.2) compares the melting points of the labelled indoles with the literature values for the non-substituted compounds.

Attempted labelling of indole and 5-methoxyindole by the above method, resulted in extensive decomposition, probably due to dimerisation. (Acid-catalysed deuteration of indole by Hinman and Bauman⁽⁶⁰⁾ resulted in a low (7%) overall yield.) This problem was overcome by using instead a base-catalysed process: the indole (0.5 g.) was dissolved in absolute alcohol (4 ml.); this solution was added to 'Analar' sodium hydroxide (0.8 g.) in deuterium oxide (5 ml.) to give a homogeneous solution, which was stirred in the dark at room temperature for 48 hours. (Tritiated water of 4 mc. per ml. activity was used instead of deuterium oxide for the tritiation). The pH of the solution was then adjusted to 6 by passage of gaseous carbon dioxide. The labelled indole was extracted with ether, isolated and purified, as for the acid-catalysed labelling procedure.

TABLE (4.2)

Melting points^a of labelled indoles compared with literature values for the non-labelled compounds.

Indole	m.p. deuteriated derivative	m.p. tritiated derivative	m.p. indole (non-labelled)	Ref.
5-bromo-	90.5 - 91°	90.5 - 91°	90 - 91°	(57)
2-t-butyl-	-	72 - 73°	73 - 74°	(56)
5-cyano-	106 - 107.5°	106 - 107.5°	107 - 108°	(58)
			104 - 106°	(59)
indole	50 - 52°	50 - 52°	50.5 - 51.5 ^{ob}	(60)
5-methoxy-	54.5 - 56.5°	55 - 56.5°	54 - 55°	(61)
			52 - 53°	(62)
2-methyl-	59 - 60°	57 - 57.5°	59 - 60°	(63)
2-methyl-5-nitro-	-	174°	176 - 176.5°	(64)
5-nitro-	132 - 134° ^c	136 - 138°	141 - 142°	(65)
6-nitro-	144 - 146° ^c	141 - 143° ^c	144 - 145°	(65)

a. Melting points (°C) are uncorrected values.

b. m.p. of 3[²H]indole.

c. Prepared by Challis and Hendry.⁽⁶⁶⁾

Spectral evidence for the position of deuteration.

Nuclear magnetic resonance spectra.

Previous workers⁽⁶⁷⁾ have shown that N.M.R. can be used to determine substitution at the alpha or beta (2 or 3) position of the indole nucleus. The signal attributed to the β -proton occurs at higher field than the signals for the N-, α - and aromatic protons. This criterion was used to determine the site of deuteration in indole and its 5-bromo-, 5-cyano- and 5-methoxy- derivatives. (A similar analysis has been used for 5-nitro-,⁽⁶⁶⁾ 6-nitro-⁽⁶⁶⁾ and 2-methyl-indole.⁽⁵¹⁾)

Spectra of the indoles, before and after deuteration, were compared and in each case only the β -proton signal (high field) was diminished in the deuterated compound (to 0 - 20% of its original intensity, as calculated from the integrated spectrum). This is illustrated by FIGURES (4.1-4) where the spectra of 5-cyano- (FIGURE (4.1)), and 5-bromoindole (FIGURE (4.2)) are compared with those of the deuterated derivatives. (FIGURES (4.3) and (4.4) respectively).

TABLE (4.3) and FIGURE (4.5) show the expected correlation* between the acidity of the β -proton and its chemical shift (τ value). Electron-withdrawing groups at other sites in the indole nucleus

* Jardine and Brown⁽⁶⁸⁾ have shown that although solvent polarity causes marked differences in chemical shift of the signal for the α -proton in indole, only small differences are found in the corresponding signal for the β -(3-position) proton. The correlation of TABLE (4.3) can therefore be satisfactorily made even though the same solvent was not used throughout.

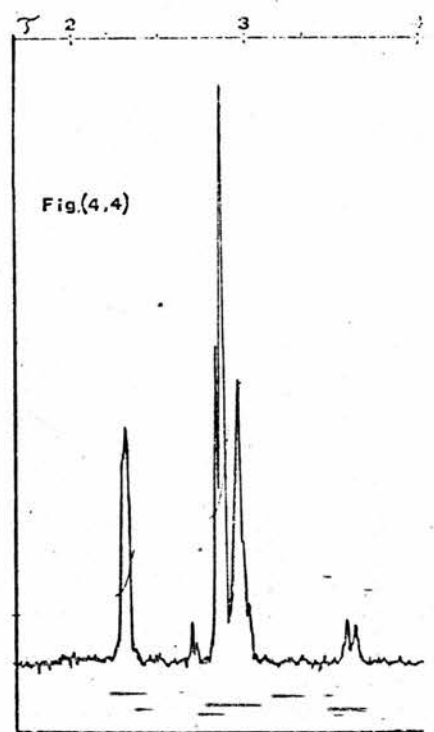
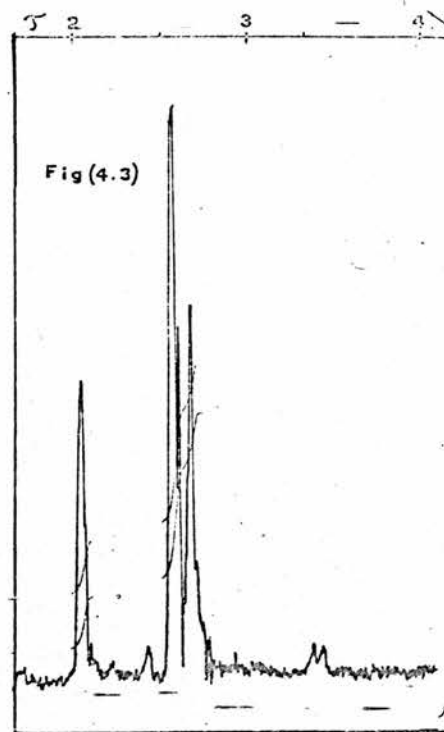
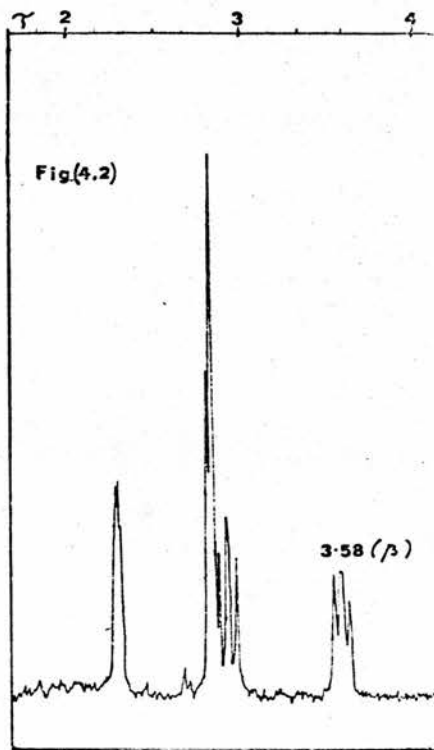
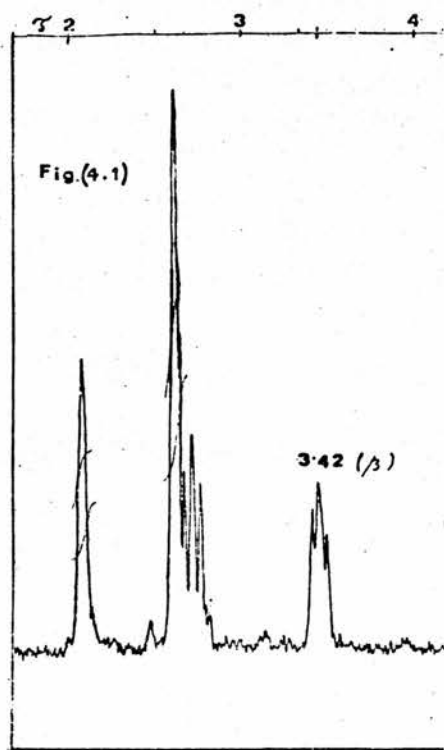


Figure (4.5). Variation of γ (β -proton) with pK of indole

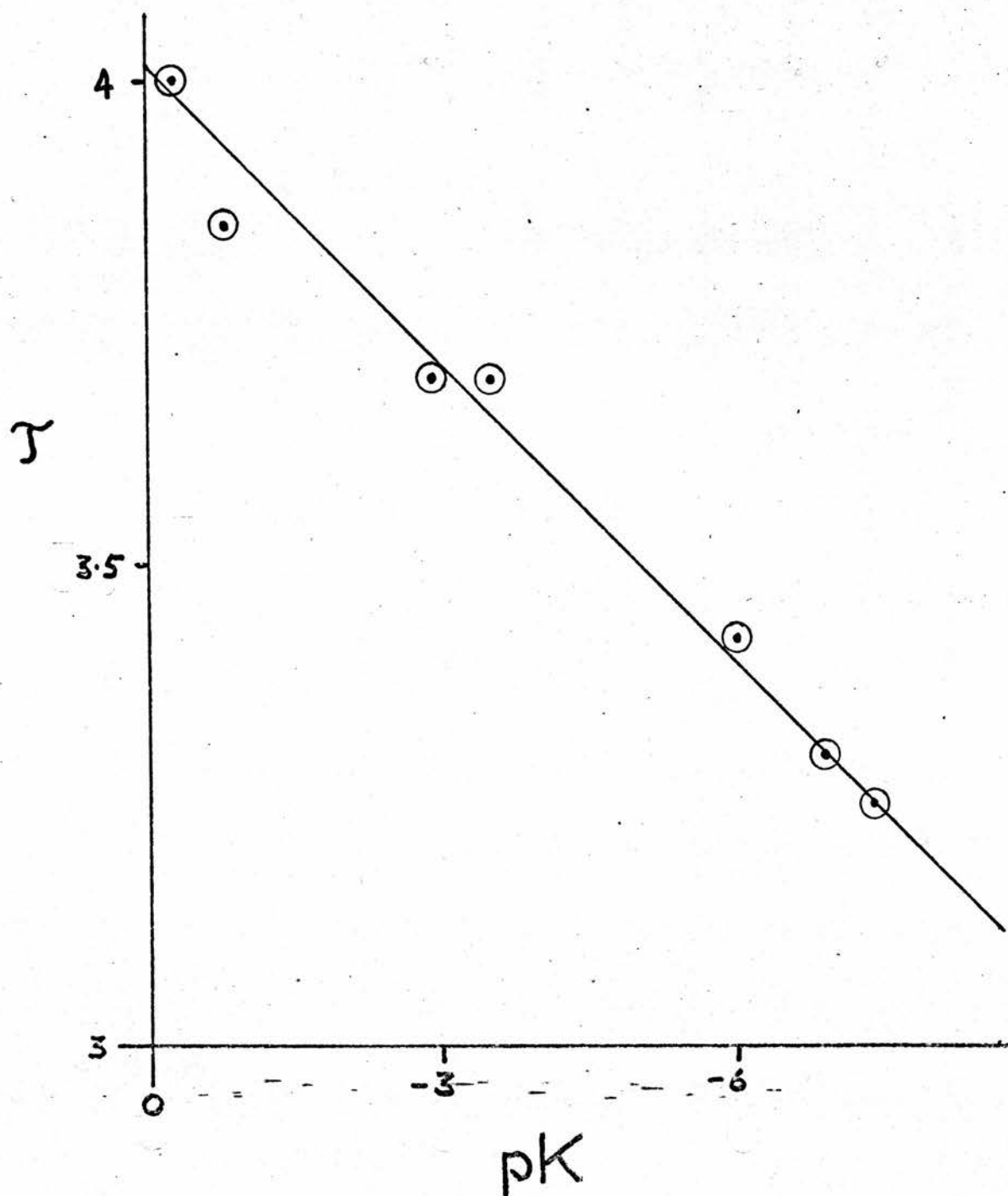


TABLE (4.3)

Variation of chemical shift (τ) of the signal for the β -proton
in indoles with acid dissociation constant (pK_A) of the
indole.

(The pK_A is that for 3-protonation)

Compound	pK_A^a	τ (β)	Solvent
1. 2-methylindole	-0.28	4.00	ClH_4
2. 2-t-butylindole	-0.80	3.85	ClH_4
3. 5-methoxyindole	-2.9	3.69	ClH_4
4. indole	-3.5	3.69	ClH_4
5. 5-bromoindole	-4.3	3.58	$CDCl_3$
6. 5-cyanoindole	-6.0	3.42	$CDCl_3$
7. 6-nitroindole	-6.9	3.33	$CDCl_3$
		3.27	D.M.S.O.
8. 5-nitroindole	-7.4	3.25	D.M.S.O.

a. The pK_A values for compounds 1,4,7,8 are those reported by Hinman and Lang;^(31c) the values for indoles 2,3 and 6 are reported for the first time in this thesis.

increase the acidity of this proton and lead to deshielding; the signal therefore appears at lower field. The converse is true for electron-releasing groups.

Infra-red spectra.

The proton on the indole nitrogen is also exchanged by the labelling procedures described above, and it was important to establish that only 3-position proto-deuteriation and proto-detrification was being followed in the kinetic experiments. N.M.R. analysis of the broad N-H absorption is difficult and subject to inaccuracy, since the signal for the N-proton either appears as a broad peak at low field, or is indistinguishable from the aromatic absorptions. The problem was overcome by infra-red analysis in the following manner. The deuteriated indole was dissolved in aqueous (50:50) ethanol, extracted immediately with ether, recovered and purified as described before. The intense N-D stretching absorption, observed by Hinman and Bauman⁽⁶⁰⁾ in the product of their deuteriation, occurs in the 2450 - 2600 cm.⁻¹ region of the spectrum as shown in TABLE (4.4).

TABLE (4.4)

	ν cm. ⁻¹	
indole	2,520	(nujol)
5-cyanoindole	2,470	(nujol)
5-methoxyindole	2,597	(carbon disulphide)
5-bromoindole	2,530	(nujol)

This absorption, which was present in the spectrum of the original

reaction product, disappeared completely after the above treatment, indicating that under the conditions used for kinetics (where the substrate was dissolved in distilled water prior to addition to the catalyst) the hydrogen isotope on the indole nitrogen had been replaced by hydrogen before initiation of the catalysed exchange process.

The spectra of substituted indoles, in KBr and nujol, have recently been discussed by Kanaoka and his co-workers.⁽⁶⁹⁾ They found that indoles bearing no 3-substituent had absorptions in the range $785 - 770 \text{ cm}^{-1}$; the absorption in this region was therefore assigned to a C-H (3-position) out-of-plane bending vibration. They were unable, however, to specify the ring C-H (2- or 3-position) which resulted in an absorption in the $725 - 710 \text{ cm}^{-1}$ range. The C-H absorptions used in the dedeuteriation experiments described in this thesis, (TABLE (4.1)) fall into either one of these two ranges, with the exception of the peak at 756 cm^{-1} in 5-methoxyindole (which may have been shifted from the $785 - 770 \text{ cm}^{-1}$ region by a solvent effect). This provides evidence that the unassigned $725 - 710 \text{ cm}^{-1}$ region can be attributed to a 3-position C-H vibration.⁽⁶⁹⁾

It was concluded from these combined spectral studies, that isotopic substitution of only the N- and 3-position protons in the indole nucleus had been achieved by the labelling experiments and that the deuterium or tritium atom attached to the nitrogen was replaced by hydrogen, prior to kinetic measurements, merely by dissolving the labelled compound in water.

Reagents.

Acetic acid buffer solutions were prepared by adding weighed amounts of 'Analar' grade sodium acetate and sodium chloride (both oven-dried at 140°) to a measured volume of 'Analar' acetic acid which had been standardised by titration with a B.D.H. "Volumetric Solution" of sodium hydroxide, using phenolphthalein as indicator. Pyridine buffers were prepared from 'Analar' pyridine and B.D.H. "Volumetric Solution" grade hydrochloric acid.

The sodium hydroxide used for kinetic runs up to 3.6M was a B.D.H. "Volumetric Solution". For the experiments at higher basicity, carbonate-free sodium hydroxide solutions were prepared by dilution of a saturated solution of 'Analar' sodium hydroxide in boiled-out water. The molarity of the solutions was determined from titration with B.D.H. standard hydrochloric acid using methyl red as indicator.

'Analar' sulphuric acid was used without further purification for the equilibrium measurements. Standard solutions were prepared by dilution, and their concentrations were checked against B.D.H. standard sodium hydroxide using methyl red as indicator.

The reaction solutions for the kinetic runs in dilute mineral acid were prepared from B.D.H. "Volumetric Solution" grade hydrochloric acid.

Deuterium oxide (isotopic purity 99.7%) was purchased from Koch-Light, and purified for kinetics by repeated distillation from alkaline potassium permanganate to a conductivity of $< 10^{-6}$ mhos.

Deuteriosulphuric acid was the kind gift of Dr. A.R. Butler.
(Department of Chemistry, University of St. Andrews, Fife, Scotland.)

Reagent grade 2:2:4-trimethylpentane, carbon disulphide and xylene were used without further purification. (For the U.V. measurements, "Spectrosol" grade 2:2:4-trimethylpentane was used). It was found that the use of sulphur-free xylene gave no detectable change in the radioactive counting experiments. Benzene was obtained from May and Baker as a "Pure Crystallisable" reagent. 'Analar' absolute alcohol was obtained from Burroughs. Hopkin and Williams anhydrous calcium sulphate and anhydrous sodium carbonate were general purpose reagents.

BIBLIOGRAPHY

1. V. Gold and D.P.N. Satchell, *Quart.Rev.*, 1955, 9, 51.
2. K.B. Wiberg, *Chem.Rev.*, 1955, 55, 713.
3. L. Melander, "Isotope Effects on Reaction Rates", Ronald Press, New York, 1960.
4. V. Gold, "Friedel-Crafts and Related Reactions", (Ed., Olah) Interscience Publishers, New York - London - Sydney, 1964, 2, 1253.
5. H. Zollinger, "Advances in Physical Organic Chemistry", (Ed., Gold) Acad.Press, London and New York, 1964, 2, 163.
6. F.H. Westheimer, *Chem.Rev.*, 1961, 61, 265.
7. J. Bigeleison, *Pure Appl.Chem.*, 1964, 8, 217.
8. R.P. Bell, *Trans. Faraday Soc.*, 1961, 57, 961.
9. A.V. Willi and M. Wolfsberg, *Chem. and Ind.*, 1964, 2097.
10. R.P. Bell, *Discuss. Faraday Soc.*, 1965, 39, 16.
11. R.F.W. Bader, *Canad.J.Chem.*, 1964, 42, 1822.
12. W.J. Albery, *Trans.Faraday Soc.*, 1967, 63, 200.
13. R.A. More O'Ferrall and J. Kouba, *J.Chem.Soc.*, 1967, B, 985.
14. R.P. Bell and J.E. Crooks, *Proc.Roy.Soc. A.*, 1965, 286, 285.
15. R.P. Bell and D.M. Goodall, *Proc.Roy.Soc. A.*, 1966, 294, 273.
16. (a) J.R. Jones, *Trans.Faraday Soc.*, 1965, 61, 95;
(b) *ibid.*, 1965, 61, 2456; (c) J.R. Jones, R.E. Marks and S.C. Subba Rao, *ibid.*, 1967, 63, 111; (d) J.R. Jones and S.C. Subba Rao, *ibid.*, 1967, 63, 120; (e) J.R. Jones, R.E. Marks and S.C. Subba Rao, *ibid.*, 1967, 63, 993.
17. R. Stewart and D.G. Lee, *Canad.J.Chem.*, 1964, 42, 439.

18. A.C. Ling and F.H. Kendall, J.Chem.Soc., 1967, B, 445.
19. A.J. Kresge, D.S. Sagatys and H.L. Chen, J.Amer.Chem.Soc., 1968, 90, 4174.
20. L. Funderburk and E.S. Lewis, J.Amer.Chem.Soc., 1964, 86, 2531; *ibid.*, 1967, 89, 2322.
21. R.P. Bell, T.A. Fendley and J.R. Hulett, Proc.Roy.Soc. A., 1956, 235, 453.
22. A.J. Kresge, Discuss. Faraday Soc., 1965, 39, 48.
23. L.C. Gruen and F.A. Long, J.Amer.Chem.Soc., 1967, 89, 1287.
24. J.L. Longridge and F.A. Long, J.Amer.Chem.Soc., 1967, 89, 1292.
25. A.F. Cockerill, J.Chem.Soc., 1967, B, 964.
26. A.F. Cockerill, S. Rottschaefer and W.H. Saunders, Jr., J.Amer.Chem.Soc., 1967, 89, 901.
27. V. Gold and D.P.N. Satchell, J.Chem.Soc., 1955, 3609.
28. A.J. Kresge and Y. Chiang, (a) J.Amer.Chem.Soc., 1959, 81, 5509; (b) Proc.Chem.Soc., 1961, 81; (c) J.Amer.Chem.Soc., 1961, 83, 2877.
29. (a) J.Colapietro and F.A. Long, Chem. and Ind., 1960, 1056; (b) J. Schulze and F.A. Long, J.Amer.Chem.Soc., 1964, 86, 331. (c) R.J. Thomas and F.A. Long, *ibid.*, 1964, 86, 4770.
30. (a) M. Koizumi, Y. Komaki and T. Titani, Bull.Chem.Soc., Japan, 1938, 13, 643; (b) M. Koizumi and T. Titani, *ibid.*, 1938, 13, 307; (c) M. Koizumi, *ibid.*, 1939, 14, 453.
31. (a) R.L. Hinman and J. Lang, Tetrahedron Letters, 1960, 21, 12; (b) R.L. Hinman and E.B. Whipple, J.Amer.Chem.Soc., 1962, 84, 2534; (c) R.L. Hinman and J. Lang, *ibid.*, 1964, 86, 3796.

32. R.M. Acheson, "An Introduction to the Chemistry of Heterocyclic Compounds", Interscience Publishers, New York and London, 1960, p. 131.
33. B.C. Challis and F.A. Long, J.Amer.Chem.Soc., 1963, 85, 2524.
34. B.C. Challis and F.A. Long, unpublished results.
35. G. Yagil, J.Phys.Chem., 1967, 71, 1034; *ibid.*, 1967, 71, 1045; Tetrahedron, 1967, 23, 2855.
36. M. Kilpatrick and R. Dean Eanes, J.Amer.Chem.Soc., 1953, 75, 586.
37. R. Gary, R.G. Bates and R.A. Robinson, J.Phys.Chem., 1965, 69, 2750.
38. V. Gold and B.M. Lowe, J.Chem.Soc., 1968, A, 1923.
39. A.A. Frost and R.G. Pearson, "Kinetics and Mechanism", John Wiley and Sons Inc., New York and London, 2nd Edition, 1961, p. 195.
40. A.J. Kresge and Y. Chiang, J.Amer.Chem.Soc., 1962, 84, 3976.
41. R.J. Bruehlman and F.H. Verhoek, J.Amer.Chem.Soc., 1948, 70, 1401; R.H. Linnel, J.Org.Chem., 1960, 25, 290; C.J. Hawkins and D.D. Perrin, J.Chem.Soc., 1962, 1351.
42. R.P. Bell, Discuss. Faraday Soc., 1965, 39, 94.
43. B.D. Butts and V. Gold, J.Chem.Soc., 1964, 4284.
44. R.P. Bell, (a) "The Proton in Chemistry", Cornell University Press, Ithaca, N.Y., 1959, p.155; (b) "Acid-Base Catalysis", Oxford University Press, New York, N.Y., 1941, p.82.
45. J.E. Leffler and E. Grunwald, "Rates and Equilibria of Organic Reactions", John Wiley and Sons Inc., New York and London, 1963, pages 238-241.
46. Chapter 10 of reference (44)a.

47. V. Gold and D.C.A. Waterman, J.Chem.Soc., (a) 1968, B, 839;
(b) 1968, B, 849.
48. M. Anbar, M. Bobtelsky, D. Samuel, B. Silver and G. Yagil,
J.Amer.Chem.Soc., 1963, 85, 2380.
49. H.S. Harned and R.A. Robinson, Trans. Faraday Soc., 1940, 36, 973.
50. G. Yagil and M. Anbar, J.Amer.Chem.Soc., 1963, 85, 2376.
51. B.C. Challis, unpublished results.
52. C.G. Swain, E.C. Stivers, J.F. Reuwer, Jr., and L.J. Schaad,
J.Amer.Chem.Soc., 1958, 80, 5885.
53. B.C. Challis, private communication.
54. C.K. Rule and V.K. La Mer, J.Amer.Chem.Soc., 1938, 60, 1974.
55. D.C. Martin and J.A.V. Butler, J.Chem.Soc., 1939, 1366.
56. A. Jönsson, Svensk.Kem.Tidskr., 1955, 67, 188.
57. J. Thesing, G. Semler and G. Mohr, Chem.Ber., 1962, 95, 2205.
58. H. Singer and W. Shive, J.Org.Chem., 1955, 20, 1458.
59. H.G. Lindwall and G.J. Mantell, J.Org.Chem., 1953, 18, 345.
60. R.L. Hinman and C.P. Bauman, J.Org.Chem., 1964, 29, 2437.
61. J.B. Bell and H.G. Lindwall, J.Org.Chem., 1948, 13, 547.
62. R.R. Hunt and R.L. Rickard, J.Chem.Soc., 1966, C, 344.
63. N.B. Chapman, K. Clarke and H. Hughes, J.Chem.Soc., 1965, 1424.
64. W.E. Noland, L.R. Smith and D.C. Johnson, J.Org.Chem., 1963,
28, 2262.
65. S.M. Parmerter, A.G. Cook and W.B. Dixon, J.Amer.Chem.Soc.,
1958, 80, 4621.
66. B.C. Challis and J.B. Hendry, unpublished results.
67. L.A. Cohen, J.W. Daly, H. Kny and B. Witkop, J.Amer.Chem.Soc.,
1960, 82, 2184.

68. R.V. Jardine and R.K. Brown, *Canad.J.Chem.*, 1963, 41, 2067.
69. Y. Kanaoka, Y. Ban, T. Oishi, O. Yonemitsu et al.,
Chem. and Pharm.Bull.(Tokyo), 1960, 8, 294.